

University of Mississippi

eGrove

---

Electronic Theses and Dissertations

Graduate School

---

2012

## Use of Geophysics to Map Subsurface Features at Levee Seepage Locaitons

Thomas Chapman Brackett

Follow this and additional works at: <https://egrove.olemiss.edu/etd>



Part of the [Geophysics and Seismology Commons](#)

---

### Recommended Citation

Brackett, Thomas Chapman, "Use of Geophysics to Map Subsurface Features at Levee Seepage Locaitons" (2012). *Electronic Theses and Dissertations*. 60.

<https://egrove.olemiss.edu/etd/60>

This Dissertation is brought to you for free and open access by the Graduate School at eGrove. It has been accepted for inclusion in Electronic Theses and Dissertations by an authorized administrator of eGrove. For more information, please contact [egrove@olemiss.edu](mailto:egrove@olemiss.edu).

USE OF GEOPHYSICAL METHODS TO MAP SUBSURFACE FEATURES AT  
LEVEE SEEPAGE LOCATIONS

A Thesis  
Presented in Partial Fulfillment of Requirements  
for the Master of Science Degree  
in the Department of Geology and Geological Engineering  
The University of Mississippi

By  
THOMAS C. BRACKETT

December 2012

**Copyright © Thomas C. Brackett 2012**

**ALL RIGHTS RESERVED**

## **ABSTRACT**

The record breaking 2011 caused moderate to severe seepage and piping along the Mississippi River levees in Northwest Mississippi. The aim of this thesis was to implement geophysical techniques at two seepage locations in order to give a better understanding of the causes of underseepage and to provide information on how to potentially mitigate the problem. Sites near Rena Lara, MS in Coahoma County and near Francis, MS in Bolivar County were chosen as study sites. Electrical Resistivity Tomography (ERT) and Electromagnetic Induction (EM) surveys were conducted on and adjacent to levees to identify seepage pathways and any geological features at the sites.

Results from geophysical surveys revealed that Francis and Rena Laura each had a prominent geomorphologic feature that was contributing to underseepage. Seepage at Francis was the result of a sand filled channel capped by a clay overburden. Permeable materials at the base of the channel served as a conduit for transporting river water beneath the levee. The seepage surfaced as sand boils where the overlying clay overburden was thin or non-existent. Investigations at the Rena Lara site revealed a large, clay-filled swale extending beneath the levee. The clay within the swale has relatively low horizontal permeability, and concentrated the seepage flow towards more permeable zones on the flanks of the swale. This resulted in the formation of sand boils at the base of the levee. Both geomorphic features at Francis and Rena Lara were identified as surface drainages using remote sensing data.



With the assistance of borehole and elevation data, geophysics was successfully used to characterize the features at each site. Properties such as permeability and clay content were derived from responses in electrical conductivity and used to build seepage models at each site. These models will hopefully be considered when determining seepage conditions and mitigation techniques at other sites along the levee.

## **DEDICATION**

...to my amazing parents for their unconditional dedication and support. I would never be where I am today if it weren't for their patience and encouragement.

## **ACKNOWLEDGEMENTS**

I would like to sincerely thank Dr. Greg Eason, Dr. Craig Hickey and Charles Swann for their time and dedication to helping me complete this thesis. Appreciation also goes to the Mississippi Levee Board, the Yazoo-Mississippi Delta Levee Board and the U.S. Army Corps of Engineer's Vicksburg and Memphis Districts for their cooperation in sharing critical data. The U.S. Corps of Engineer's Engineering Research and Development Center also deserves acknowledgement for allowing me to use geophysical equipment. Lastly, I would like to thank the faculty and my peers in the Geology and Geological Engineering department for their constant support and encouragement throughout my career at Ole Miss.

## TABLE OF CONTENTS

1. Introduction.....	1
i. Piping Mechanics.....	2
ii. Predicting Seepage Occurrence Using Geology.....	3
iii. Mitigation.....	6
i. Landside Berms and Levee Aprons.....	6
ii. Relief Wells.....	7
2. Thesis Objectives.....	8
3. Study Area.....	9
i. Francis.....	9
ii. Rena Lara.....	10
4. Preliminary Data.....	15
i. Elevation Data.....	15
ii. Borehole Data.....	15
5. Geologic Setting.....	19
i. Regional Geology.....	19
ii. Local Geology and Geomorphology.....	21
i. Francis Geology and Geomorphology.....	21
ii. Rena Lara Geology and Geomorphology.....	31
6. Geophysical Methods.....	39
i. Electromagnetic Induction (EM).....	39
ii. Electrical Resistivity Tomography (ERT).....	43
7. Data Surveying and Processing.....	45
i. Survey Plan and Implementation.....	45
i. Francis Survey.....	47
ii. Rena Lara Survey.....	50
iii. Survey Limitations.....	50
ii. Data Processing.....	53
i. Software.....	53
ii. Interpolation Methods.....	57
8. Geophysical Results and Interpretation.....	58
i. Francis Results.....	58
i. Francis EM Data.....	59
ii. Francis ERT Data.....	59
iii. Francis Geological Interpretation.....	66

ii.	Rena Lara Results.....	68
i.	Rena Lara EM Data.....	68
ii.	Rena Lara ERT Data.....	68
iii.	Rena Lara Geological Interpretation.....	69
9.	Discussion of Results.....	74
i.	Seepage Model.....	74
i.	Francis Seepage Model.....	74
ii.	Rena Lara Seepage Model.....	75
ii.	Geophysics and Seepage Modeling.....	76
10.	Applications of Results.....	81
11.	Recommendations for further work.....	82
i.	Suggestions for Supplemental Geophysical Surveys at Francis.....	82
ii.	Suggestions for Supplemental Geophysical Surveys at Rena Lara...	83
	References.....	86
	Appendices.....	88

## LIST OF FIGURES

1.1	Cross section illustrating how surface features may influence seepage pathways. Sand boils are noted by black plus-signs (Modified from USACE, 1956).....	5
3.1	Topographic map of the study area with sand boils from the 2011 flood event. Sites include Francis in northern Bolivar County and Rena Lara in southern Coahoma County.....	11
3.2	Aerial imagery of Francis site during 2011 flood showing locations of sand boils. The brown background colors west of the levee indicates flood waters.....	12
3.3	Aerial imagery of Rena Lara during 2011 flood event showing locations of sand boils. The blue dot marks a seepage scarp on the toe of the levee discovered in January 2012.....	13
3.4	Water seeping from a scarp in the apron at the Rena Lara site. The photo was taken in January 2012 when there was no flood water present on the river-side of the levee.....	14
4.1	Location of 10 boreholes drilled at the Francis site. Wells FRA-1.11c to FRA 9.11c were drilled using a CPT test. Well FRA-1.11T was drilled and logged using USCS standards.....	17
4.2	Location of 16 boreholes drilled at the Rena Lara site. Each well was drilled and logged using USCS standards.....	18
5.1	Typical cross section of Mississippi River valley and alluvial deposits (Modified from USACE, 1956). The relatively impermeable top stratum is composed of paleo-meander deposits.....	20
5.2	Map of surface geomorphic features at study area. Features were delineated by Fisk (1944) using aerial imagery.....	24
5.3	Drawing adapted from Saucier (1994) showing components of the fluvial system. Comparison shows these components are analogous to the ones seen at Francis.....	25

5.4	LIDAR image at Francis showing the orientation of a small drainage trending beneath the levee. The sand boils surfaced within this drainage in 2011.....	26
5.5	Locations of cross-sections created from Francis borehole data.....	27
5.6	Cross section A-A' shows a pinching-out of the silt and silty sand to the north of the site, yielding a direct sand to clay contact.....	28
5.7	Cross-section B-B' shows a pinching out of the silty-sand towards borehole 2.11c.....	29
5.8	Cross-section C-C' shows the sand to clay contact does not intersect borehole 6.11c on the river-side of the levee.....	30
5.9	Both DEM (above) and Fisk (1944) maps show multiple meander loops trending towards the study area. The apparent meander complexes are shown and their features are shown on the DEM map.....	33
5.10	Smaller scale features seen in the elevation data (above) reflect ridge and swale topography near the site. The LIDAR indicates that the active drainage may follow one of these swales.....	34
5.11	Index to cross-sections created from Rena Lara borehole data.....	35
5.12	Cross-section X-X' shows a clay plug and undulating silt and sand units beneath the levee. This is indicative of ridge and swale deposits and is reflected in the elevation data.....	36
5.13	Cross-section Y-Y' shows the clay plug continuing to the river-side of the levee.....	37
5.14	Cross-section Z-Z' shows an elevation profile across the levee along with information from boreholes 10-RG-83 and 9-LG-83. The section shows how the clay body thickens towards the land-side of the levee as well as the elevation of the seepage scarp.....	38
6.1	Diagram showing the generation of magnetic fields from electromagnetic induction. Adapted from USACE (1995).....	41

6.2	Pictures showing horizontal dipole (a) and vertical dipole (b) modes for the EM 34 (Llopis et. al, 2007).....	42
6.3	Diagram of the orientation of the measuring and current electrodes in the dipole-dipole array (Dunbar et. al, 2007).....	44
7.1	Map of EM survey grids at Francis. The large grid in the field and the grid on the levee apron both have 20m station spacing, while the smaller grid near the sand boils has 10m station spacing.....	48
7.2	Map of ERT surveys at Rena Lara. The survey lines were designed to cross the surface drainage and seepage pathway perpendicularly.....	49
7.3	Map of EM survey grids at Rena Lara. The station spacing was kept at 10m throughout all grids.....	51
7.4	Map of ERT survey at Rena Lara. The survey line was designed to cross the seepage pathway perpendicularly.....	52
7.5	Flow chart of EM data processing. The data required manual formatting before it could be manipulated.....	55
7.6	Flow chart of ERT data processing. The raw data required less formatting compared to the EM data.....	56
8.1	Conductivity profile of the EM 34 Horizontal Dipole. The profile shows an area of high conductivity near the surface that is interpreted to be a clay overburden.....	61
8.2	Conductivity profile of the EM 34 Vertical Dipole. The readings were too heavily influenced by the high conductivity material at the surface to read conductivity at depth.....	62
8.3	ERT Lines at Francis. A highly conductive material is present at the surface of each survey line. There is also a zone of low conductivity in Lines 2.2 and 3.....	63



8.4a	Conductivity (mS/m) section of Line 3. The high conductivity zone is continuous along the surface. There is a low conductivity zone at the same depth as Line 2.2.....	64
8.4b	Conductivity (mS/m) section of Line 2.2. The high conductivity zone is discontinuous. There is also a low conductivity zone at 5m (16 ft.).....	64
8.4c	Conductivity (mS/m) section of Line 2. A high conductivity zone is encountered at the near surface at around 60m (197 ft.).....	65
8.5	Plan view of low conductivity/ high permeability zone on the ERT line. The boundary of the zone is marked by green dashed lines. The zone appears to follow the trend of the seepage pathway and the surface drainage.....	67
8.6	Conductivity profile of EM 34 Vertical Dipole. The results show a high conductivity zone extending across the apron. This zone also lines up the drainage next to the levee.....	70
8.7	Conductivity profile of EM 34 Horizontal Dipole. The results show the high conductivity zone extending more parallel along the apron.....	71
8.8	ERT line at Rena Lara. The high conductivity zone is wedge-shaped and lines up with the drainage near the levee.....	72
8.9	Conductivity (mS/m) section of Line 1. The results show a wedge-shaped feature of highly conductive material. This is interpreted to be a clay-filled swale.....	73
9.1	Model of seepage at Francis. The clay overburden and the high permeability zone beneath it both influence sand boil occurrence.....	78
9.2	Model of seepage at Rena Lara. The clay-filled swales running beneath the levee focus seepage towards adjacent, more permeable zones. Modified from Wilson (2003).....	80

11.1	Map of suggested ERT surveys for supplemental surveying at Francis. The ERT lines should continue to cross the drainage perpendicularly in order to further identify the feature.....	84
11.2	Suggested grids for supplemental EM data. The layout of the grids is designed to further identify the clay-filled swale and detect a clay overburden.....	85

## **CHAPTER 1**

### **INTRODUCTION**

Levee breaches along the Mississippi River have long been a problem with potentially disastrous consequences. Although there has not been a significant levee breach in Mississippi since 1927, authorities must continue to monitor seepage occurring beneath the levee. When seepage becomes concentrated into localized channels, a process known as piping occurs (Wilson, 2003). Piping may remove the foundation material beneath a levee, potentially resulting in a collapse. The most common indicator that piping has occurred is a sand boil on the dry-side of the levee.

The United States Army Corps of Engineers (USACE) mitigates underseepage by building berms or installing relief wells around sand boils. Both of these methods are designed to lower the hydrostatic gradient acting on the levee and terminate the flow of foundation materials. In areas where surface geology and other factors promote piping, seepage mitigation may only serve as a “band aid” for a specific area. Once a boil has been controlled, another sand boil may appear locally where there a relief well or berm is not present.

Due to this phenomenon, it is important to understand the factors that promote seepage and characterize the path the seepage is taking beneath the levee. Mapping geologic features beneath the levee may help in understanding these factors.

## 1.1 Piping Mechanics

Seepage is the result of the differential hydrostatic pressure created when flood water rises on the river-side of the levee. Since most modern levees are constructed with a clay “cap”, seepage is concentrated beneath the levee (Smith, 1997). As hydraulic pressures forces water beneath the levee, a hydraulic gradient develops in the underlying alluvial material, or substratum. The gradient causes flow to develop from the river side toward the landside portion of the levee. The flow emerges where finer-grained overburden materials at the landside toe of the levee are thin or absent (USACE, 1956). The fine-grained overburden material is commonly referred to as top stratum and acts as a resisting force to the upward flow of seepage. When the submerged unit weight of the top stratum becomes less than the upward seepage forces, a critical hydraulic gradient is reached (Terzaghi, 1929). The equation for critical gradient is listed below.

$$i_c = \frac{\gamma'}{\gamma_w} \quad <1.1>$$

Where  $\gamma'$  is the submerged unit weight of the landside topstratum, and  $\gamma_w$  is the unit weight of water (Terzaghi, 1929).

At critical hydraulic gradient, the toe of the levee may heave or rupture, greatly weakening the stability of the levee (Wilson, 2003). Another phenomenon that may occur during these conditions is a sand boil. Sand boils are more common than general seepage because of the heterogeneity of the substratum (Wilson, 2003). Water usually flows through zones of higher permeability in the substratum and surfaces through weak areas in the top stratum (Wilson, 2003). When the flow is bound in this manner, sand boils are created and serve as an indication of piping. The size and severity of the sand boil is a result of differences in hydraulic gradient (Wilson, 2003). As piping continues, and soil continues to be removed, a subsurface void begins

to develop from the boil and progresses beneath the levee. The erosion created by the void can severely compromise the foundation of the levee (USACE, 1956).

## **1.2 Predicting Seepage Occurrence Using Geology**

Since under seepage is controlled by geologic deposits beneath the levee, emphasis has been placed on the nature and properties of these deposits. Studies post-dating the Mississippi River flood of 1927 have focused on trying to find a relationship between floodplain deposits and sand boils. In 1941, the USACE began to study the relationship between thicknesses of permeable substratum and overlying clay top stratum as the principal factors that control sand boil formation (USACE, 1941). Fourteen years later, the USACE was able to model seepage using an empirical formula. Input variables include thickness of top stratum and substratum, dimensions of the levee, hydrostatic head, permeability and other quantifiable data (USACE, 1956). Fisk (1944) and Kolb (1975) focused on delineating permeable and impermeable alluvial features with aerial photography and concluded that the angle and location of these features with respect to the levee have a strong influence on underseepage. Figure 1.1 shows how a point bar deposit may focus seepage flow beneath a levee due to its configuration of fine-grained material.

Combining maps constructed by Fisk (1944) with modern remote sensing imagery, allows investigators to delineate certain geomorphic features that may promote underseepage. The sheer size and complexity of geomorphic features presents a problem when trying to narrow down the exact location for the seepage outlet. Paleo-channel systems can average 0.5 mi (0.8km) in width and can be superimposed by smaller, more recent fluvial features (Fisk, 1944). The USACE, thus, deems it a priority to conduct ground based investigations of geomorphic

features around and beneath the levee system. Traditionally, this has been done by drilling several boreholes near the levee to determine sediment properties and to construct subsurface cross sections. This method, however, is time consuming, expensive and involves estimation when interpreting conditions between boreholes.

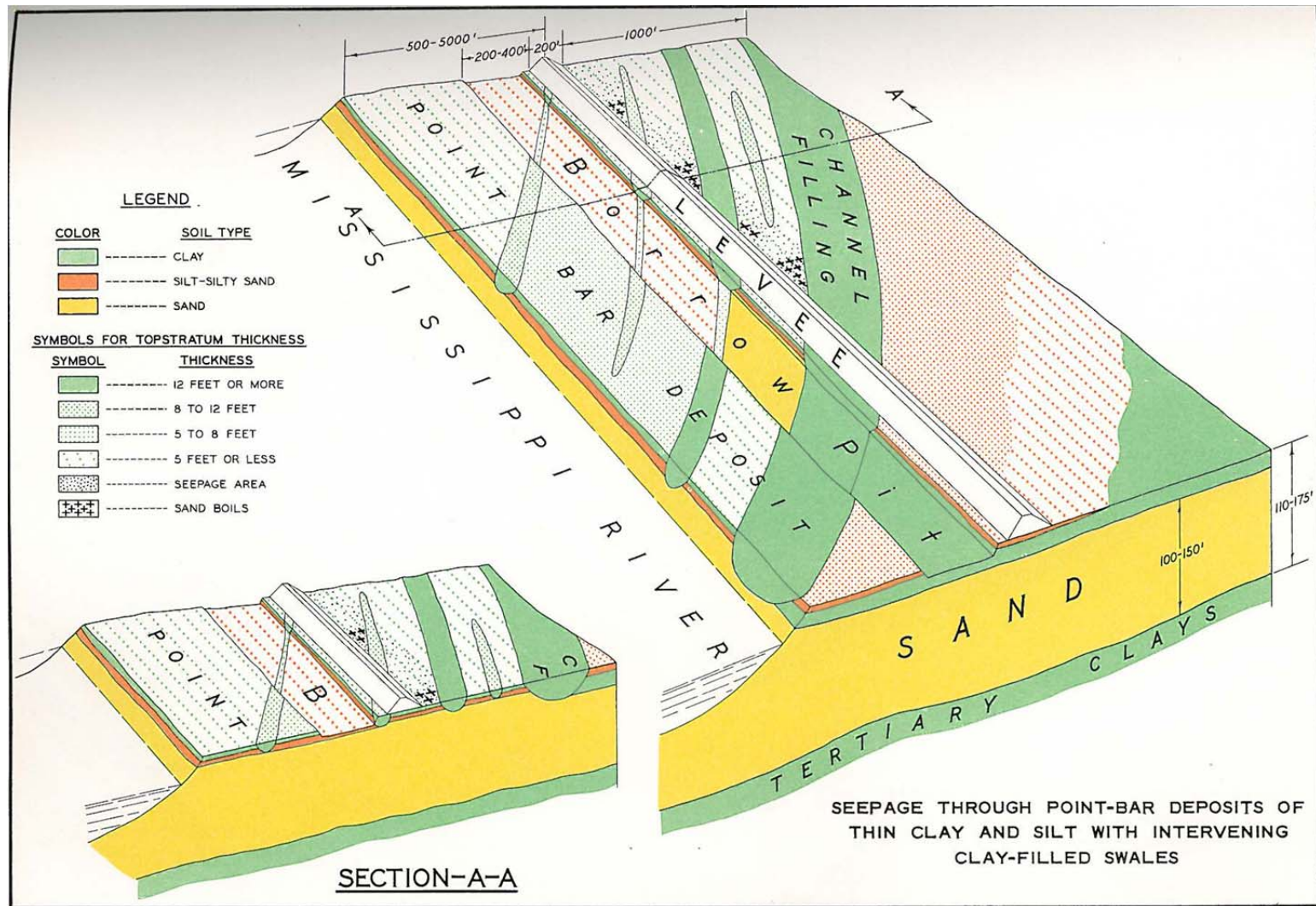


Figure 1.1 Cross section illustrating how surface features may influence seepage pathways. Sand boils are noted by black plus-signs (Modified from USACE, 1956).

### **1.3 Mitigation**

As seepage begins to develop, measures must be taken to prevent the piping caused by the seepage and reduce the pressure acting on the landside portions of the levee (USACE, 1956). This prevention is usually done in two different stages. As a boil begins to form on the land side of the levee, immediate action must be taken to lower the hydraulic head between the sand boil elevation and the floodwater elevation. Sand bags are piled around the boil to reduce the pressure/head gradient, thus lowering the erosion rate. An earthen berm may also be built around the seepage/boil area if the amount of discharge is more substantial. The second stage of mitigation is to construct a more permanent method for seepage control. Various measures may be taken to control levee underseepage and are chosen based on factors such as cost, property rights, foundation materials, etc. (USACE, 1956). Each measure focuses on one or all of the contributing factors associated with piping. This thesis will focus on the two measures commonly used in Mississippi, landside berms and relief wells (Nimrod and Thompson, 2011).

#### **1.3.1 Landside Berms and Levee Aprons**

A landside berm may be used to increase the unit weight of overburden at the seepage outlet, thus reducing the critical gradient. Berms may be localized around the seepage area or may be built as an extension of the levee toe. Berms that extend from the levee toe over large spans of the levee are referred to as levee aprons or blankets (USACE, 1956). In most cases the apron is constructed of semi-permeable material. This material allows the upward movement of water through the berm to lower the hydrostatic head (USACE, 2005).



### **1.3.2 Relief Wells**

The second most common seepage control measure in Mississippi is relief wells. Relief wells utilize a different technique in controlling piping erosion. Instead of inhibiting the seepage flow with overburden materials, relief wells allow controlled flow without allowing foundation materials to be removed (USACE, 1956). Relief wells are installed into the substratum and screened to filter out foundation material entering the well. The well opening is also extended at least 1 foot above the ground surface to reduce the hydraulic head (Williams, 2009). The USACE (1956) has outlined other design specifications when implementing a relief well system. The location and depth of each well is designed to intercept a majority of the subsurface seepage so that the flow will be controlled. Wells are designed to penetrate at least 50% of the alluvial aquifer in the substratum. The dimensions of the well screen and filter are dependent on subsurface material. Relief well systems usually consist of a straight line of wells near the seepage area. The initial spacing and overall length of the relief well system is based on calculated hydraulic heads, which are derived from piezometer data. These calculations assume a lateral homogeneity in the subsurface.

## **CHAPTER 2**

### **Thesis Objective**

The objective of this thesis was to use geophysical methods as a means to characterize anomalies in the subsurface that may contribute to levee underseepage and piping. Two different geophysical methods were employed at two sites where seepage occurred. Characterization of the anomalies was performed by:

- A) Determining the spatial relationship between anomalies and locations of sand boils in the area.
- B) Analyzing the spatial relationships between anomalies and geomorphic features delineated on surface geology maps and elevation data.
- C) Comparison of trends in the geophysical data with borehole data in the area.
- D) Determining how geophysical data (conductivity) is related to soil properties such as grain size, porosity and permeability.
- E) Exploring how subsurface anomalies could influence the hydraulic gradient present during flood stage.

## **CHAPTER 3**

### **Study Area**

The levees within the lower Mississippi River area have a history of underseepage dating back to the construction of the modern levee system (USACE, 1956). The USACE (1956) used three sites within this study area (Stovall, Francis and Farrell, Mississippi) as examples for seepage control measures. A seepage study conducted by the USACE in 2000 led to the installation of over 200 relief wells along the levee near Hillhouse, MS (Chasteen, 2000). This thesis will focus on the main-line Mississippi River levees in southern Coahoma County and northern Bolivar County. The two levee segments will be studied due to their seepage occurrence during the most flood event in 2011. Although these study locations are in different counties, Corps districts and levee board districts, they are within close proximity to each other (7.5 miles/12 km). Figure 3.1 shows a map of the general study area.

#### **3.1 Francis**

The first study site is 0.5 miles (0.8 km) west of Francis, Mississippi, in Bolivar County, within the jurisdiction of the USACE Vicksburg District and the Mississippi Levee Board District. During the 2011 flood event, three main sand boils were mitigated at this location. The first sand boil(s) occurred at the toe of the clay apron in the landside, man-made drainage trench. In order to control the seepage, temporary levees were built extending across the trench on each side of the sand boils to create a berm. Impounding water above the seepage area lowered the

hydrostatic head acting on the top stratum and slowed the seepage (Nimrod and Thompson, 2011). After the first sand boils were mitigated, two more sand boils surfaced approximately 300 feet (90 m) to the northwest. These boils were controlled by the construction of sand bag berms. Figure 3.2 shows the location of the sand boils at Francis.

### **3.2 Rena Lara**

The second study site discussed in this thesis was 1.3 miles (2 km) north of Rena Lara, Mississippi, in Coahoma County, in the jurisdiction of the USACE Memphis District and the Yazoo-Mississippi Delta Levee Board District. Four sand boils surfaced in this area during the 2011 flood event (Figure 3.3). Each sand boil was sand-bagged in order to temporarily mitigate the potential for piping. Recent field investigations at the site reveal that water was seeping from the clay apron on the landward toe of the levee (Figure 3.4). The seepage seemed to be minor, but had been occurring over the span of several months. The scarp created by the seepage indicated that minor levee erosion was also occurring.

## Sites for Levee Surveys

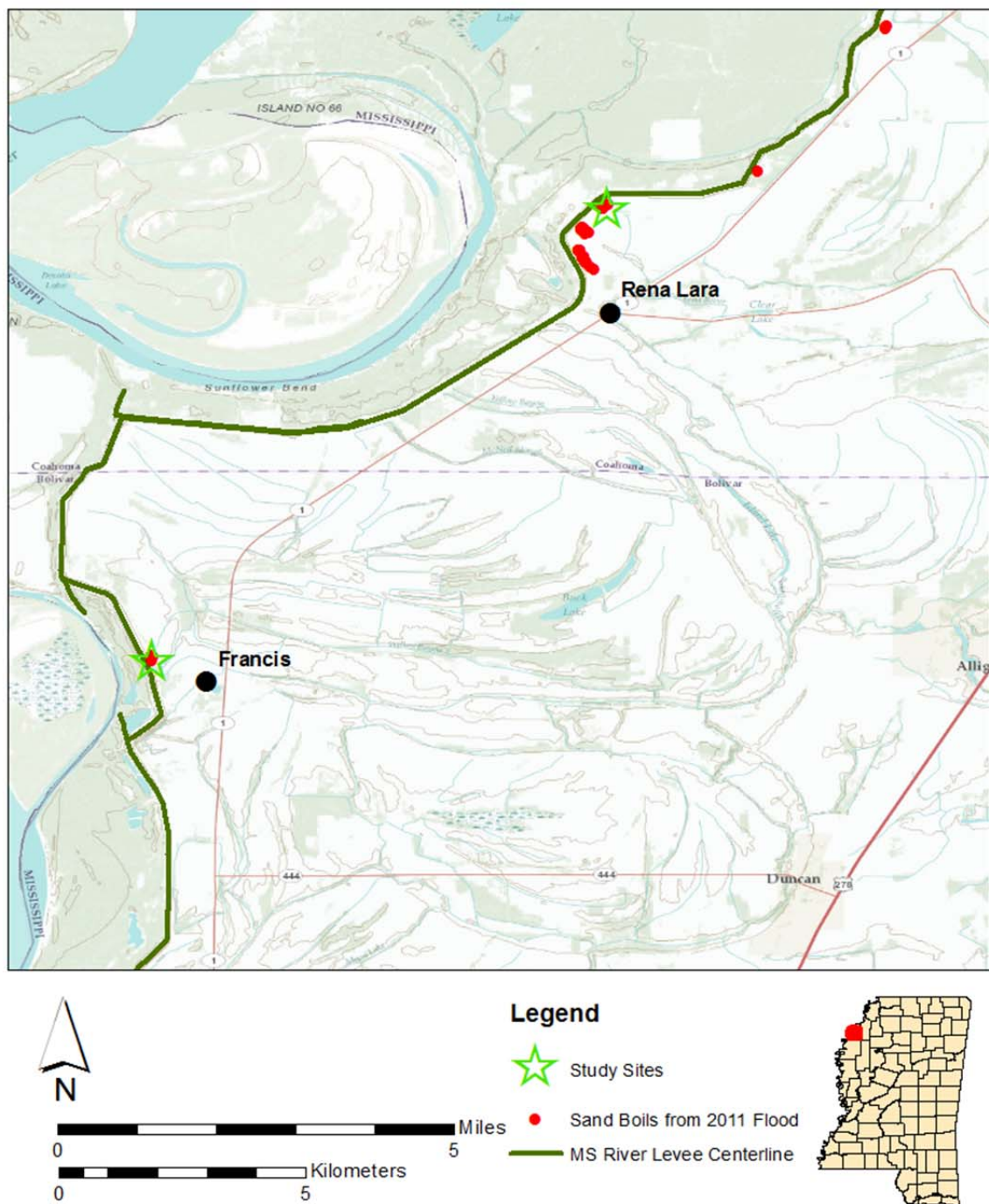


Figure 3.1 Topographic map of the study area with sand boils from the 2011 flood event. Sites include Francis in northern Bolivar County and Rena Lara in southern Coahoma County.

## Francis Sand Boils

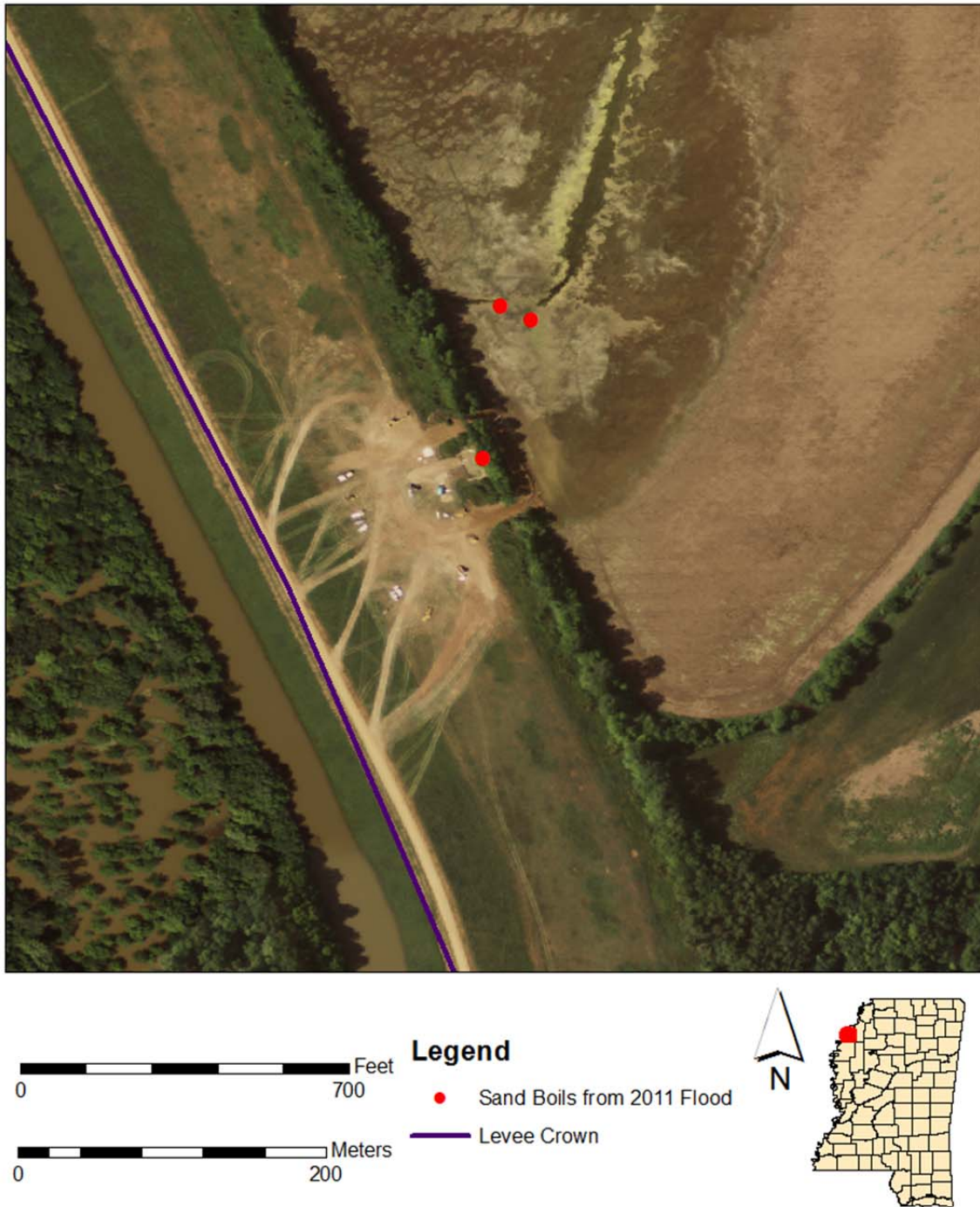


Figure 3.2 Aerial imagery of Francis site during 2011 flood showing locations of sand boils. The brown background colors west of the levee indicates flood waters.



## Rena Lara Sand Boils

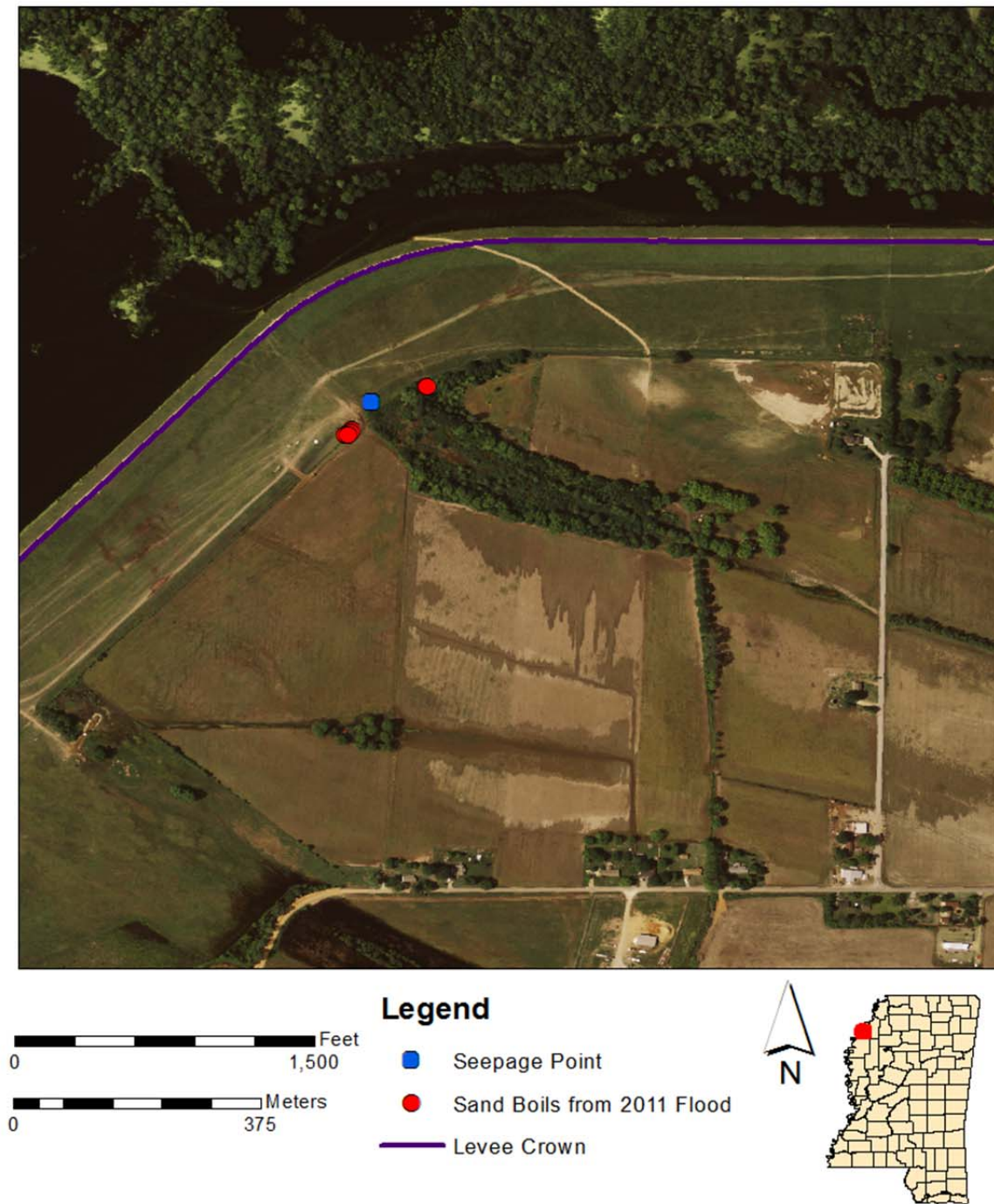


Figure 3.3 Aerial imagery of Rena Lara during 2011 flood event showing locations of sand boils. The blue dot marks a seepage scarp on the toe of the levee discovered in January 2012.



Figure 3.4 Water seeping from a scarp in the apron at the Rena Lara site. The photo was taken in January 2012 when there was no flood water present on the river-side of the levee.



## **CHAPTER 4**

### **Preliminary Data**

Before acquiring geophysical data, ancillary data was gathered at both seepage locations. The purpose of the data was to provide more site-specific information regarding the geology at the sites. Clues to both the surface and subsurface features present would, in the design of the geophysical survey methodologies, help with the interpretation of the geophysical data and complement any results drawn from the data results.

#### **4.1 Elevation Data**

Two forms of remote sensing data were used to delineate surface features at the seepage sites. The first set of data is the 7.5-minute Digital Elevation Model (DEM) images produced by the U.S. Geological Survey. Because of the coarse resolution (30m/9ft), the DEMs were used to locate larger-scale features in the study area such as paleo-channels. Light Detection and Ranging (LIDAR) data was also utilized. LIDAR data produces a more accurate form of digital elevation model with vertical accuracies as high as 15 cm (6 in.) (Aronoff, 2005). Due to the large data size and high resolution associated with the system, LIDAR was used in locating smaller-scale features such as local drainage segments and drainage divides.

## **4.2 Borehole Data**

Due to the range of the uncertainty sometimes associated with geophysical data, boreholes at each site were important for constructing subsurface profiles and reconciling geophysical results with characteristics such as grain size and moisture content. Ten boreholes were drilled at the Francis site by the USACE in October, 2011(Figure 4.1). Wells FRA-1.11c to FRA 9.11c reached a depth of 50 feet (16m) using a Cone Penetrometer (CPT) test. The cone penetrometer data was interpreted to include lithology (Appendix A). Well FRA-1.11T was logged using the Unified Soil Classification System (USCS) and was drilled to a depth of approximately 160 feet (50m) (Appendix A).

Thirty-three wells were drilled at the Rena Lara levee as part of a 1983 seepage study. Wells 5-14 were utilized during this research because of their proximity to the seepage site. Both a field boring log and a lab-based, USCS log were created for each boring (Appendix B). The USCS log proved more accurate in determining the specific soil type and stratum thicknesses. The eight logs were drilled to an average depth of 40 feet (12 m).

## Francis Boreholes

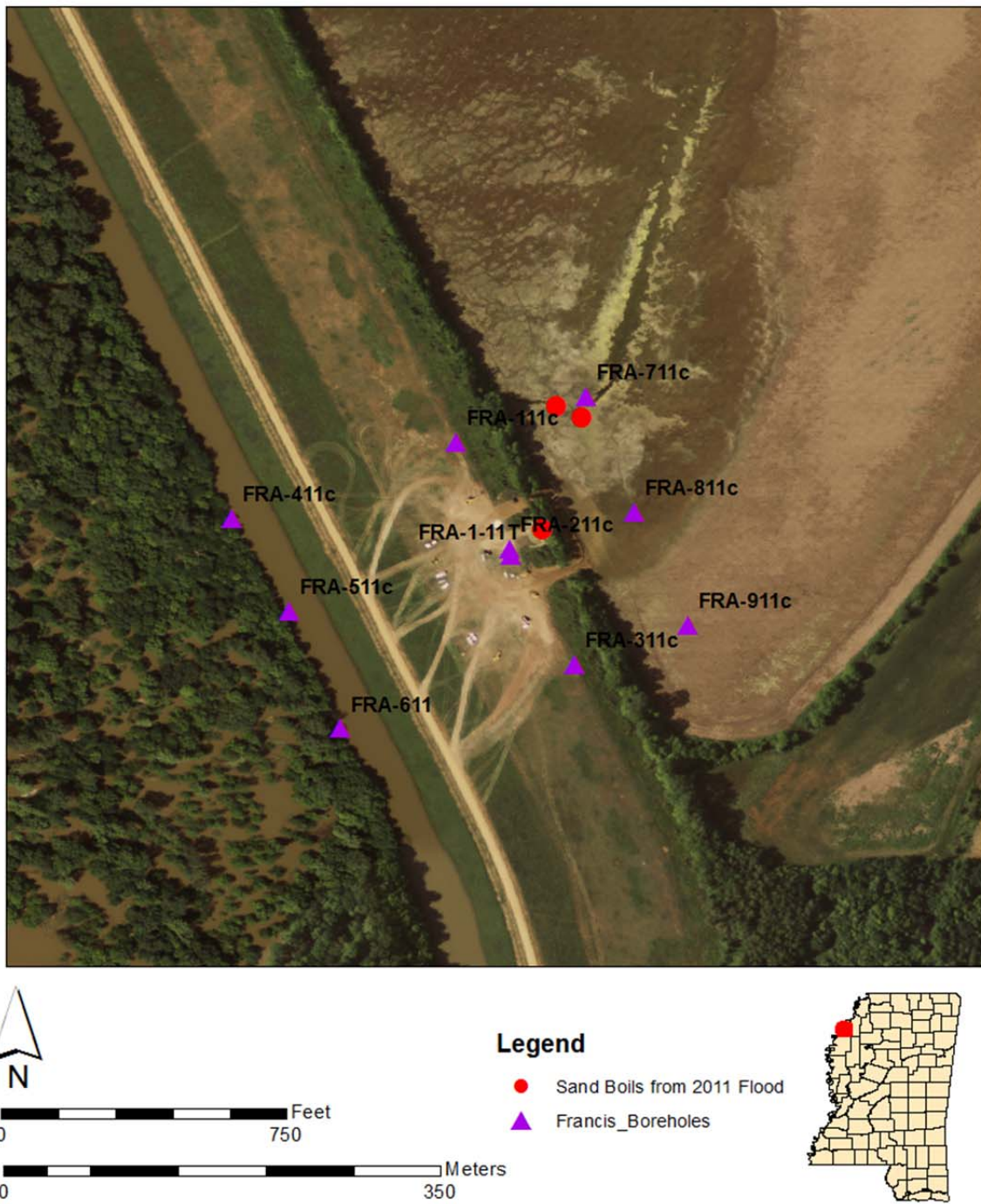


Figure 4.1 Location of 10 boreholes drilled at the Francis site. Wells FRA-1.11c to FRA 9.11c were drilled using a CPT test. Well FRA-1.11T was drilled and logged using USCS standards.

## Rena Lara Boreholes

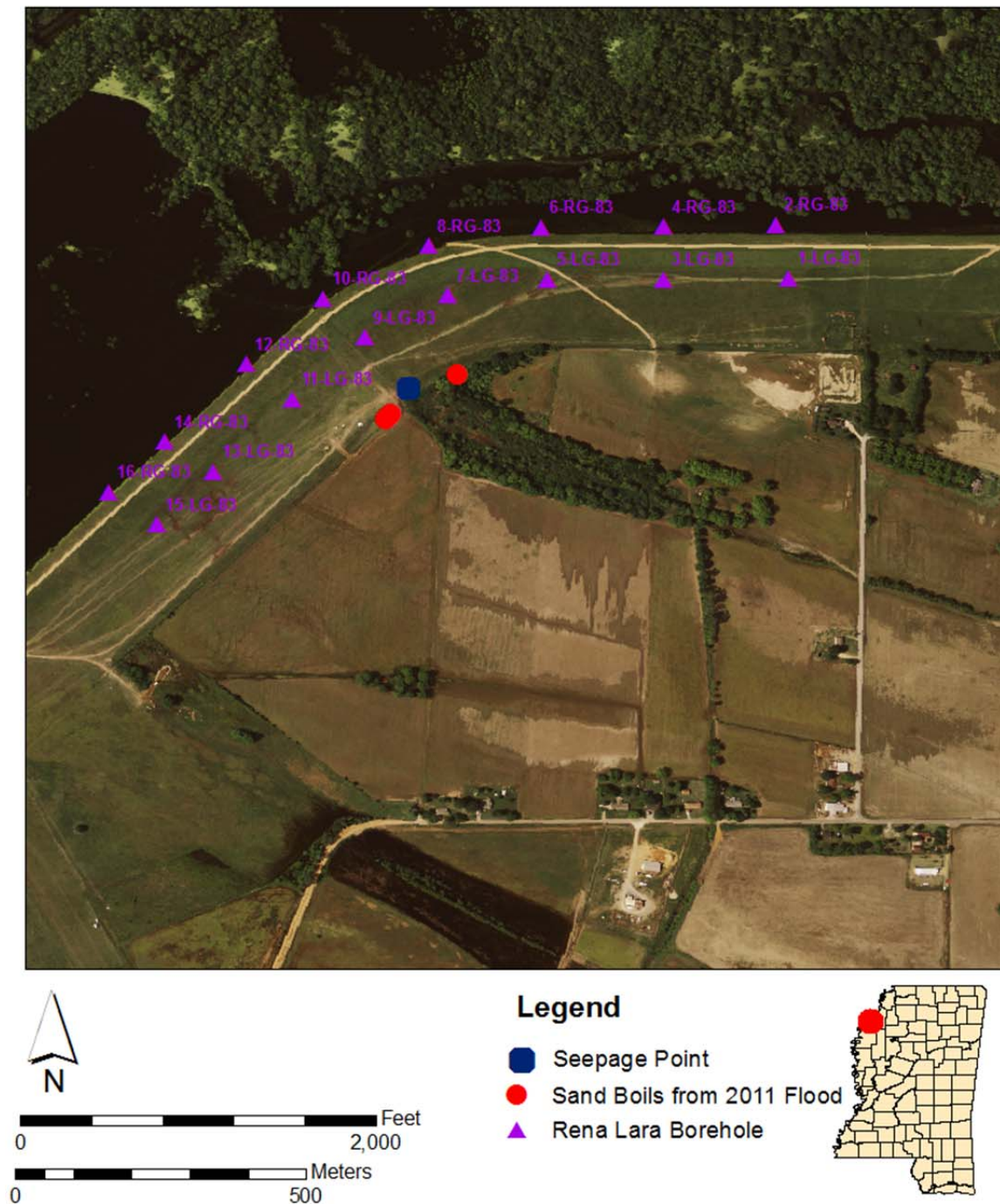


Figure 4.2 Location of 16 boreholes drilled at the Rena Lara site. Each well was drilled and logged using USCS standards.

## **CHAPTER 5**

### **Geologic Setting**

#### **5.1 Regional Geology**

Coahoma and Bolivar Counties lie within the Mississippi portion of the Mississippi River flood plain, which extends from Memphis to Vicksburg (Saucier, 1994). The flood plain is bound to the east by the edge of the Mississippi River flood plain and to the west by the current Mississippi River channel. It is composed of Holocene and Pleistocene-aged meander deposits formed by the migration of the Mississippi River across its floodplain. The fluvial depositional environments include point bars, channel-fill deposits, natural levees and back swamp deposits (Saucier, 1994). Figure 5.1 shows depositional features typically associated with a meander environment. These features are marked by lateral and vertical discontinuities and vary greatly in grain size. Collectively, recent fluvial deposits form a relatively impermeable top stratum sequence. Below the top stratum is a permeable substratum consisting of predominately coarser-grained sand. This substratum averages 150 feet (46m) thick in the study area and also varies greatly in grain size and permeability (USACE, 1956). Below the substratum are Tertiary units which compose the valley floor.

The coarser-grained substratum that lies beneath the study area comprises the alluvial aquifer. The aquifer is confined below by the Tertiary clays and above by the top of the fining upward sequence. These fine-grained sediments are often formed as back swamp deposits. The aquifer is



recharged in areas where water can infiltrate more permeable deposits, such as point bars. The aquifer averages 125 feet (38 m) and is capable of yielding 7000 gpm where agricultural demand is high (Saucier, 1994). The hydrologic connectivity between this aquifer and flood waters have been investigated as a cause for underseepage beneath local levees (Saucier, 1994).

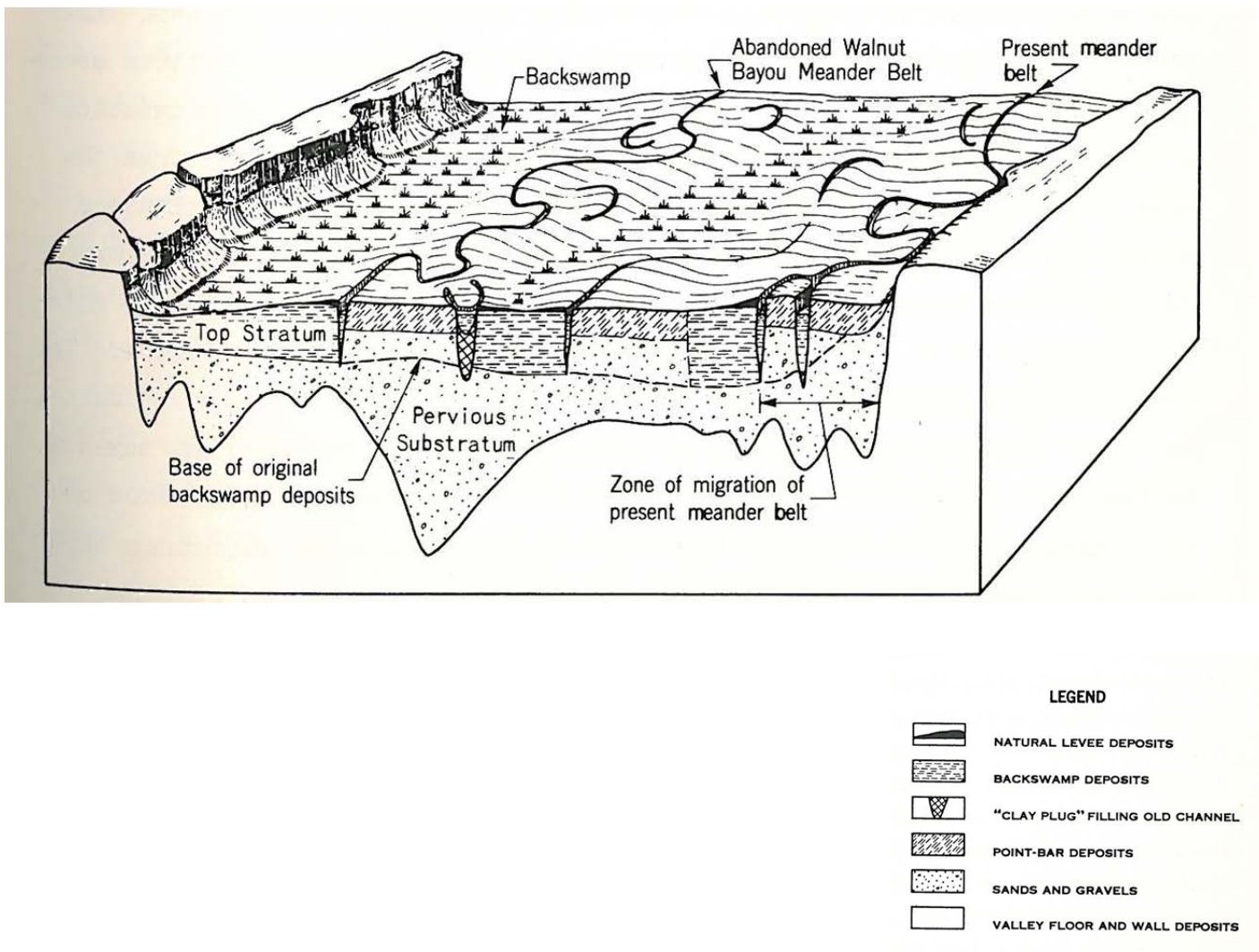


Figure 5.1 Typical cross section of Mississippi River valley and alluvial deposits (Modified from USACE, 1956). The relatively impermeable top stratum is composed of paleo-meander deposits.

## **5.2 Local Geology and Geomorphology**

In order to make geologic interpretations at Francis and Rena Lara, major paleo-channels were first identified in the study area. The locations of the sites in relationship to these paleo-channels could be used to predict what geomorphic features dominated the site. For example, if the site was located on the inside of a large meander, the geology is expected to be dominated by point bar features. These assumptions were later verified using preliminary data.

### **5.2.1 Francis Geology and Geomorphology**

Interpretation of digital elevation data was used to determine surface geomorphology at both sites. Geomorphologic maps constructed by Fisk (1944) were used as a guide (Figure 5.2). The LIDAR data at the Francis site indicates a large paleo-meander extending landward from beneath the levee between the community of Francis and the actual sand boil site. Considering the geometry of the deposit and the flow of the current river channel, the sand boil site seems to be on the convex portion of the abandoned meander. Saucier (1994) notes that the convex portion of meander bends typically host point bar deposits near the channel with overbank/backswamp deposits occurring further away. It is also expected that the deposits will decrease in grain size as the distance from the meander increases. Figure 5.3 illustrates how each of the features in the LIDAR imagery can be associated with those typically found in a meander belt system and shows that the sand boils (labeled as blue dots) are located near the overbank/backswamp portion of the meander system. The sand boils are also located within an active drainage that flows from the landside of the levee (Figure 5.4). The active drainage is superimposed on the older meander deposits, and appears to be influenced by these geomorphic features in terms of its shape and

course. Most drainage associated with the current Mississippi River channel tends to drain in a direction away from the river (Saucier, 1994). This is confirmed at the Francis site by examining the elevation data. It is also believed that the artificial levee at the site was constructed on top of the drainage. The boreholes drilled at the site show that the levee is underlain by a clay-rich overburden averaging 10 feet (3m) thick. Below the clay overburden, the sediment coarsens into silt, and eventually a thick sand unit which is assigned to the permeable substratum. Some wells indicate a sharp transition between the fine-grained overburden into sand where the silt is thin or non-existent. The sand unit may also contain thin gravel beds. Well FRA 1.11T was drilled until it reached the Tertiary at approximately 140 feet (44m) below the flood plain, which marks the base of the permeable flood plain deposits.

Wells drilled through the levee apron on the land side of the levee show that the apron is composed of 9-12 feet (3-4m) of silty sand. Three cross sections were constructed from the available borehole data (Figure 5.5). Cross section A-A' (Figure 5.6) indicates that the southern borehole has a typical fining upward sequence of sand, sandy silt, silt and clay. Towards the northern borehole, the silt and silty sand layer pinches out as the clay layer becomes thicker. Cross section B-B' (Figure 5.7) also shows a thinning of this sandy silt layer, resulting in a direct contact between sand and clay. Cross section C-C' indicates that this clay-sand contact does not continue through to the river-side boreholes (Figure 5.8). The sharp contact between sand and clay in boreholes FRA 2.11c and FRA 7.11c is believed to indicate sand lenses that may be attributed to a subsurface channel feature. The lens may be the result of an abandoned channel that was filled with coarser sediment and then capped with clay. Although more subsurface data is needed, if the same lens is intersected by both of the boreholes, it trends in the same direction



as the surface drainage. This correlation suggests that the surface drainage is also reflected in the subsurface.

## Surface Geomorphology at Francis and Rena Lara

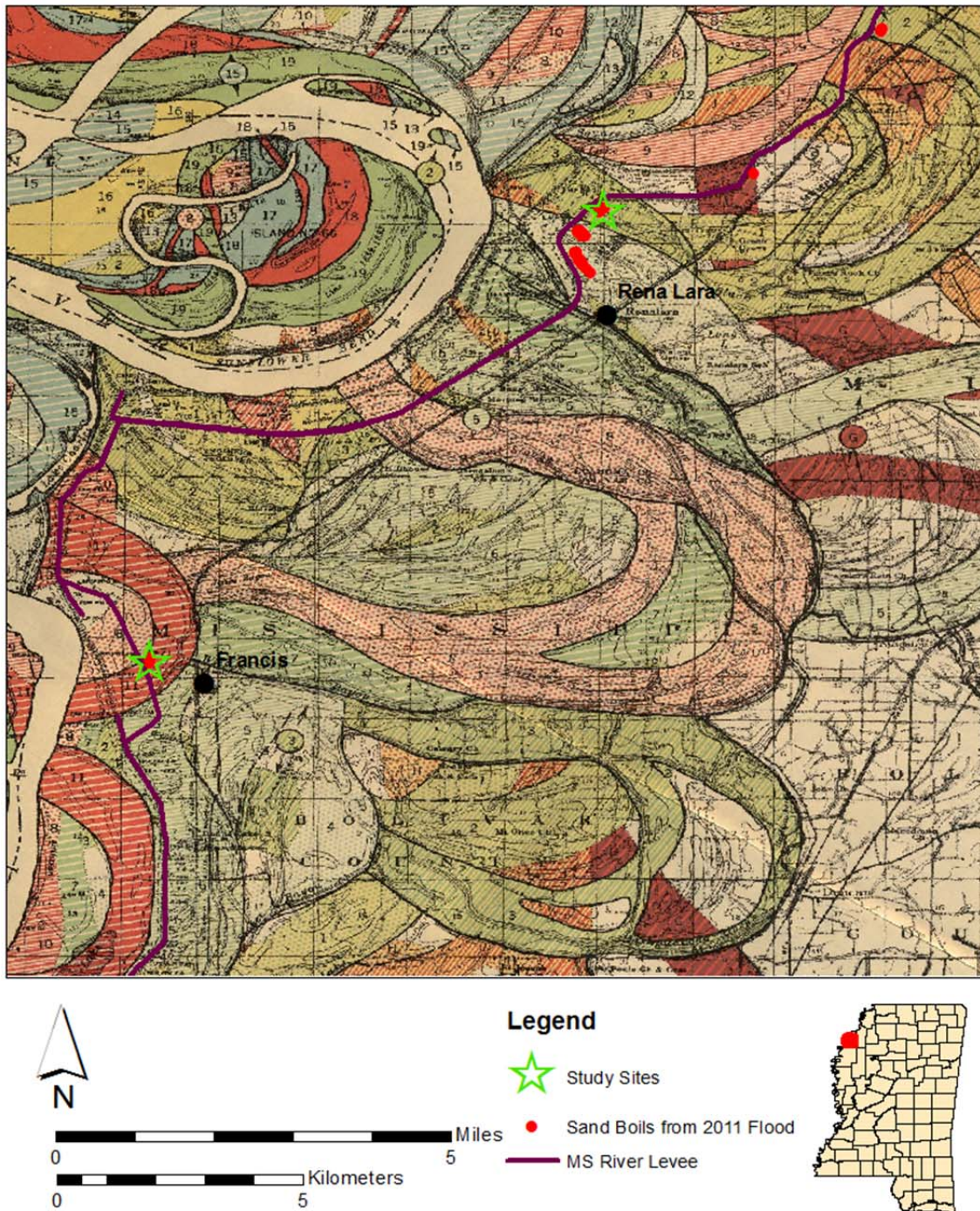


Figure 5.2 Map of surface geomorphic features at study area. Features were delineated by Fisk (1944) using aerial imagery.



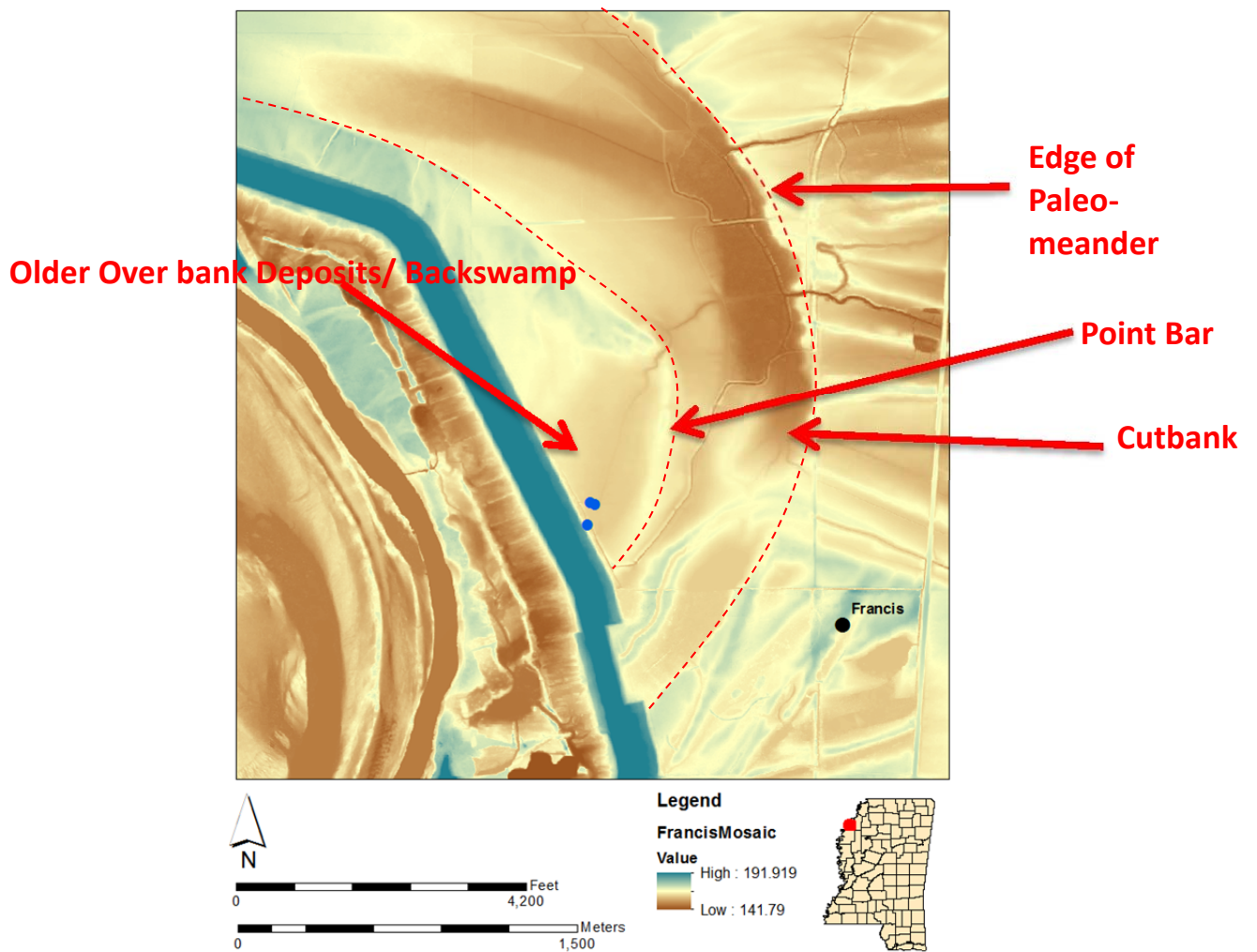
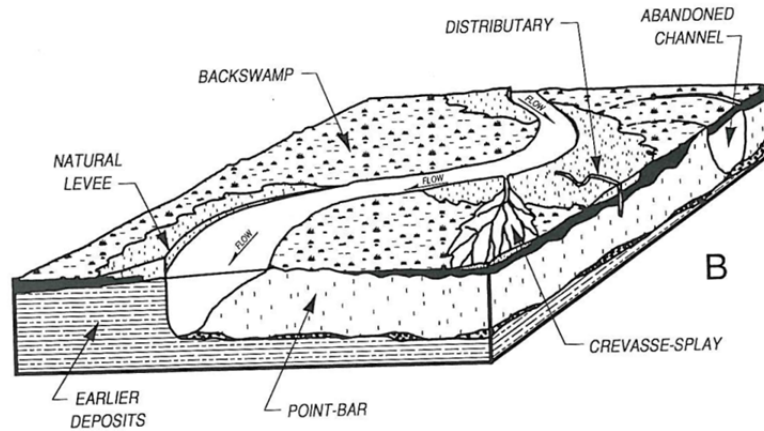


Figure 5.3 Drawing adapted from Saucier (1994) showing components of the fluvial system. Comparison shows these components are analogous to the ones seen at Francis.

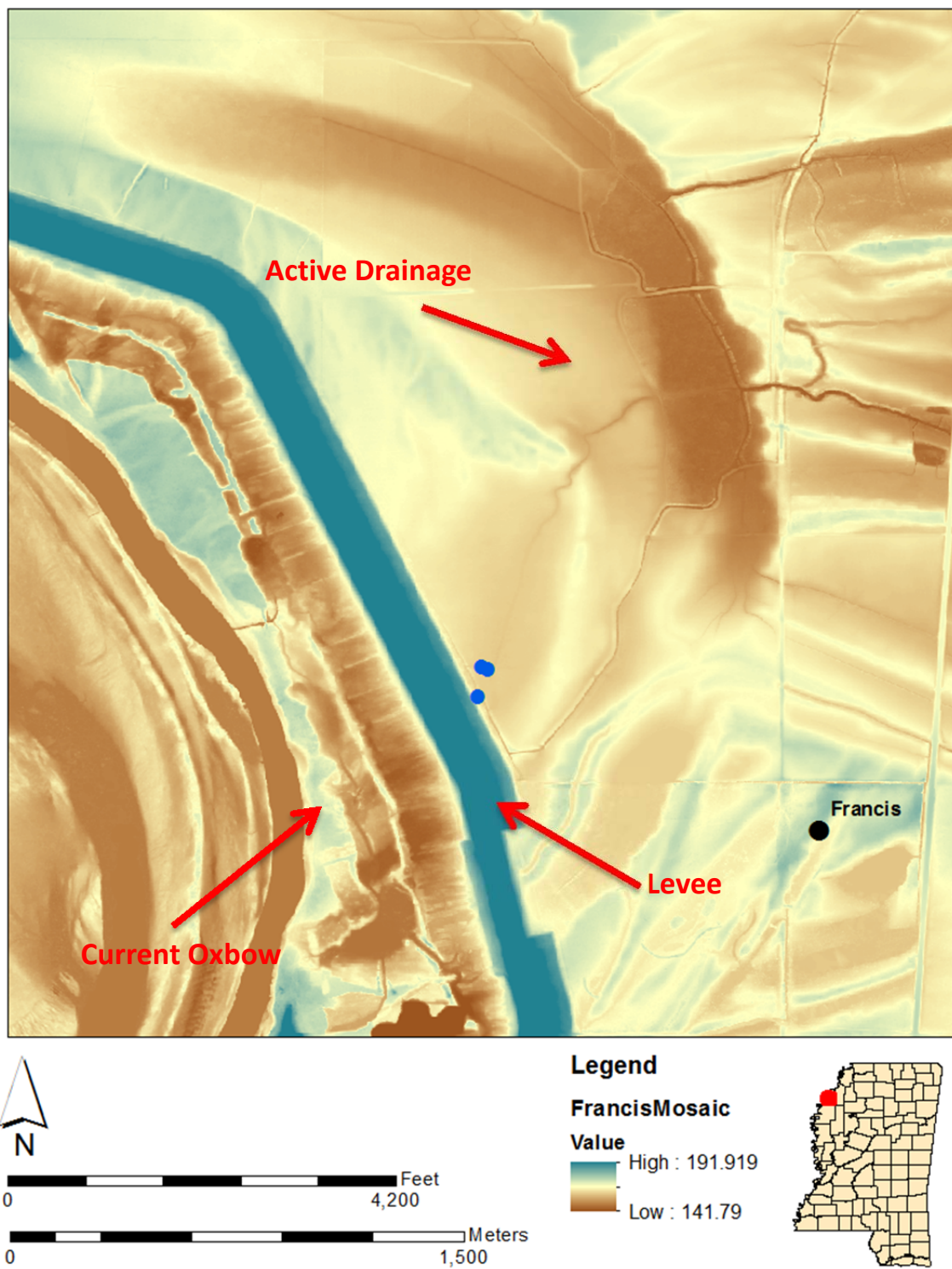


Figure 5.4 LIDAR image at Francis showing the orientation of a small drainage trending beneath the levee. The sand boils surfaced within this drainage in 2011.

## Francis Cross-Sections

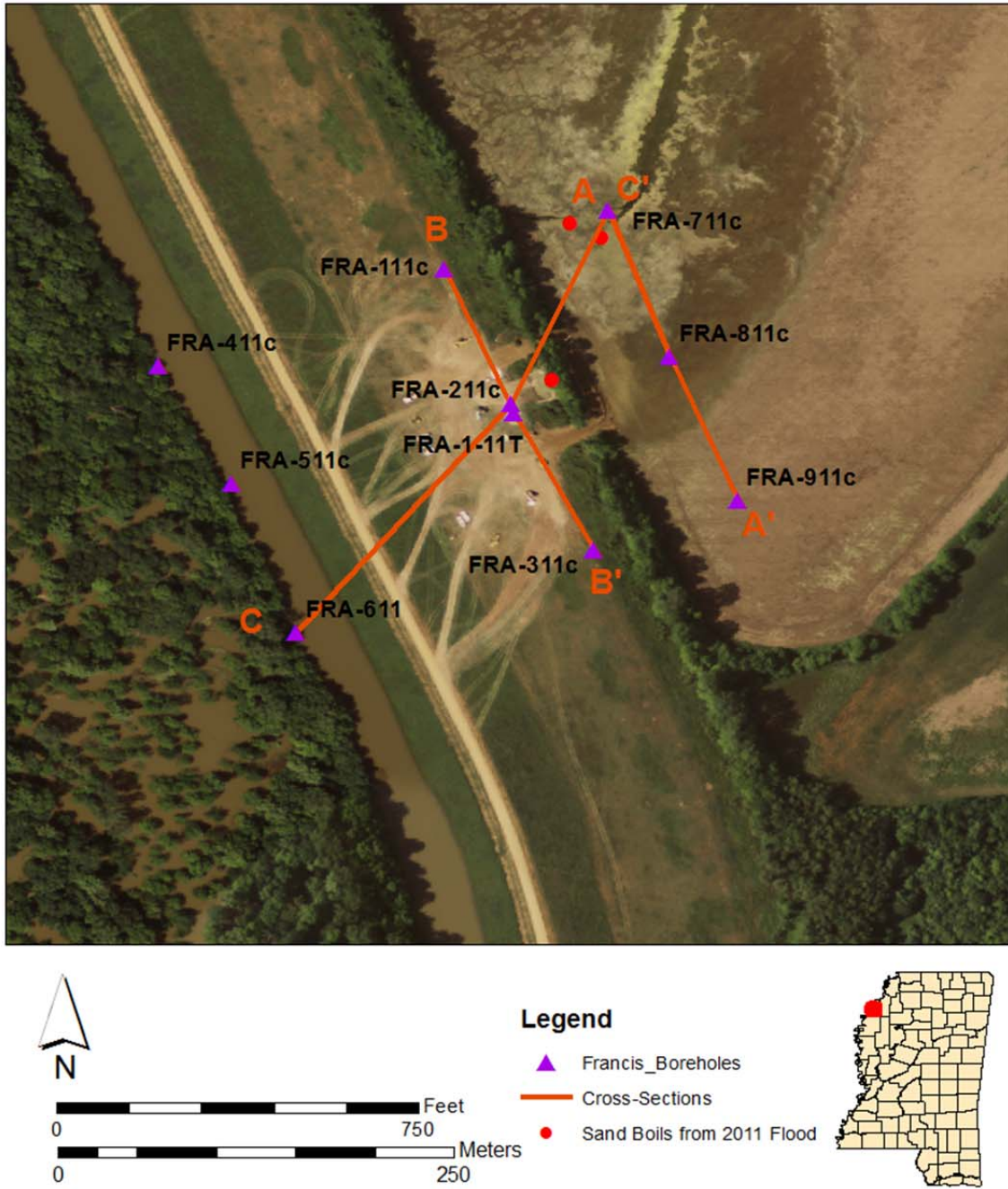


Figure 5.5 Locations of cross-sections created from Francis borehole data.



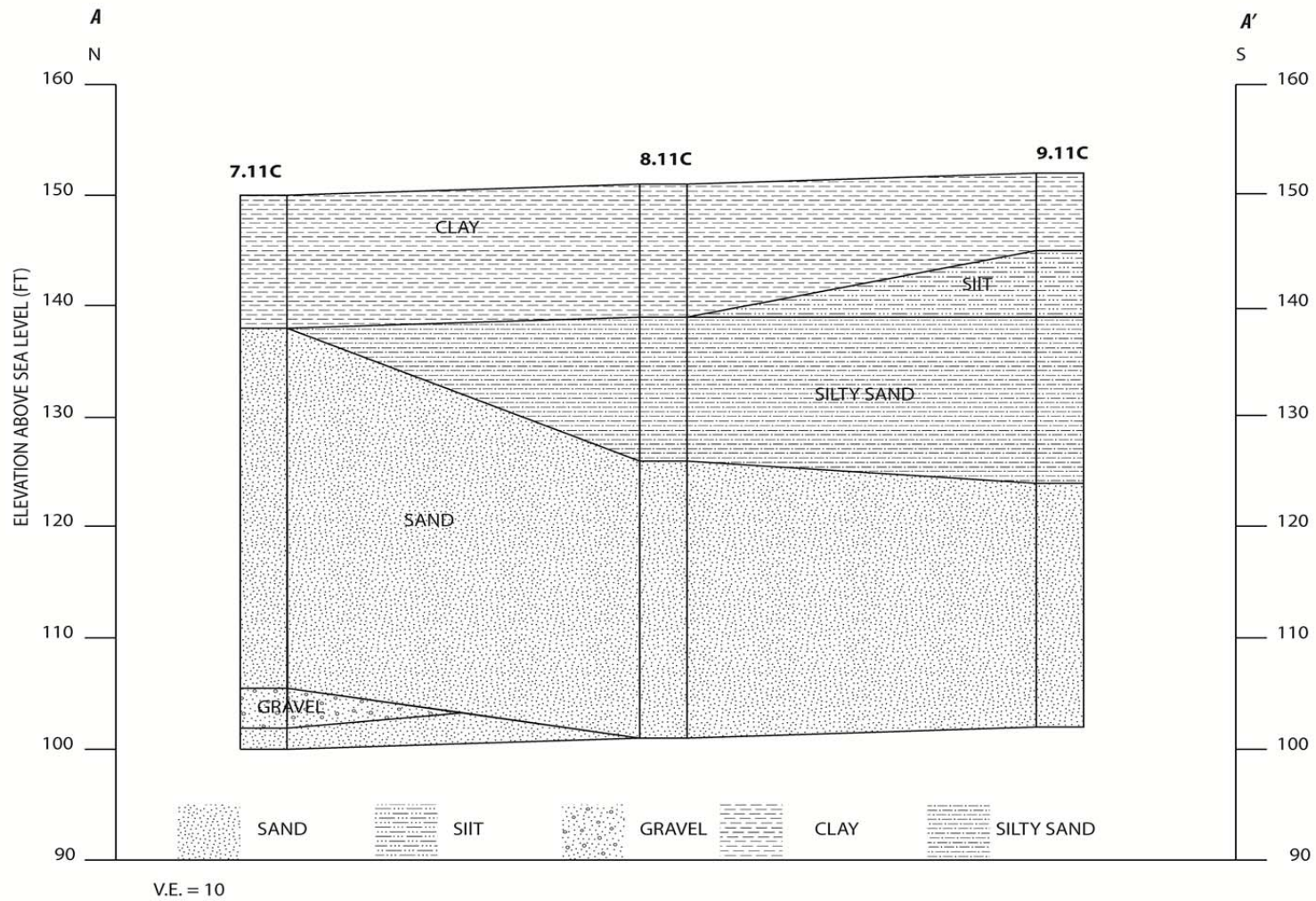


Figure 5.6 Cross section A-A' shows a pinching-out of the silt and silty sand to the north of the site, yielding a direct sand to clay contact

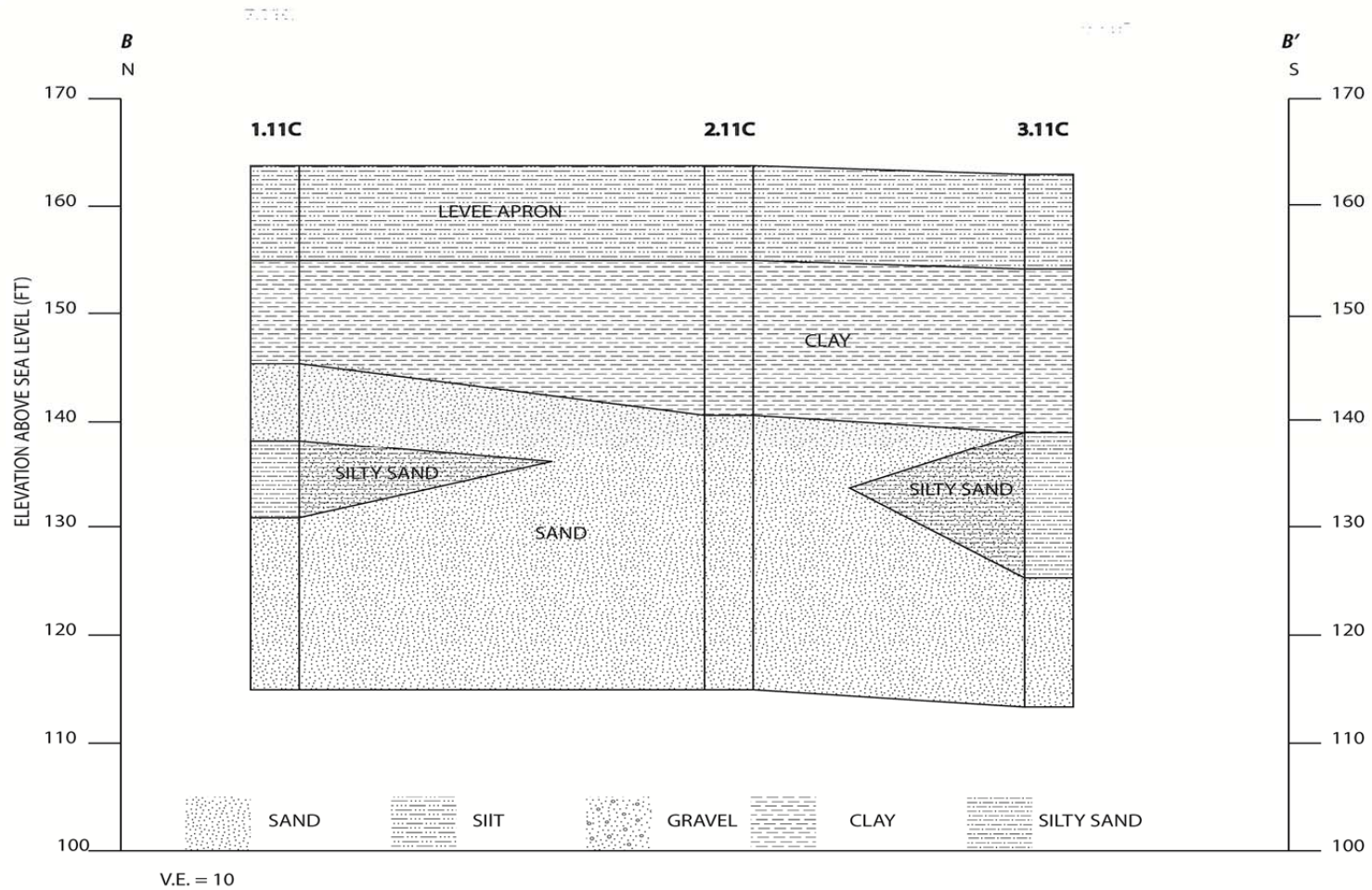


Figure 5.7 Cross-section B-B' shows a pinching out of the silty-sand towards borehole 2.11c.

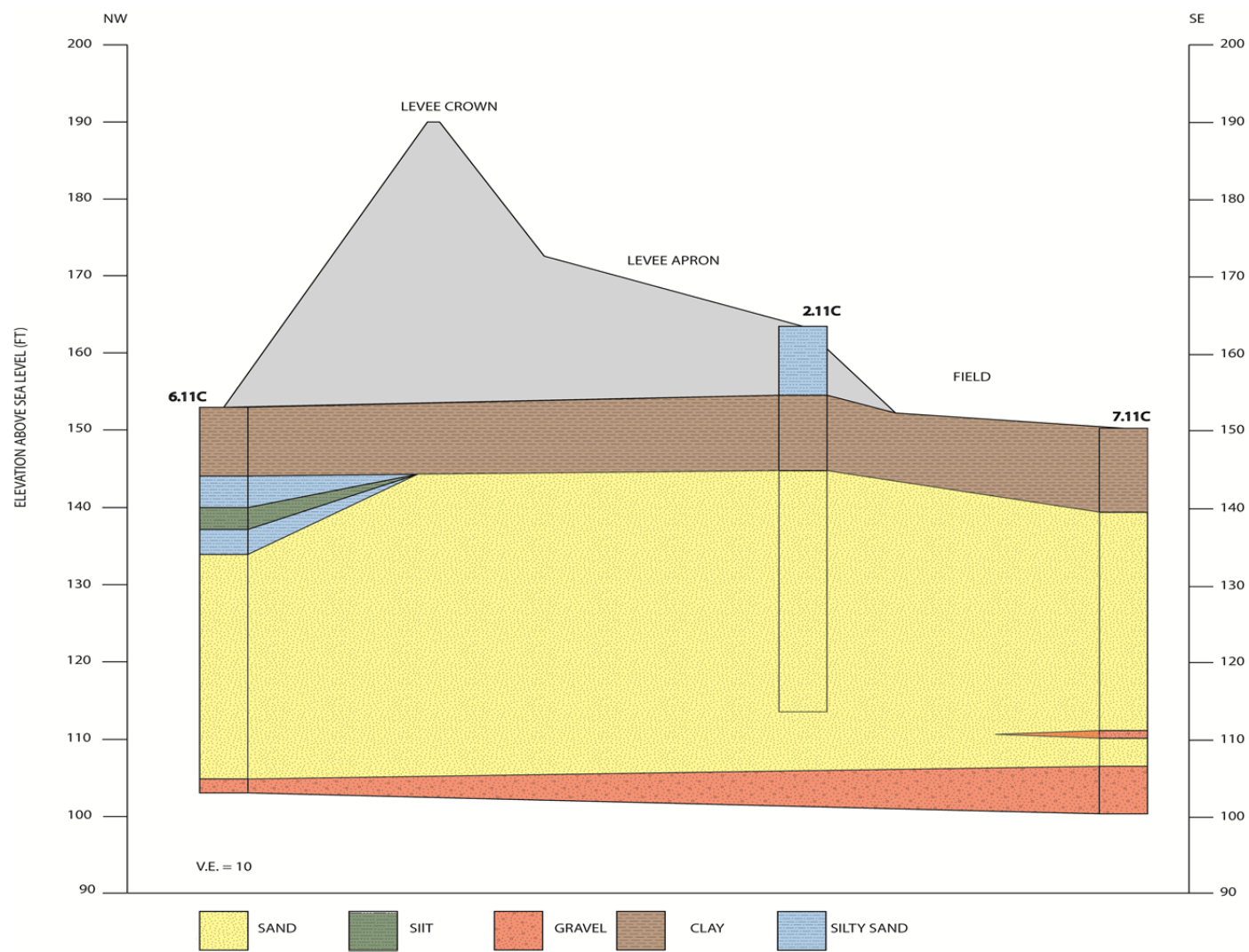


Figure 5.8 Cross-section C-C' shows the sand to clay contact does not intersect borehole 6.11c on the river-side of the levee.



### 5.2.2 Rena Lara Geology and Geomorphology

The DEM data for the area shows multiple abandoned meander features converging at the Rena Lara site. The geology at the site may be dominated by one or all of the three meander features shown in Figure 5.9. The distance from each of the features, however, makes this assumption difficult. Fisk (1944) suggests that the site lies on several, meander features, with segments of each superimposing the other. Because these interpretations were made using large-scale imagery, it is difficult to determine exactly which part of the meander feature(s) is most significantly influencing the geomorphology. Some smaller scale drainage features were located using the LIDAR topographic data. The topography data on the land side of the levee (Figure 5.10) indicates the presence of ridge and swale deposits. An active drainage similar to the one at the Francis site can also be seen in the LIDAR imagery. The drainage appears to flow away from the levee to the east and appears to be influenced by the swales created by a previous meander. The drainage feature can be seen on the LIDAR data on both sides of the levee, suggesting that the levee was built on top of the feature. Figure 5.10 also shows that the seepage scarp and sand boils are adjacent to the drainage.

Borehole data and LIDAR elevation data were used to create surface and subsurface profiles of the site (Figure 5.11). These data show that the levee at the Rena Lara site is composed predominately of clay. It is difficult, however, to distinguish between the base of the levee and the top stratum clays because the similar nature of the clays. Cross-section X-X' shows a thick clay plug in the center of the profile (Figure 5.12). The sands and silty sand beneath the clay undulates through the section, supporting the assumption that the levee was built over and existing ridge and swale deposit. Cross-section Y-Y' shows that both the clay plug and the undulating sand and sandy silt continue beneath the levee (Figure 5.13). Wells 9-LG-83 and 10-

RG-83 are located along the surface drainage feature described above and are also where the clay plug is thickest. This plug indicates that the drainage was once much deeper (20-30 ft. /6-10 m) and is now filled with clay. Cross-section Z-Z' is a profile of the levee from the river-side to the land-side (Figure 5.14). The section shows how the clay plug thickens towards the land-side of the levee and the elevation of the seepage on the levee apron.

## Geomorphologic Features at Rena Lara

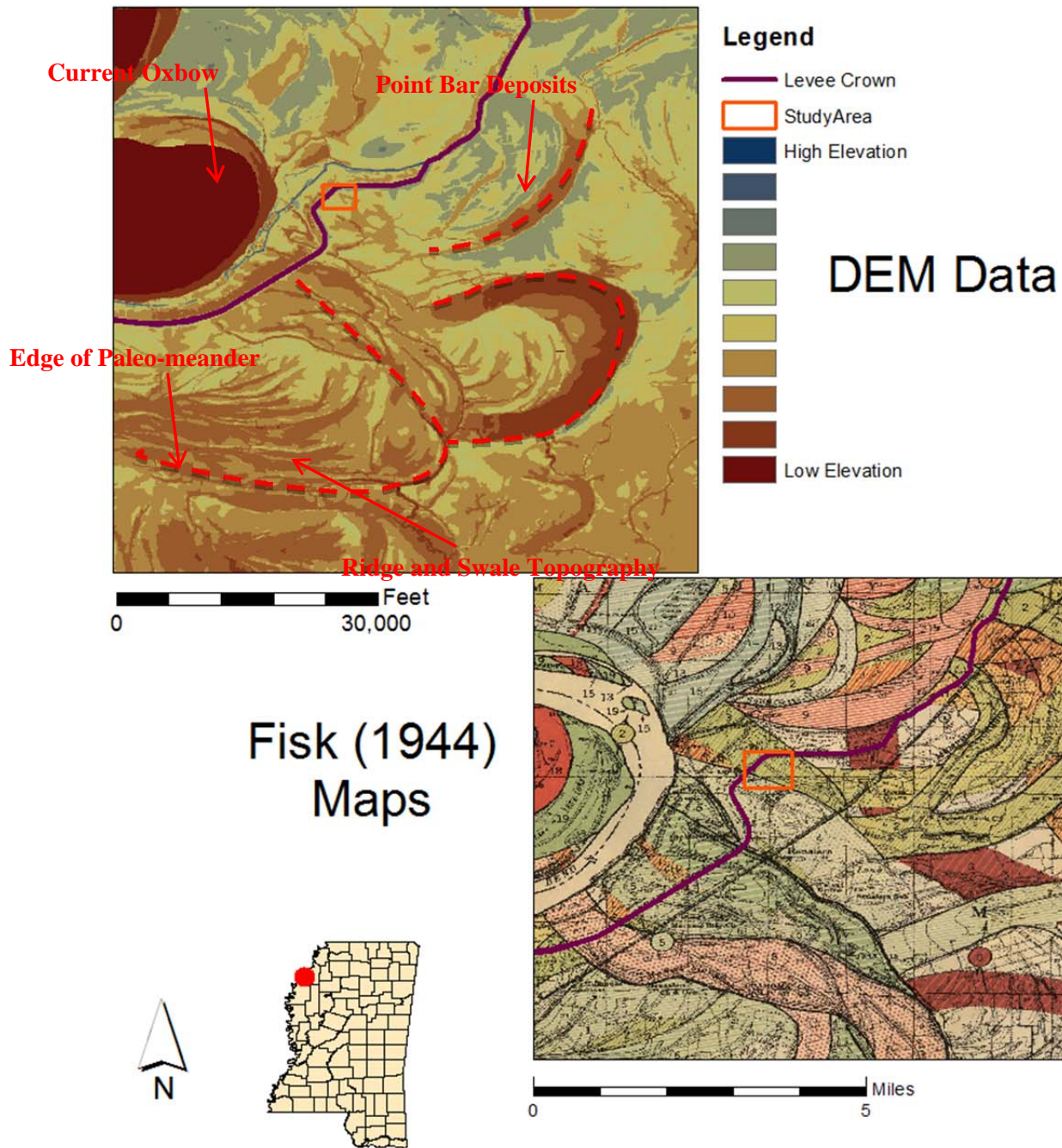


Figure 5.9 Both DEM (above) and Fisk (1944) maps show multiple meander loops trending towards the study area. The apparent meander complexes are shown and their features are shown on the DEM map

## Geomorphologic Features at Rena Lara

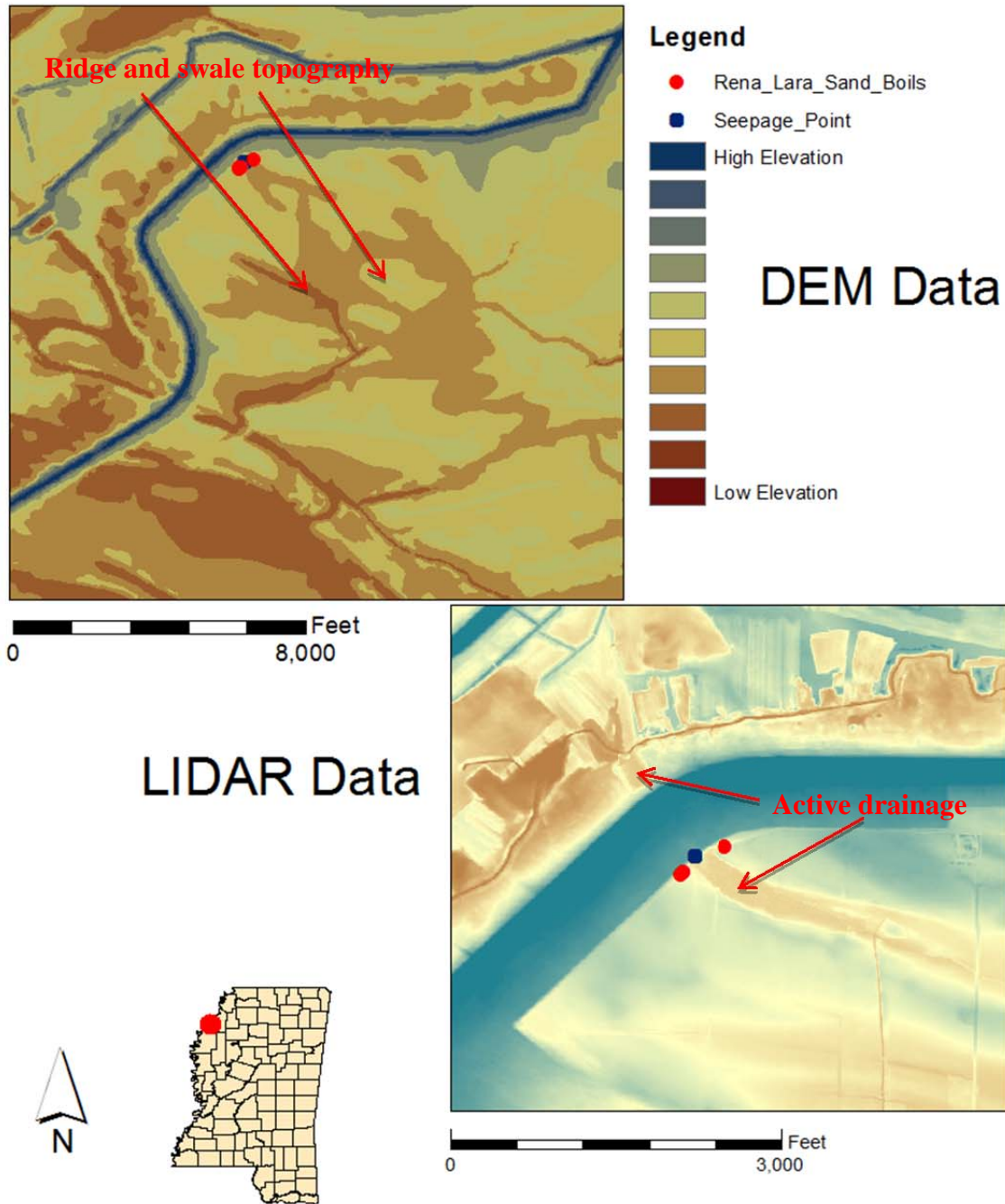


Figure 5.10 Smaller scale features seen in the elevation data (above) reflect ridge and swale topography near the site. The LIDAR indicates that the active drainage may follow one of these swales.



## Rena Lara Cros Sections

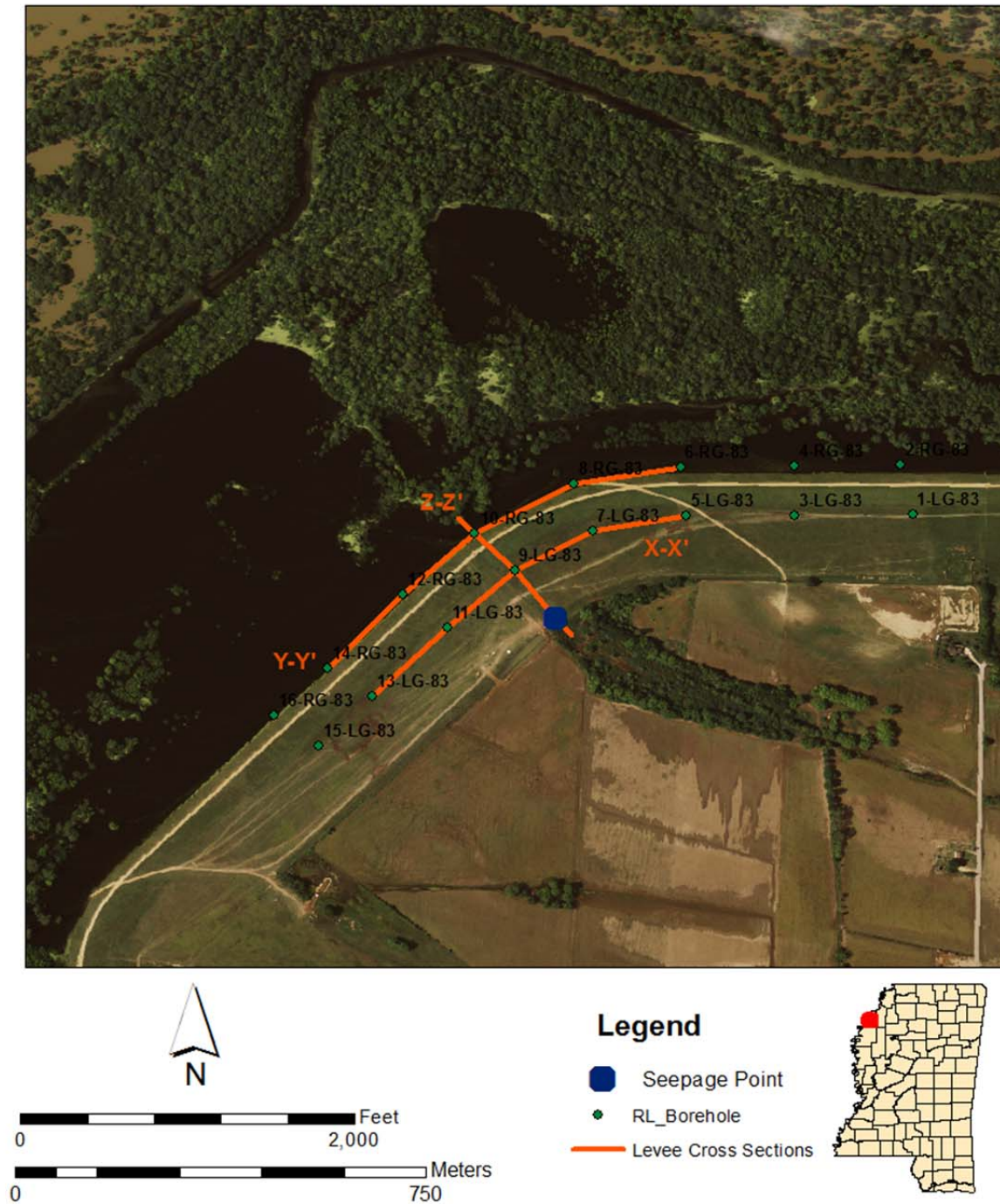


Figure 5.11 Index to cross-sections created from Rena Lara borehole data.

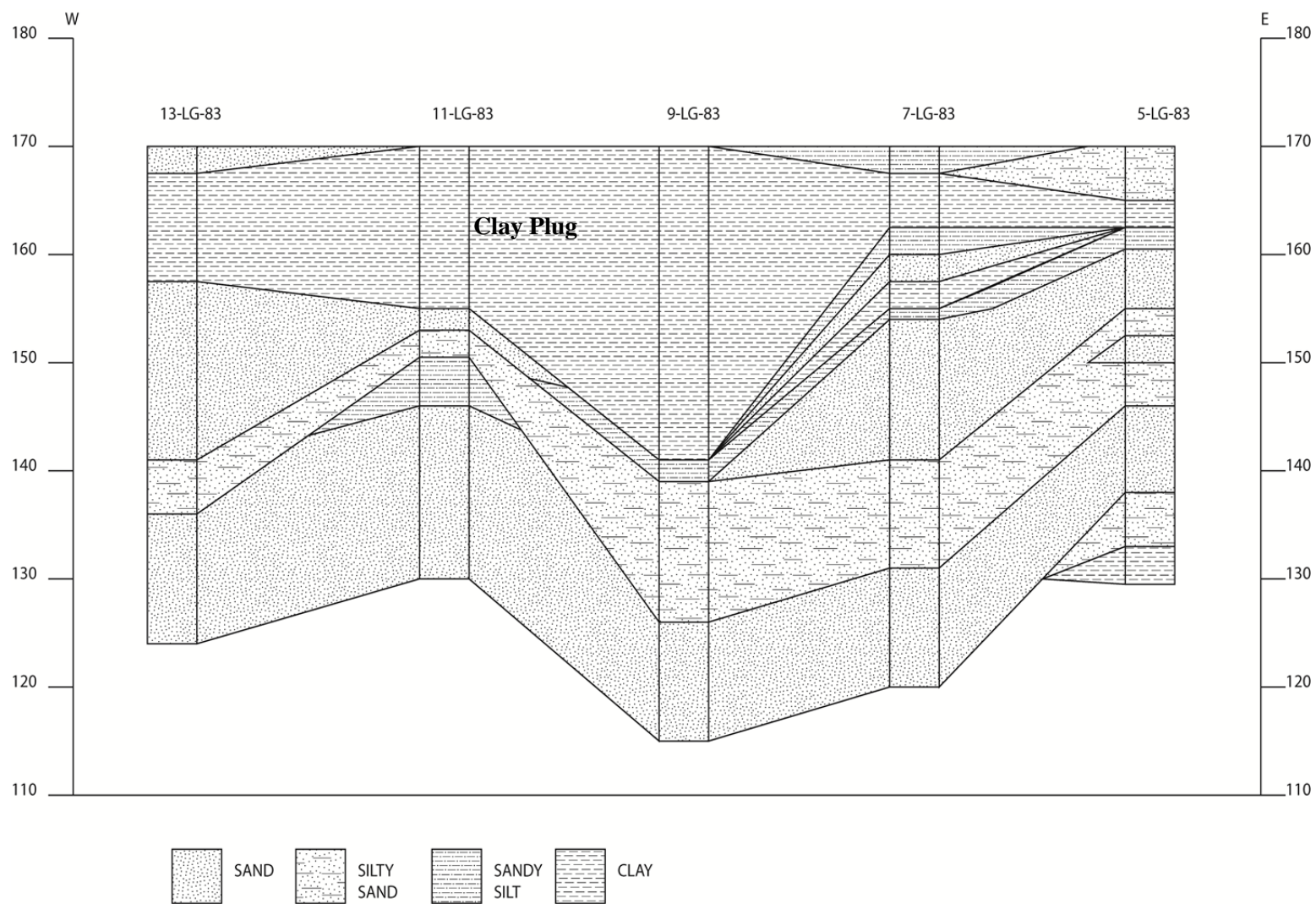


Figure 5.12 Cross-section X-X' shows a clay plug and undulating silt and sand units beneath the levee. This is indicative of ridge and swale deposits and is reflected in the elevation data.

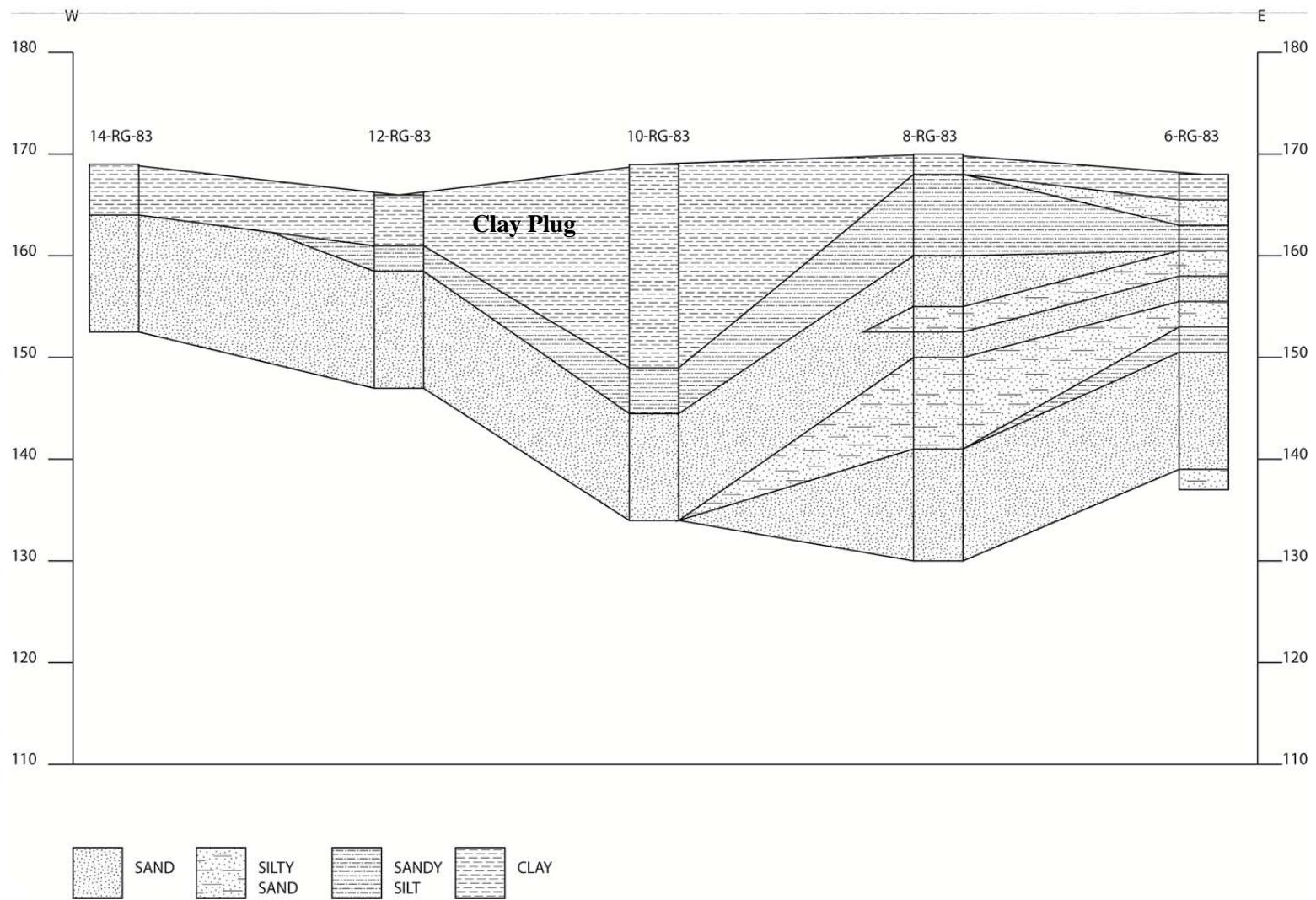


Figure 5.13 Cross-section Y-Y' shows the clay plug continuing to the river-side of the levee.



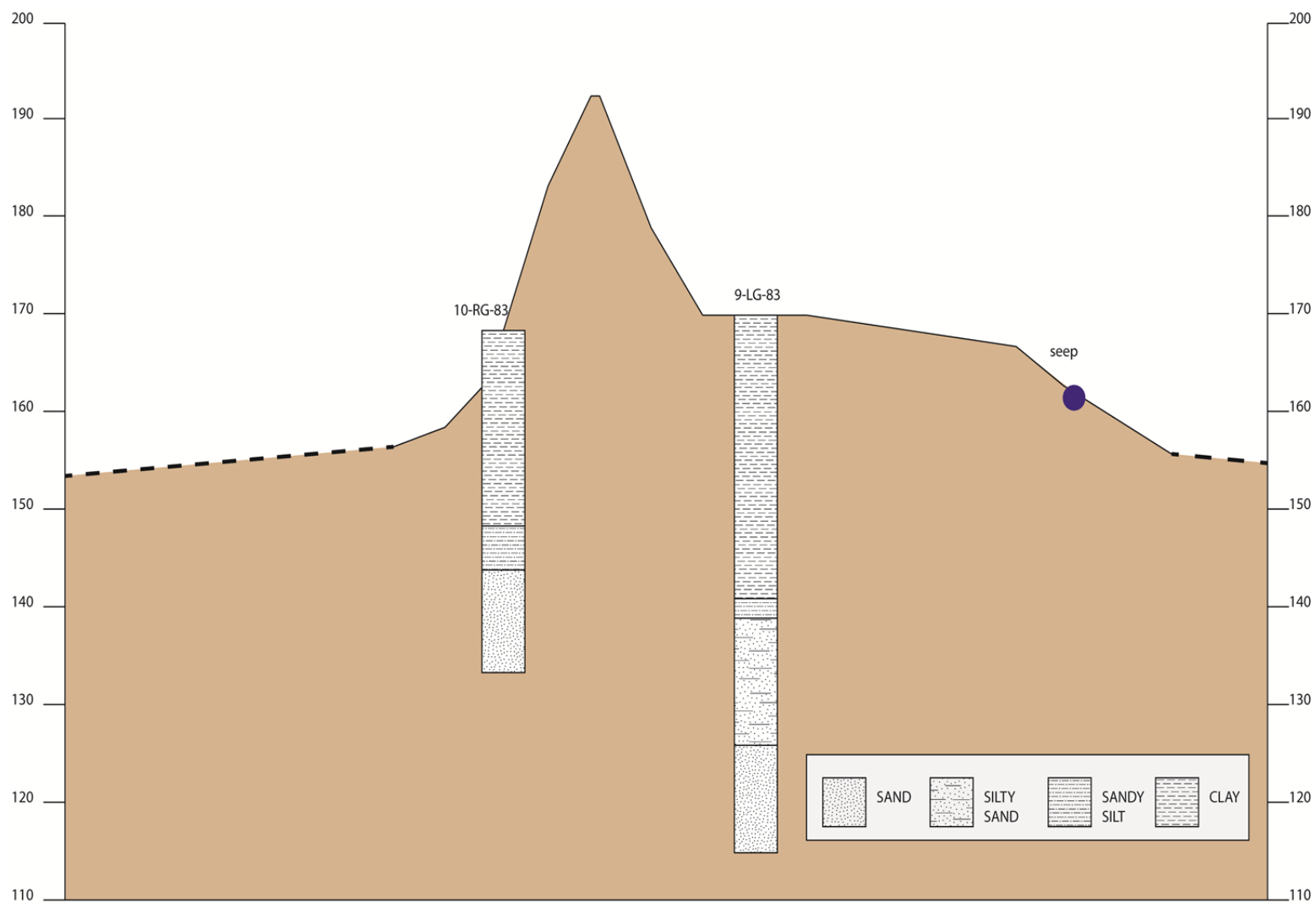


Figure 5.14 Cross-section Z-Z' shows an elevation profile across the levee along with information from boreholes 10-RG-83 and 9-LG-83. The section shows how the clay body thickens towards the land side of the levee as well as the elevation of the seepage scarp.



## **CHAPTER 6**

### **Geophysical Methods**

This investigation used two geophysical methods, electromagnetic induction and electrical resistivity, for defining subsurface features. These two methods were based on parameters including the geometry of geomorphologic features, soil properties and levee dimensions.

#### **6.1 Electromagnetic Induction (EM)**

The first and primary geophysical method used during this thesis was electromagnetic (EM) induction. Recent studies conducted by Dunbar et al. (2007) and Llopis et al. (2007) have proven this method is successful in delineating shallow geologic features. Electromagnetic induction detects the apparent electrical conductivity of subsurface materials, which is influenced by pore water fluid, presence of conductive materials and the amount of void space. (Llopis et al., 2007). Electromagnetic surveys were conducted using a Geonics EM<sub>34</sub>. The instrument consists of a transmitter and receiver coil separated by a known distance. Current passing through the transmitter coil generates a magnetic field. As lines of force from the magnetic field penetrate the ground, an eddy current is induced through conductive material in the subsurface. This eddy current in turn produces a secondary magnetic field. The receiver is configured to measure the differences between the primary field induced by the transmitter coil, and the

secondary field induced by the eddy current (USACE, 1995). A generalized model of this process is pictured in Figure 6.1. Differences between the primary and secondary currents are used to measure the apparent conductivity in millisiemens per meter (mS/m) to identify anomalous areas in the subsurface (Llopis et al., 2007).

The EM<sub>34</sub> system allows for varying investigation depths by changing the orientation and separation of the two coils. The greater the separation distance of the coils (10, 20 or 40m), the greater the depth of investigation. Positioning the two coils upright creates a horizontal dipole mode (Figure 6.2a). In horizontal dipole, the system is more sensitive to near-surface materials. In vertical dipole mode, the coils are laid flat on the ground surface (Figure 6.2b) and the depth of investigation is deeper with less influence from the near-surface (Llopis et. al, 2007). For a multilayered system, however, the shallower, more conductive layer tends to contribute more to the secondary magnetic field (McNeill, 1980). Because of this phenomenon, the depth of investigation, especially in horizontal dipole mode, is greatly influenced by the relative conductivity in the near surface. In total, there are 6 possible modes for EM<sub>34</sub> operation, two for each spacing. Table 6.1 shows the approximate depth of investigation for each mode. For this study, the 10 meter vertical and horizontal dipole modes were used because most of the anomalies were believed to be within the first 50 feet of the surface. At each measurement station, the two dipoles were recorded along with a GPS coordinate.

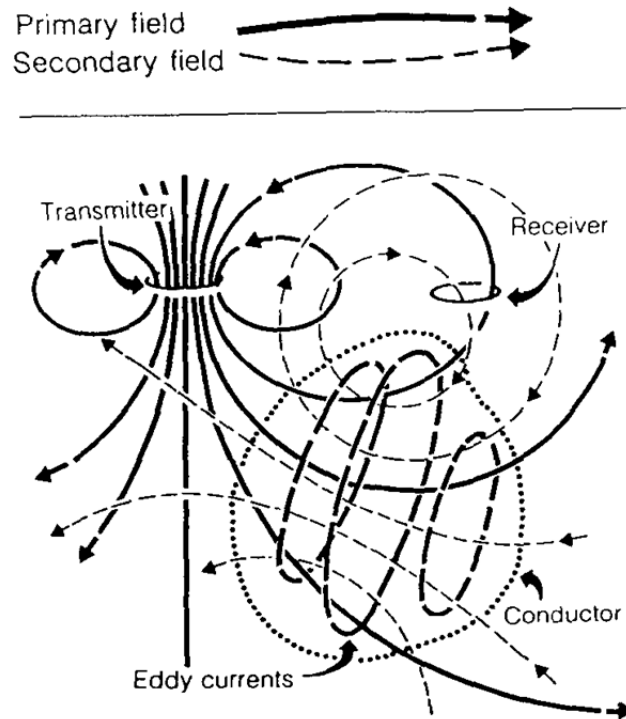


Figure 6.1 Diagram showing the generation of magnetic fields from electromagnetic induction. Adapted from USACE (1995)

**Table 6.1 Exploration Depth vs. Coil Spacing**

	Exploration Depth (meters)	Exploration Depth (meters)
Intercoil Spacing (meters)	Horizontal Dipoles	Vertical Dipoles
10	7.5	15
20	15	30
40	30	60

Table 6.1 Estimated exploration depths of EM<sub>34</sub> with varying coil spacing. Adapted from McNeill (1980).

a)



b)



Figure 6.2 Pictures showing horizontal dipole (a) and vertical dipole (b) modes for the EM 34 (Llopis et. al, 2007)

## **6.2 Electrical Resistivity (ERT)**

Electrical Resistivity Tomography (ERT) surveys can be utilized at selected locations to construct resistivity profiles of the subsurface (Sorensen and Chowdhury, 2010). Because resistivity is the inverse of the conductivity, ERT surveys can be used to supplement results from EM data. The electrical resistivity of the stratum is measured by applying an electrical direct current (DC) between two implanted electrodes and measuring the difference of potential between two additional electrodes (USACE, 1995). Resistivity is recorded in units of ohm-meters. In most cases, the set of electrodes are implanted along a survey line. The actual order or configuration of the electrode array is dependent on the type of investigation, geometry of the stratum, expected resistivity and depth of investigation. The Dipole-Dipole array was used in this study to focus on lateral changes in resistivity (USACE, 1995). The array consists of the two current electrodes (I) followed by the two measuring electrodes (V) (Figure 6.3). The spacing between the two sets of electrodes is dependent on the depth of investigation, with greater spacing targeting greater depths (USACE, 1995). Like the EM system, the conductivity at the near surface will also have an influence on the investigation depth.

The ERT device used in this study was a Stinger R8. The system consists of two 12-volt batteries and four series strings (14 electrodes per string). The spacing between the two pairs of electrodes was systematically changed by altering which electrodes generated the current and which measured the current, beginning with the center and working outwards. Each time a resistivity profile was measured, 28 of the 56 electrodes were moved to the end of the line in what is called a “roll-along”. This process was repeated until the end of the survey line was reached. The GPS coordinate for the beginning and ending of the survey line, as well as each roll-along was recorded.

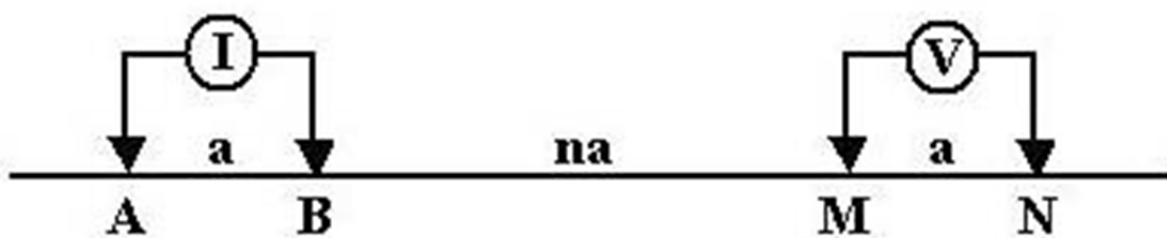


Figure 6.3 Diagram of the orientation of the measuring and current electrodes in the dipole-dipole array (Dunbar et. al, 2007).

## **CHAPTER 7**

### **Geophysical Surveying and Processing**

#### **7.1 Survey Plan and Implementation**

The main purpose of geophysical surveys at each site was to locate and characterize potential seepage pathways in the subsurface near the levee. The design of the geophysical surveys was based on information about the depth, dimensions and orientation of these potential pathways inferred from preliminary investigations of the sites. At both sites, the sand boils surfaced in or near surface drainages. Since the drainages appear to influence seepage pathways, it was determined that the surveys must, at a maximum, span the width of the drainages. The ERT and EM surveys were designed to begin at some distance away from the sand boils/drainage and cross the drainage perpendicularly. The goal was to intersect the seepage pathway and give background readings to compare with any anomalous results. Seepage tends to occur at the base of the top stratum through sand-filled geomorphologic deposits (USACE, 1956). Thus, it was important to determine the thickness of the top stratum at both sites. Borehole data at both the Francis and Rena Lara sites showed that the top stratum was approximately 30 ft. (10m) thick. The maximum exploration depth, therefore, was set at 50 feet (15 m) to allow for variation in feature thickness. Once the target dimensions for the surveys had been set, other factors had to be taken into consideration such as topography and vegetation that

would inhibit the layout. Table 7.1 indicates the dates surveying was conducted and when each survey was completed.

**Table 7.1 Timeline for Geophysical Surveying**

Date	Francis Surveying	Rena Lara Surveying
April 9-10, 2012	EM Grid 3, ERT Line 2 and 3	
May 17-18, 2012	EM Grid 1 and 2, ERT Line 2.2	
May 25 – June 1, 2012		All EM and ERT Lines

Table 7.1 Timeline of geophysical surveying at Francis and Rena Lara sites.

### **7.1.1 Francis Survey**

Figure 7.1 shows the distribution of EM 34 collection points. At each station, a GPS coordinate was recorded halfway between the receiver and transmitter coil to insure that the measurement was recorded at the station location. The size, station spacing and geometry of each grid would influence the time required to conduct the survey, as well as the resolution of the data. The grids also included several borehole points in order to correlated geophysical results with geologic data. Grid 1, located in the land-side of the levee, was designed to incorporate a large portion of the drainage that trends towards the levee. The station spacing within the grid was set to 20 m (65 ft.), in order to detect gradual changes in soil moisture, grain size and allow any subsurface structure to be detected with the vertical dipole. Grid 2 focused on the sand boil area. Station spacing was set to 10 meters to detect the seepage pathway between the sets of



boils. The collection points from grid 1 overlapped grid 2 to ensure that there were numerous data points around the sand boils. Lastly, grid 3, located on the levee apron, was designed to monitor the continuity of any feature or seepage pathway trending from the land-side and perpendicular to the levee. The stations were spaced 20 m apart in grid 3.

Three ERT lines collected at Francis are shown in Figure 7.2. Each line runs from south to north and was designed to intersect as many boreholes as possible to provide subsurface geologic control. Electrode spacing during the ERT acquisition was kept at one meter in order to assure higher resolution in the data. Line 2.2 and Line 3 were oriented so that they might intersect the potential seepage pathway both in front of, and behind the sand boils. Line 2 begins further south from the boils to record the resistivity away from the sand boil area.

## EM 34 Survey

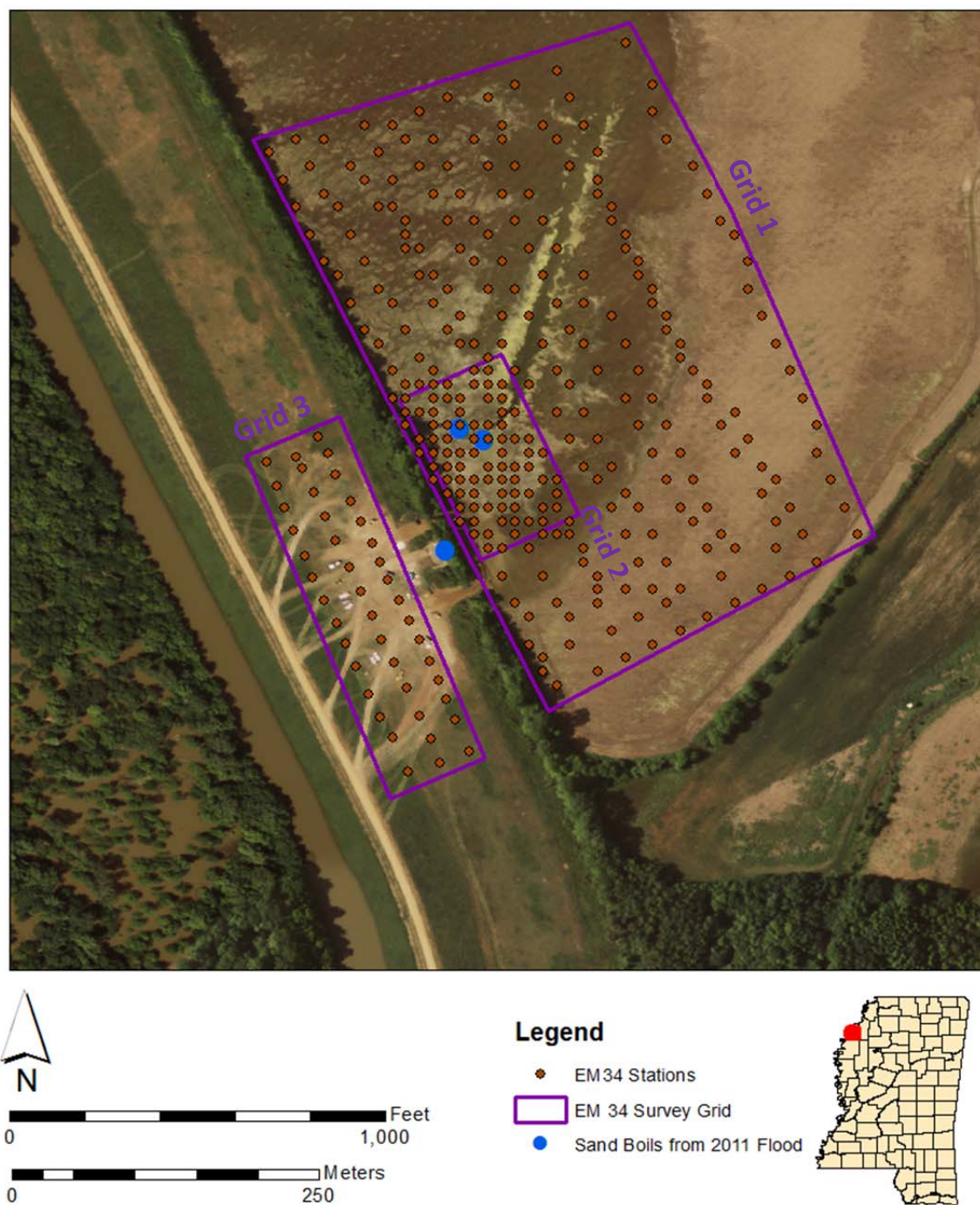


Figure 7.1 Map of EM survey grids at Francis. The large grid in the field and the grid on the levee apron both have 20m station spacing, while the smaller grid near the sand boils has 10m station spacing.

## ERT Lines

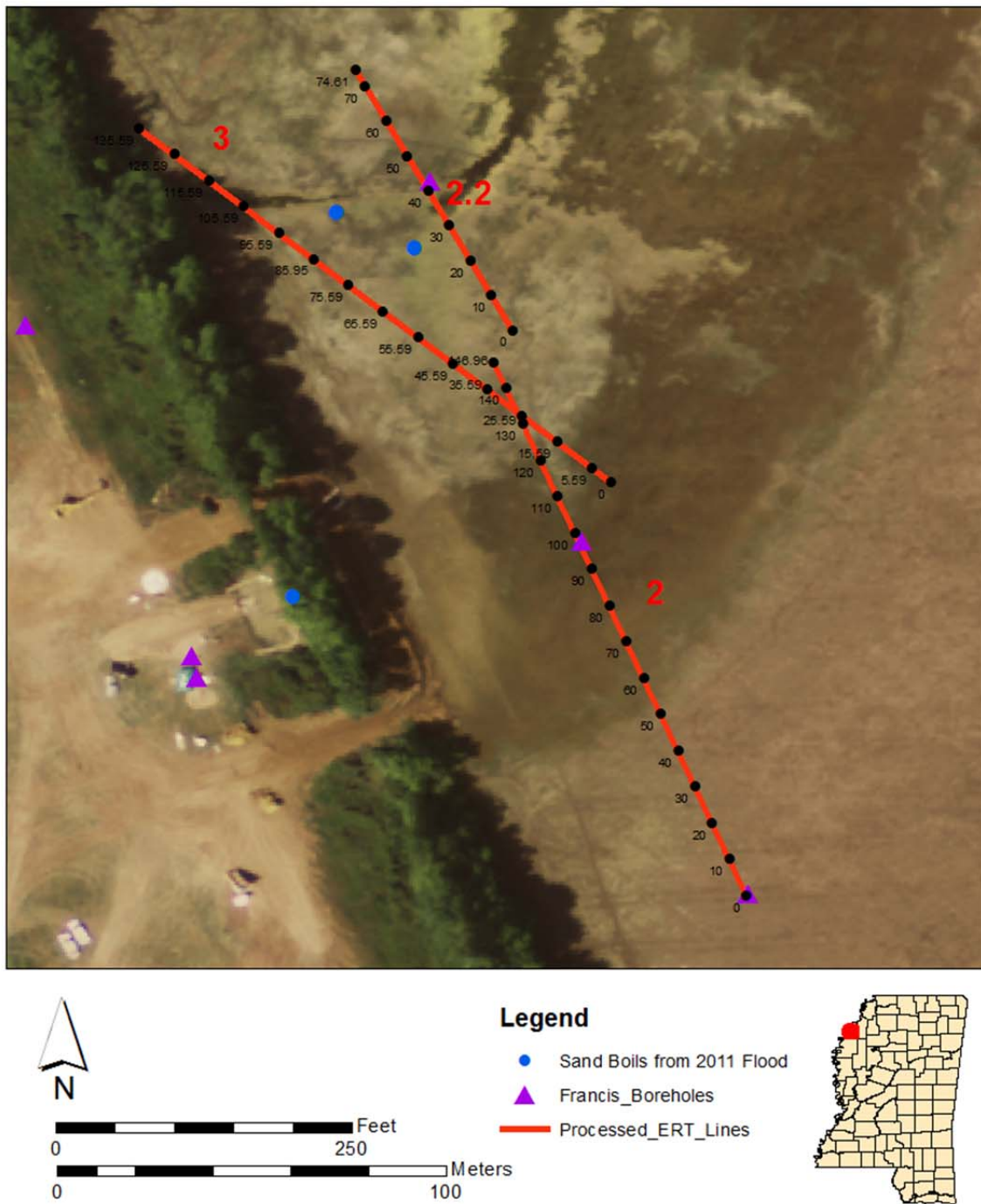


Figure 7.2 Map of ERT surveys at Rena Lara. The survey lines were designed to cross the surface drainage and seepage pathway perpendicularly.

### **7.1.2 Rena Lara Survey**

Due to the thick vegetation in the drainage at Rena Lara, and the location of the sand boils, it was decided that all geophysical surveys would be conducted on the levee apron. Figure 7.3 shows the grid design for the EM 34 at Rena Lara. The length of the survey spanned over 500 m (1640 ft.) of levee apron in order to incorporate the large drainage feature running beneath the levee. Four grids were constructed by dividing the apron into rectangles. A barbed wire fence running across the levee apron divided Grid 1 from the rest of the survey. The widths of the grids were bound by the toe of the levee and the toe of the apron. The EM survey was carried out using the same technique as the Francis EM survey. Stations were spaced 10 m (32 ft.) apart with each station being halfway between each coil during the recording.

The ERT implementation at Rena Lara differed from that at Francis, in that the survey was composed of one continuous line. The survey begins approximately 130 m (430 ft.) south of the sand boils, near the toe of the apron, and extends around the apron until it crosses the drainage feature (Figure 7.4). Because the ERT profile must be a straight line, 10-degree bends were made in the line in order to stay parallel to the slightly-curving levee. Two meter electrode spacing was used in order to investigate beneath the 10 feet (3m) thick levee apron.

### **7.1.3 Survey Limitations**

The three main limitations that emerged during data acquisitions were topography, vegetation and highly resistive near surface materials. Large wooded areas in the study area prevented surveying on the river side of the levee at both sites. The drainage ditch that borders



## Rena Lara EM

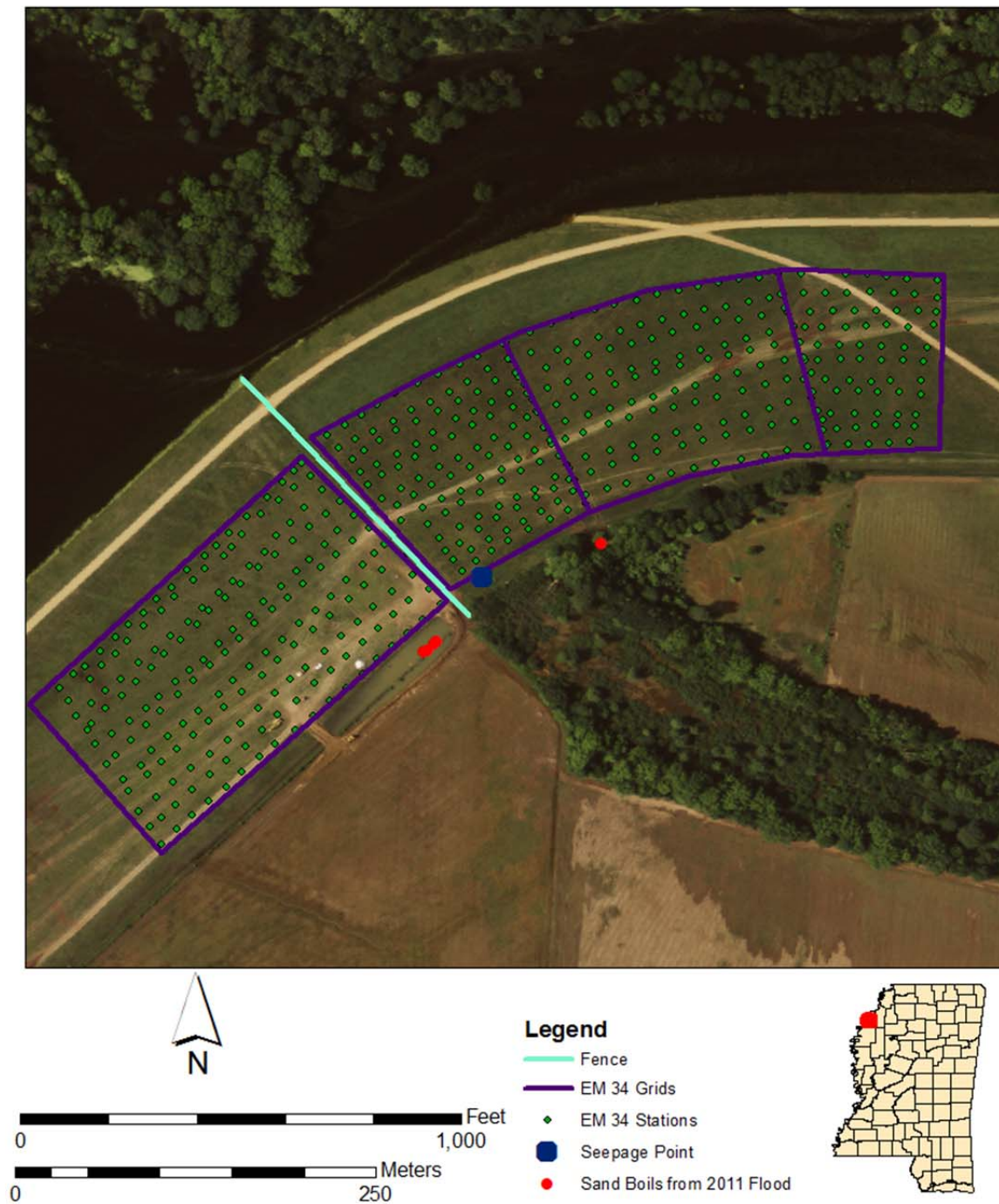


Figure 7.3 Map of EM survey grids at Rena Lara. The station spacing was kept at 10m throughout all grids.

## Rena Lara ERT

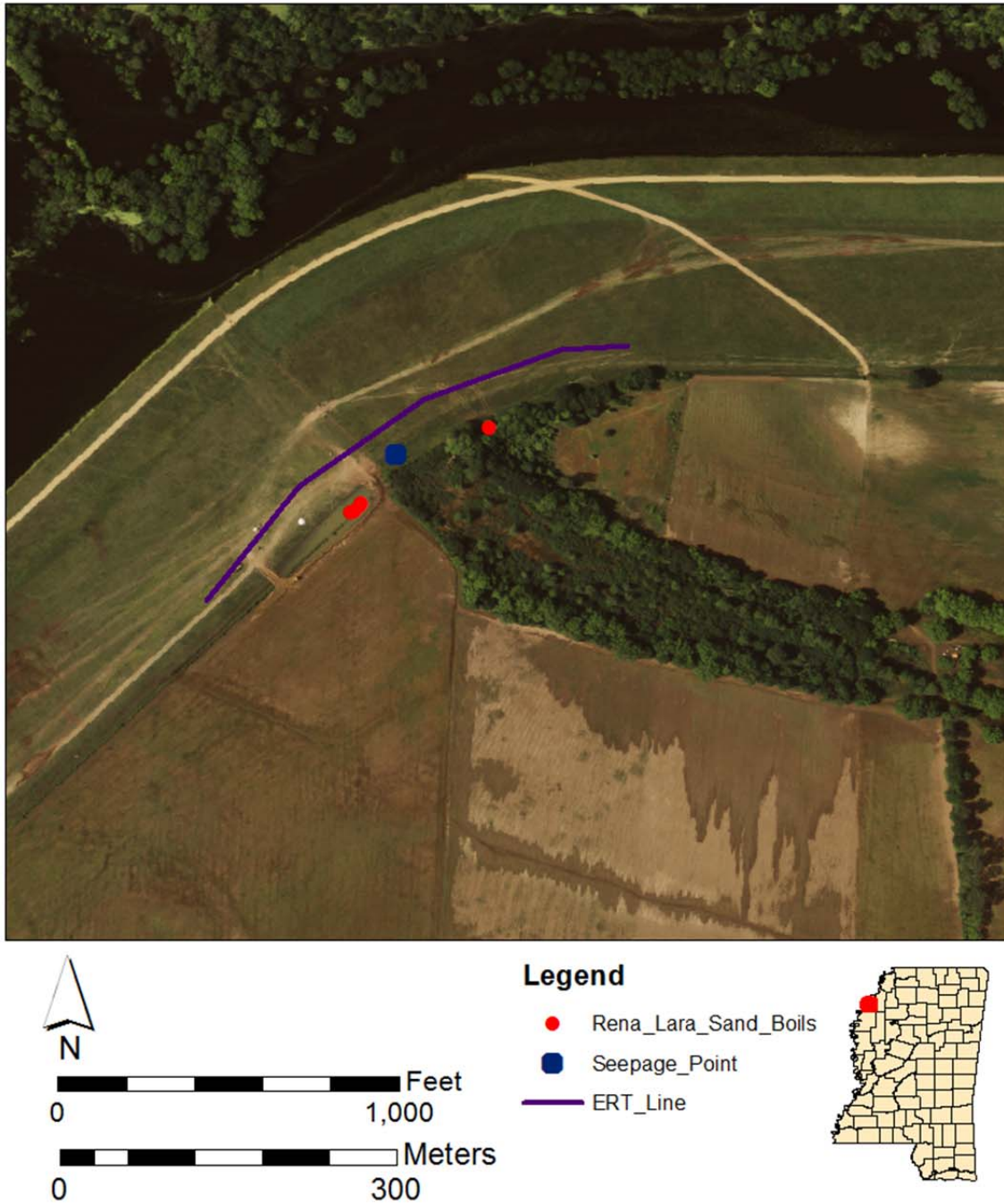


Figure 7.4 Map of ERT survey at Rena Lara. The survey line was designed to cross the seepage pathway perpendicularly.

the levee apron was also steep and heavily vegetated so the equipment could not be used. The survey areas, therefore, were restricted to flat areas with little vegetative cover. Highly resistive materials at the surface were problematic in gathering quality ERT data. Dry, porous material increased the contact resistance between the electrode and the ground surface and greatly inhibited the flow of current into the subsurface. This was noticed at both sites while performing ERT measurements on the levee apron. The apron was composed of well-drained, silty-sand which proved to be highly resistive. In order to address this problem, ERT surveys were conducted after substantial rainfall.

## **7.2 Data Processing**

Geophysical data from both the Francis and Rena Lara sites were processed using identical methods in order to ensure consistency within the results. Expertise from manufacturers of the EM and ERT systems was also used throughout the processing to improve accuracy.

### **7.2.1 Software**

Both the ERT and EM system required different methods of processing and manipulating data after collection. The EM processing required a manual input of the vertical and horizontal dipole readings and the station locations into a table format. Once in table format, the data was imported into ArcMap for spatial interpretation. Unlike the EM processing, ERT values were recorded by the Stinger R8 system and formatted before being uploaded. Once uploaded to a computer, Earth Imager is used to calculate the true resistivity of the subsurface through an

inversion process. After the inversions, a resistivity section was created giving a resistivity values for each X and Y location on a grid. The X, Y and resistivity matrix could then be exported as a table and then imported into Surfer to build an interpolated resistivity section. Both the ERT and EM processing are outlined in the flow charts in Figures 7.4 and 7.5.



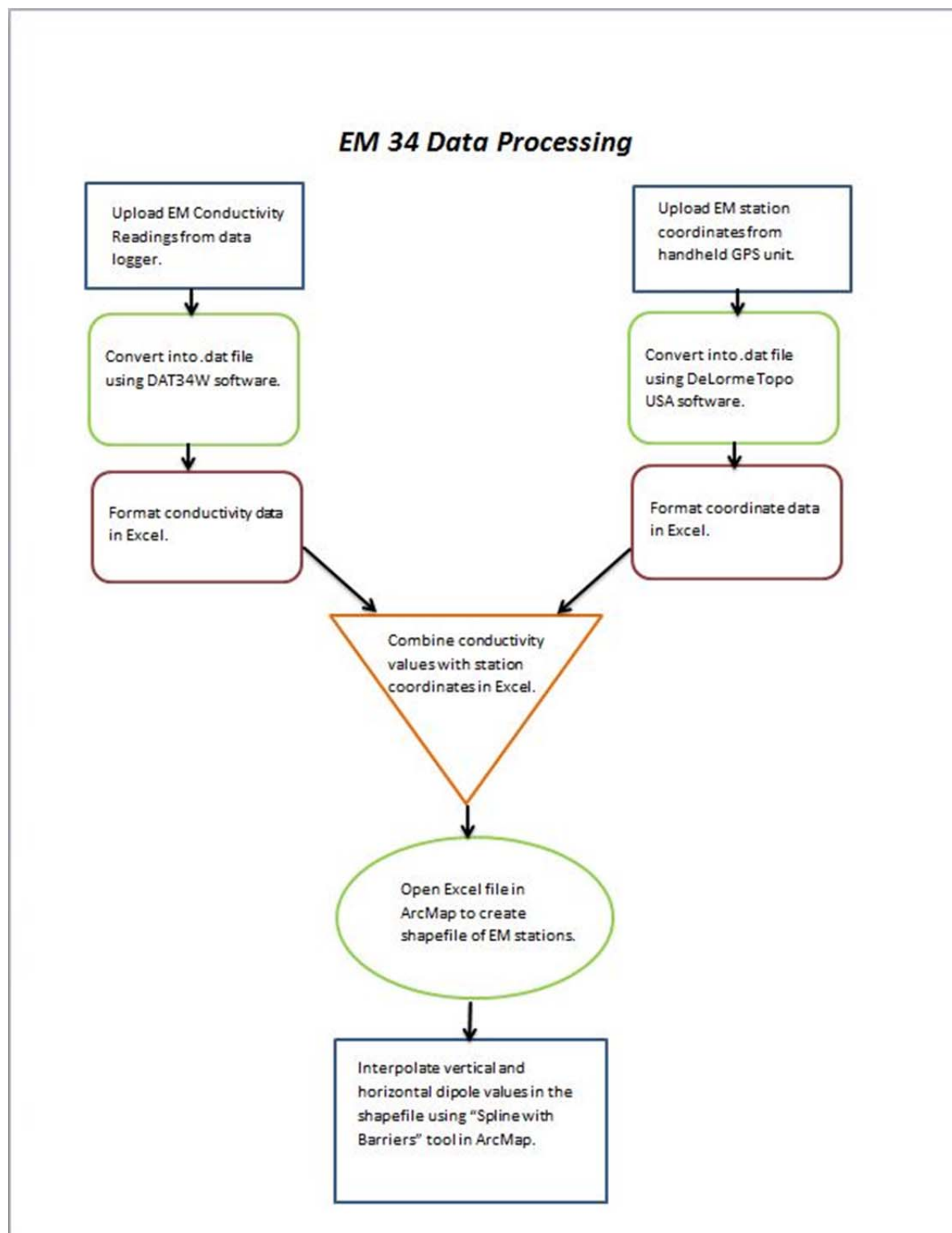


Figure 7.5 Flow chart of EM data processing. The data required manual formatting before it could be manipulated.

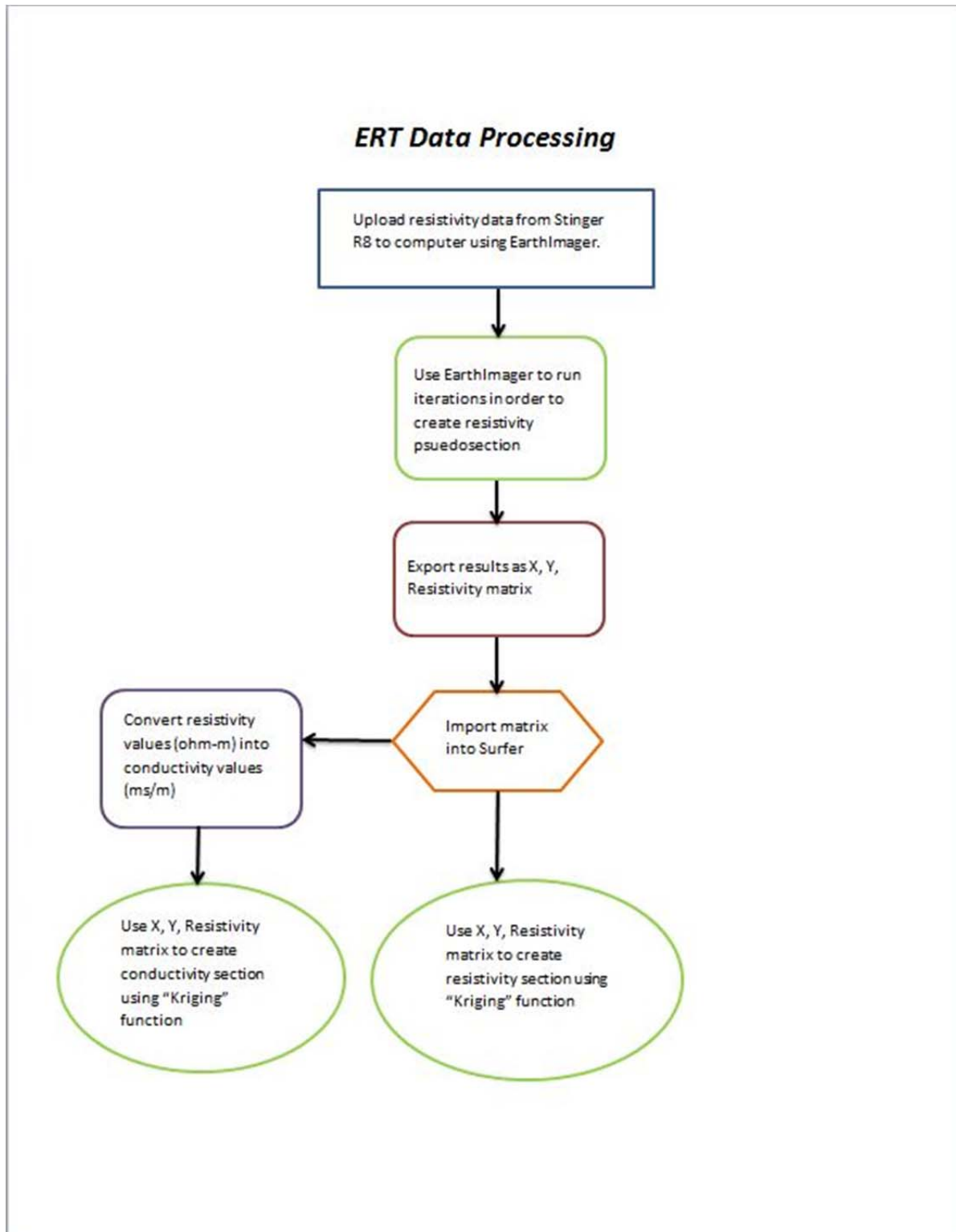


Figure 7.6 Flow chart of ERT data processing. The raw data required less formatting compared to the EM data.

### 7.2.2 Interpolation Methods

In order to construct two dimensional models of EM data, the points were interpolated using a spline function to assign conductivity and resistivity values to the entire profile. Arc Map was used to accomplish this task. A shapefile of the EM point values was interpolated using the “Spline with Barriers Tool”. The spline function creates a smooth interpolated surface that passes through the input data points (ESRI, 2010). The “Spline with Barriers Tool” allowed the spline function to be executed within a defined area in order to prevent the interpolation to extend too far from the data locations. This process created a raster surface that was assigned a color ramp to reflect the trends in conductivity. This was also advantageous because the model could be spatially referenced to objects such as sand boils and boreholes.

The Surfer program was used to generate ERT cross-section profiles. A kriging interpolation technique was used to produce a resistivity model for each ERT line. Kriging was chosen because it gave a more accurate depiction of trends in the ERT data compared to other functions. These trends were consistent with those observed in the borehole and elevation data. The resistivity values were then converted from ohm-m to mS/m and kriged again to produce a conductivity profile. This proved useful in comparing ERT with EM data and gaining more resolution of the near-surface conductivity. The resistivity values from the ERT data were converted to conductivity values by using the following equation:

$$1 \text{ ohm} - m = \frac{1}{1000} \text{ mS/m} \quad <7.1>$$

## **CHAPTER 8**

### **Geophysical Results and Interpretation**

Before proceeding to geophysical interpretation, the relationship between conductivity and local materials was established. Both Francis and Rena Lara sites have a surface layer with an abundance of clayey material, underlain by coarser silts and sands. While surface moisture conditions varied during geophysical surveying, borehole data and preliminary investigations indicated that all sediment beneath the levee material at the sites was partially to fully saturated. The variances in conductivity, therefore, are largely influenced by the properties of the materials, such as grain-size, porosity, permeability, and clay content. In order to test this hypothesis, conductivity results were compared to borehole data in Appendices A and B. Data at both sites reveals that the conductivity readings from EM and ERT data are proportional to the thickness and amount of clay present in the subsurface. Background studies, such as the one conducted by McNeill (1980), confirm that the presence of slightly moistened clay may substantially increase electrical conductivity, due to the ability of clay grains to exchange cations at a large capacity (McNeill, 1980).

#### **8.1 Francis Results**

Using the borehole data and information derived from McNeill (1980) regarding clay content and conductivity, interpretations were made relating conductivity and grain size. It was

determined that the higher the conductivity, the thicker the clay at the survey location. This also allowed inferences to be made between conductivity and permeability, with the higher the conductivity correlating with lower permeability (Shevnin et al., 2006).

### **8.1.1 Francis EM Data**

Figures 8.1 and 8.2 show the plan-view conductivity profiles produced by the EM<sub>34</sub>. The EM<sub>34</sub> horizontal dipole mode reflects the near surface conductivity of the site. Comparing results from the EM and ERT conductivity profiles suggested that the horizontal dipole mode was measuring the response in the first 1-2 meters (3-7 ft.) of the material. The results show that the material on the land-side field of the levee is more conductive than the levee apron itself. This high-conductivity material is due to the 2-3 meter (7-10 ft.) thick clay overburden identified in the borehole data. The conductivity of the material is believed to be highest (70-80 m/m) where the clay is thickest (Figure 8.1). It was also noted that near the two existing sand boils in the field, the conductivity is slightly lower; suggesting that the overburden at the sand boil locations is thin or non-existent. The high conductivity zone tends to follow the small drainage that trends toward the levee.

The EM<sub>34</sub> vertical dipole results show no apparent trend in conductive materials (Figure 8.2). Based on previous knowledge of the EM system, it is suggested that the high conductivity material in the near surface has significant influence on the EM<sub>34</sub> vertical dipole's inability to measure the conductivity at depth (McNeill, 1980). It was difficult, therefore, to determine the approximate depth that the EM 34 vertical dipole was measuring.

### 8.1.2 Francis ERT Data

Figure 8.3 shows the results of the ERT collection at the Francis site. The results indicate that a high conductivity clay overburden is present to a depth of 1-2 meters (3-7 ft.) below the surface, validating results found in the EM and borehole data. Line 2 (Figure 8.4a) shows that the clay is encountered approximately 60 meters (197 ft.) from the starting point of the survey. The conductive feature is present at the same depth in Line 2.2 (Figure 8.4 b). Although the highly conductive feature spans almost the entire length of the survey line, it is discontinuous. Line 3 (Figure 8.4c) shows that the clay is nearly continuous along the survey line.

Another trend seen in the Francis ERT results is the presence of a lower conductivity material present in lines 2.2 and 3 (Figure 8.4). The anomaly is located at a depth of 5-10 meters (16-32 ft.) and has a conductivity range between 0 and 20 mS/m. Figure 8.5 shows the location of the anomaly in plan-view. The lower conductivity feature appears to be co-located with the surface drainage feature. The borehole logs suggest this low conductivity anomaly to be a sand body. This subsurface feature is interpreted to be a channel associated with the present day drainage.



## EM 34 Horizontal Dipole Results

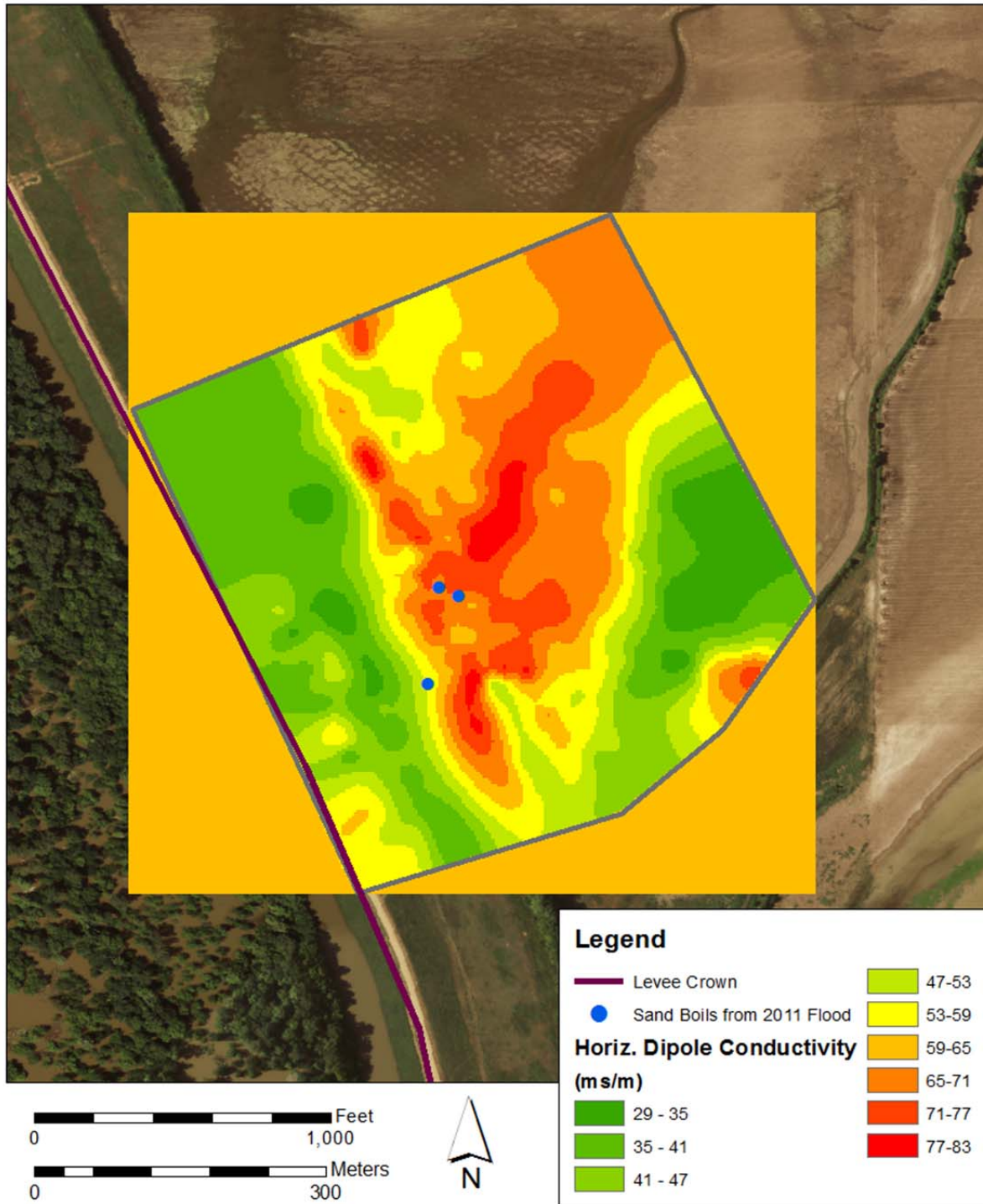


Figure 8.1 Conductivity profile of the EM 34 Horizontal Dipole. The profile shows an area of high conductivity near the surface that is interpreted to be a clay overburden.

## EM 34 Vertical Dipole Results



Figure 8.2 Conductivity profile of the EM 34 Vertical Dipole. The readings were too heavily influenced by the high conductivity material at the surface to read conductivity at depth.



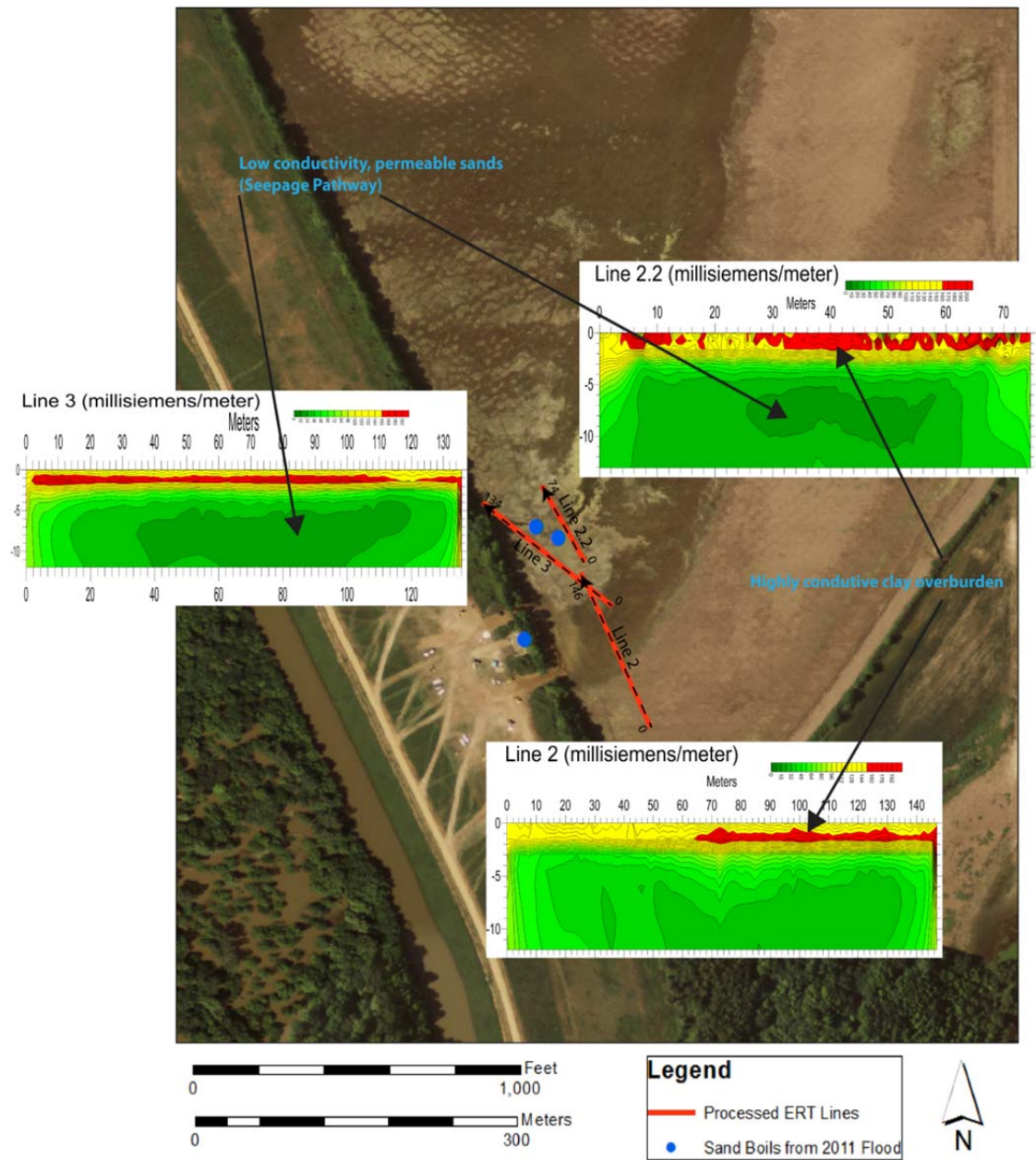


Figure 8.3 ERT Lines at Francis. A highly conductive material is present at the surface of each survey line. There is also a zone of low conductivity in Lines 2.2 and 3.

## Line 2 (millisiemens/meter)

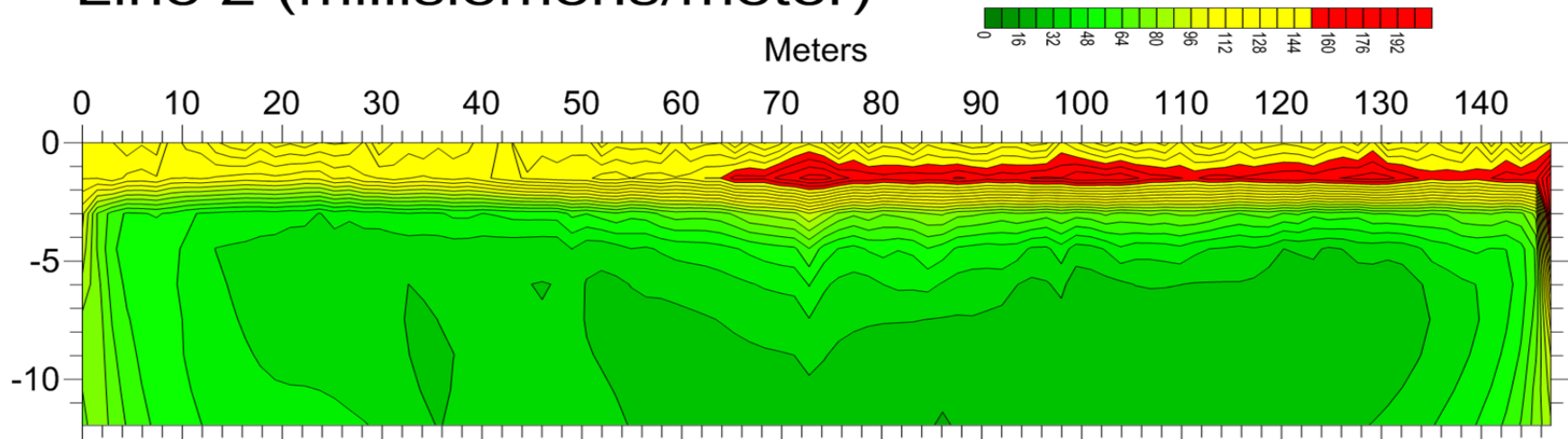


Figure 8.4a Conductivity (ms/m) section of Line 2. A high conductivity zone is encountered at the near surface at around 60m (197 ft.)

## Line 2.2 (millisiemens/meter)

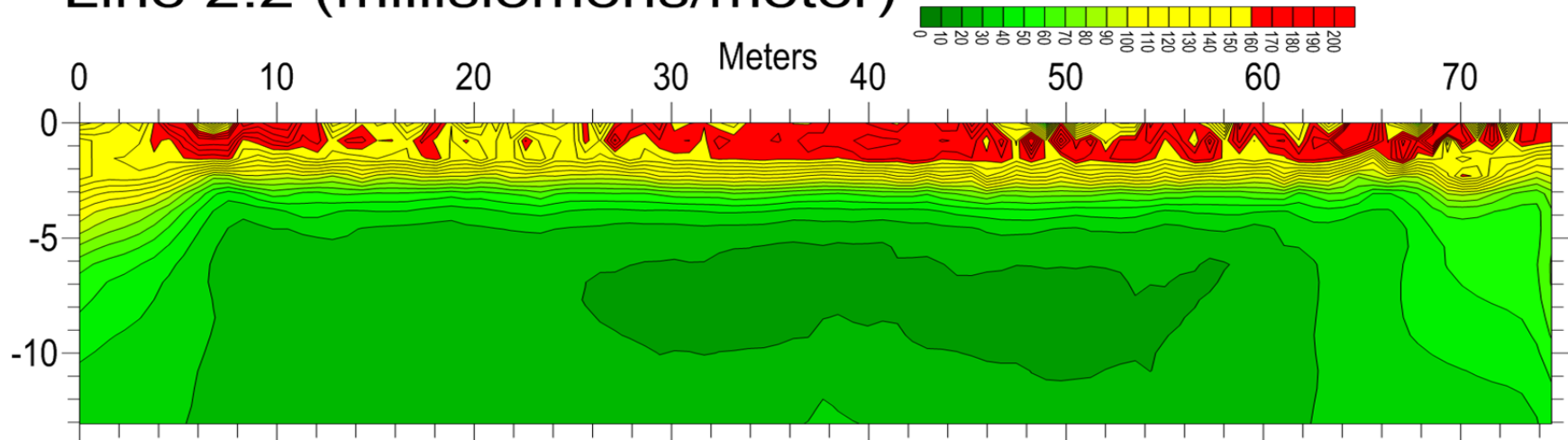


Figure 8.4b Conductivity (ms/m) section of Line 2.2. The high conductivity zone is discontinuous. There is also a low conductivity zone at 5m (16 ft.)

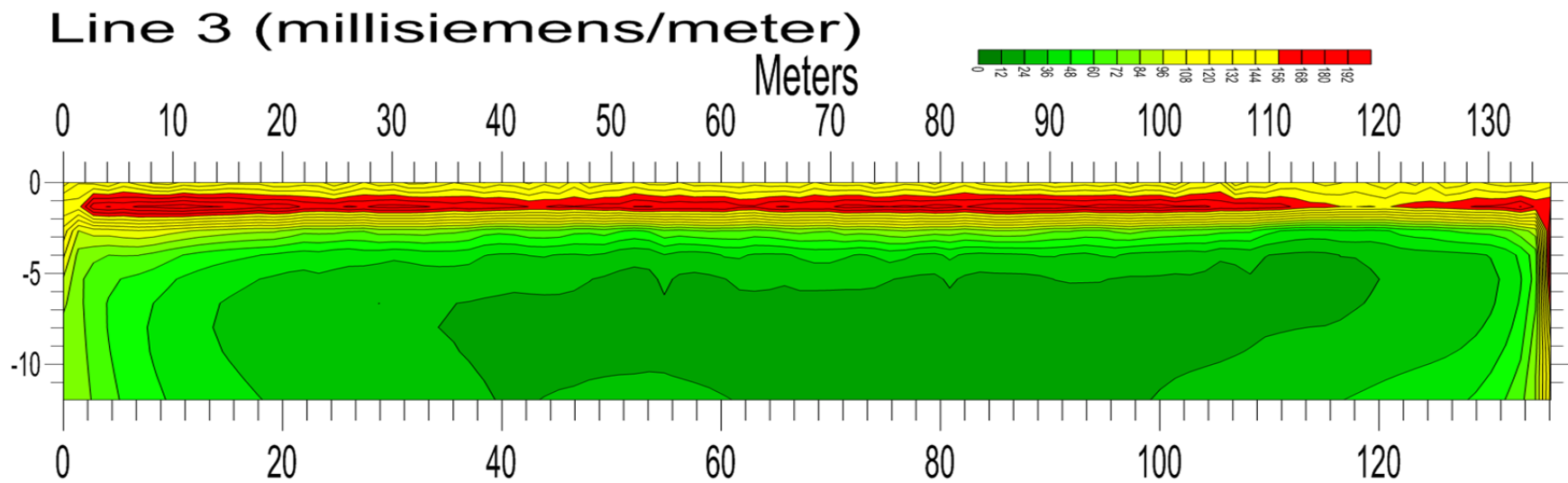


Figure 8.4c Conductivity (ms/m) section of Line 3. The high conductivity zone is continuous along the surface. There is a low conductivity zone at the same depth as Line 2.2.

### **8.1.3 Francis Geological Interpretation**

The ERT, EM and geologic data from Francis were compiled in order to determine the dominant geologic features present at the site. Based on this information, it was determined that there were two prominent features influencing seepage activity. The first feature was the clay overburden that dominates the top 2 meters (7 ft.) of the material on the land-side of the levee. Although the clay tends to be confined to the drainage, it is believed to be analogous to the fine-grained top-stratum previously discussed in Section 1.1. The second prominent feature at the site is the drainage channel trending towards the levee. Based on LIDAR data, the drainage appears to extend beneath the levee towards the river. The ERT sections show that the feature also has some subsurface expression consisting of permeable material. The locations of the high permeability (low conductivity) anomalous zones are labeled in Figure 8.5. From this, it appears that the drainage feature was once a distributary channel that was filled with coarser grained sand then capped by the clay overburden. The sharp transition between high conductivity (low permeability) zones and low conductivity (high permeability) zones in lines 2.2 and 3 can be attributed to the clay to sand contact previously discussed in section 5.2. The extent of the high permeability zone was traced in Figure 8.5.



## Conductivity Zones Found in ERT Lines 2.2 and 3

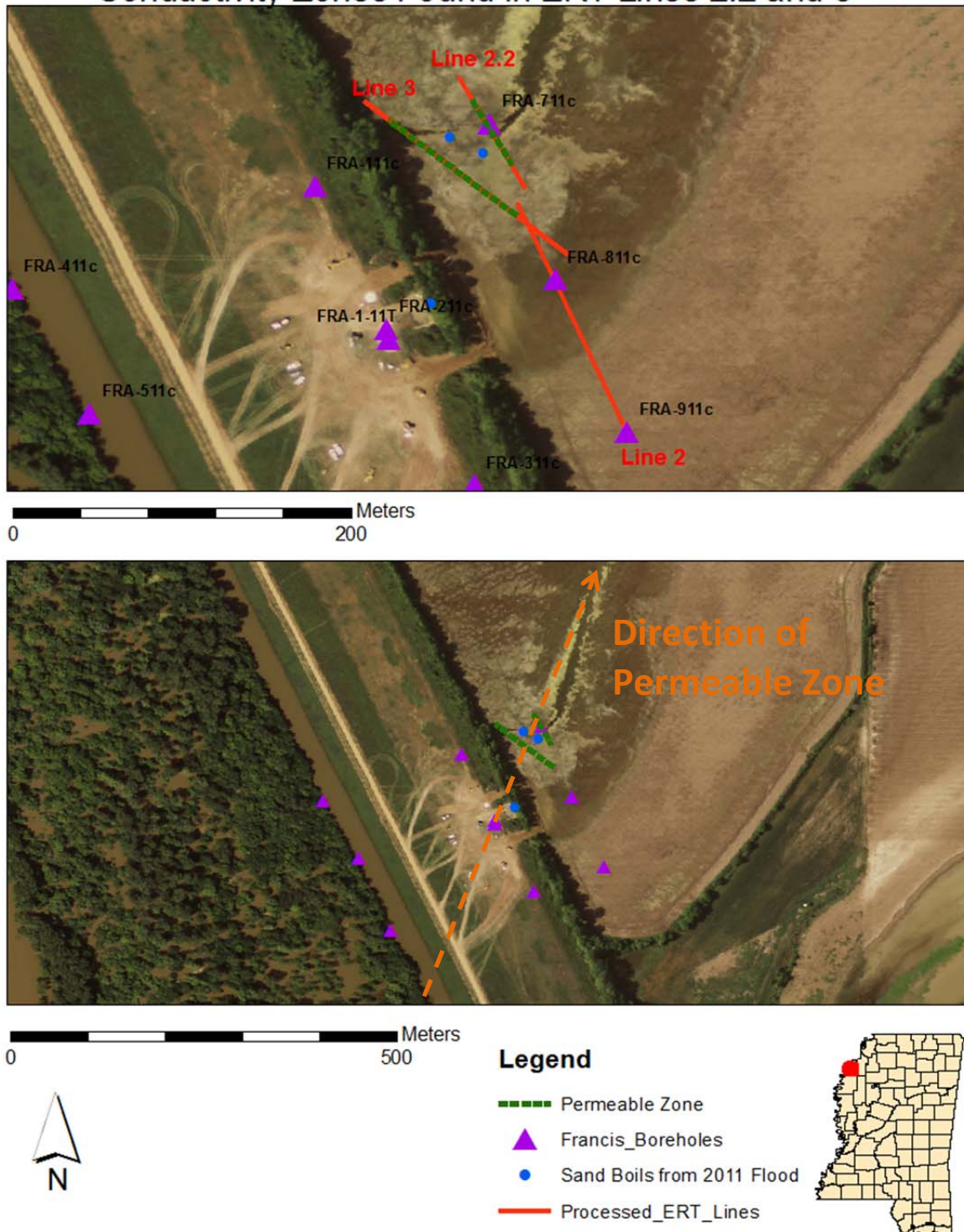


Figure 8.5 Plan view of low conductivity/ high permeability zone on the ERT line. The boundary of the zone is marked by green dashed lines. The zone appears to follow the trends of the seepage pathway and the surface drainage.

## **8.2 Rena Lara Results**

The geophysical surveying and interpretations at Rena Lara were made after geophysical processing had concluded for the Francis site. The same inferences, therefore, were made regarding the correlation between electrical conductivity, clay content and permeability.

### **8.2.1 Rena Lara EM Data**

Figures 8.6 and 8.7 show the plan-view conductivity profiles produced by the EM<sub>34</sub>. Comparing the conductivity measurements with the ERT data, it is estimated that the EM horizontal dipole measured 0-4 meters (0-13 ft.) below the surface, and the vertical dipole measured 0-10 meters (0-32 ft.) below the surface. Both dipole measurements indicate a high conductivity zone beneath the levee apron averaging 50 mS/m. The vertical dipole shows that the zone extends across the apron perpendicular to the levee (Figure 8.6). The horizontal dipole suggests that the zone extends laterally (parallel) across the apron (Figure 8.7). The high conductivity zone is interpreted to be the clay-filled swale that was delineated using the borehole data.

### **8.2.2 Rena Lara ERT Data**

Figure 8.8 shows the ERT line taken on the levee apron at Rena Lara. Based on borehole data, the apron averages 10 ft. (3m) in thickness. Electrodes were spaced at a 2 meter (7 ft.) interval in order to survey at a greater depth below the apron. The vertical profile of the high conductivity zone seen in the EM data is shown in the section (Figure 8.9). The zone is thickest

at approximately 200 meters (650 ft.) along the ERT line and appears as a wedge-shaped feature. The center of the feature coincides with the drainage discussed in section 5.2.2.

### **8.2.3 Rena Lara Geological Interpretation**

The ERT, EM and borehole data indicate that there is a clay-rich zone that runs beneath the levee at the Rena Lara site. The zone is believed to be a result of a swale that was filled with finer grained material. The swale appears to be influencing the path of the drainage that is located on the land-side of the levee. Similar to the Francis site, the drainage is indicative of the geologic feature(s) that dominate the Rena Lara site. The drainage at the Rena Lara site differs, however, because it is filled with finer-grained material instead of coarser grained sand capped by clay.

## EM 34 Horizontal Dipole Results

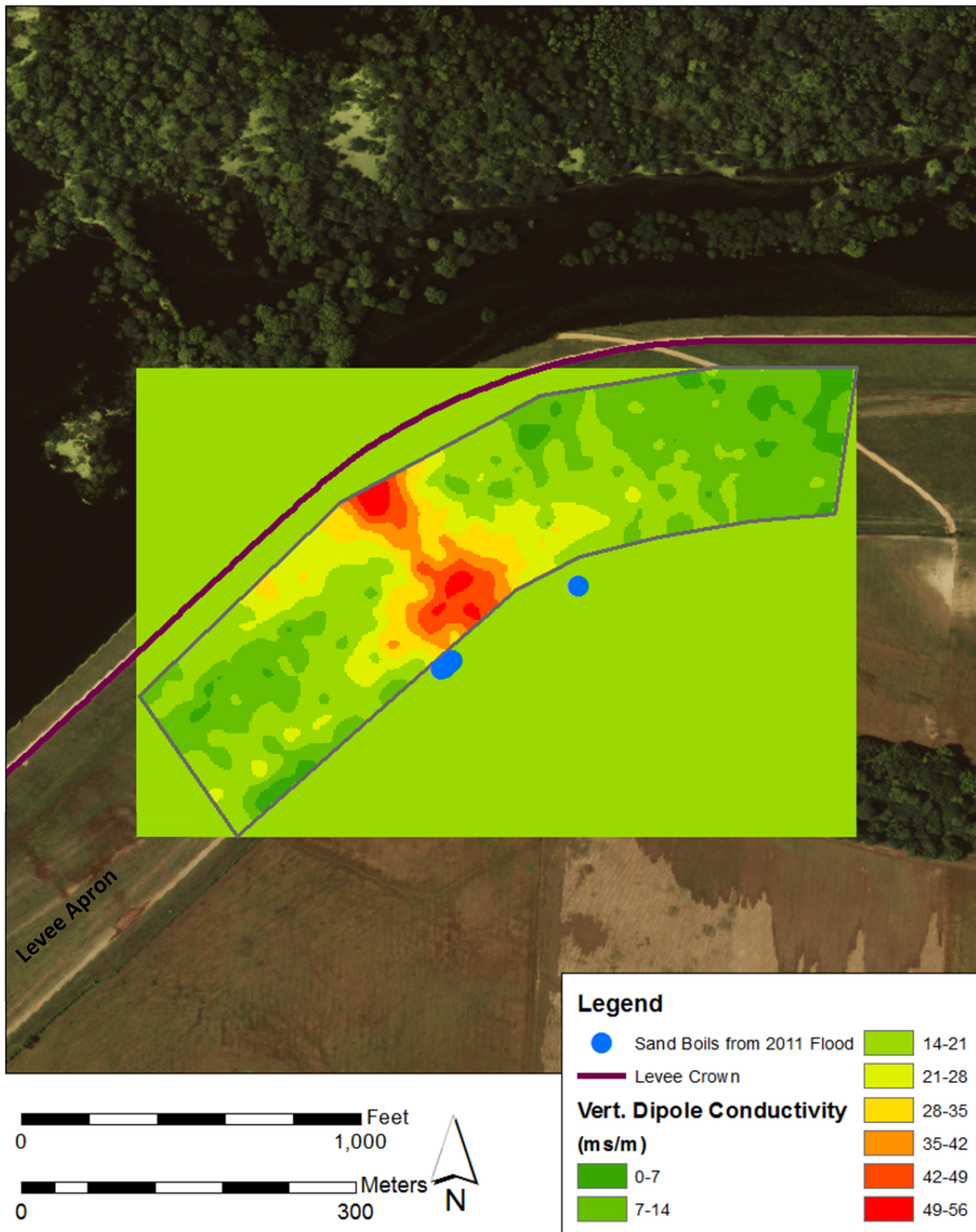


Figure 8.6 Conductivity profile of EM 34 Vertical Dipole. The results show a high conductivity zone extending across the apron. This zone also lines up the drainage next to the levee.



## EM 34 Horizontal Dipole Results

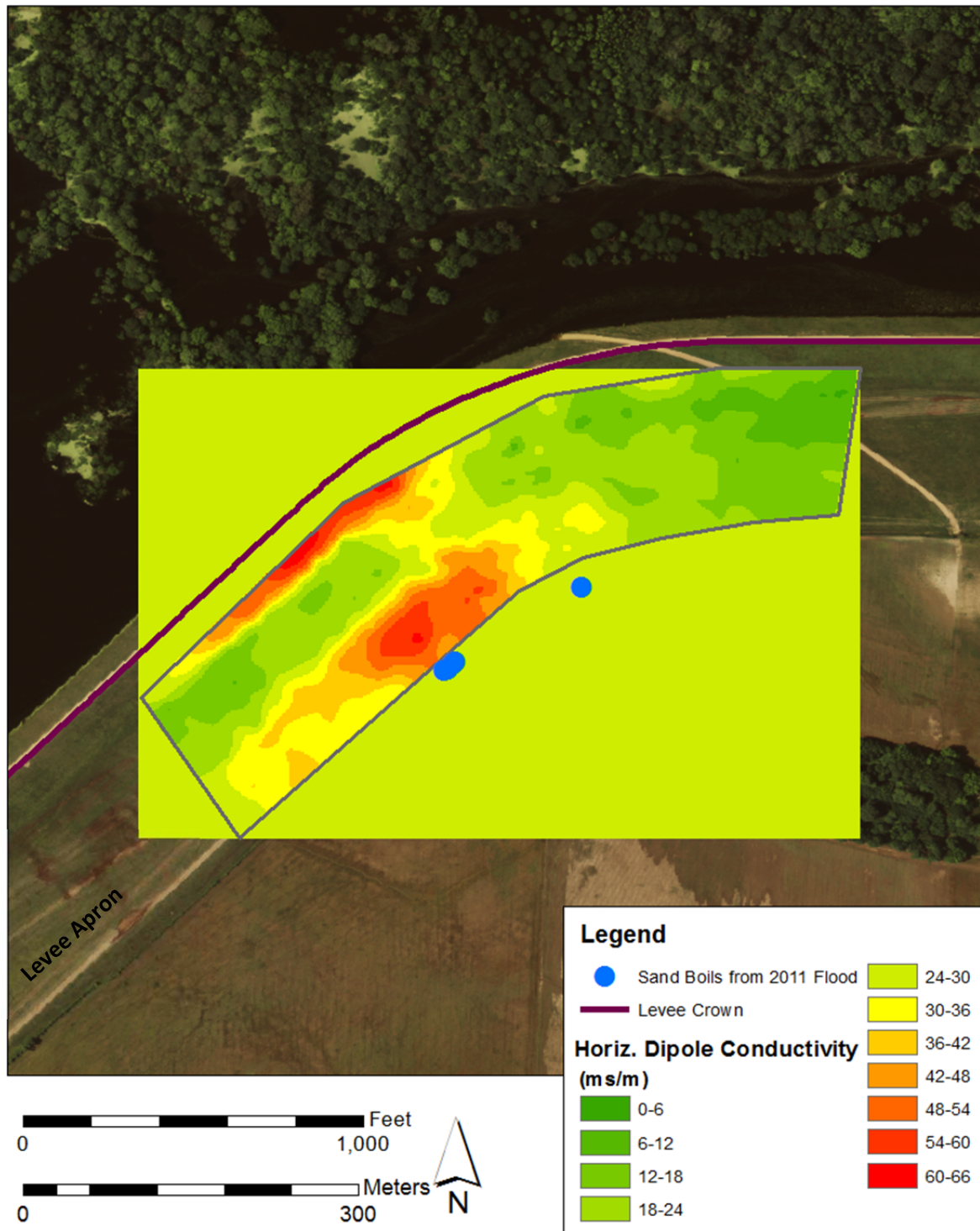


Figure 8.7 Conductivity profile of EM 34 Horizontal Dipole. The results show the high conductivity zone extending more parallel along the apron.

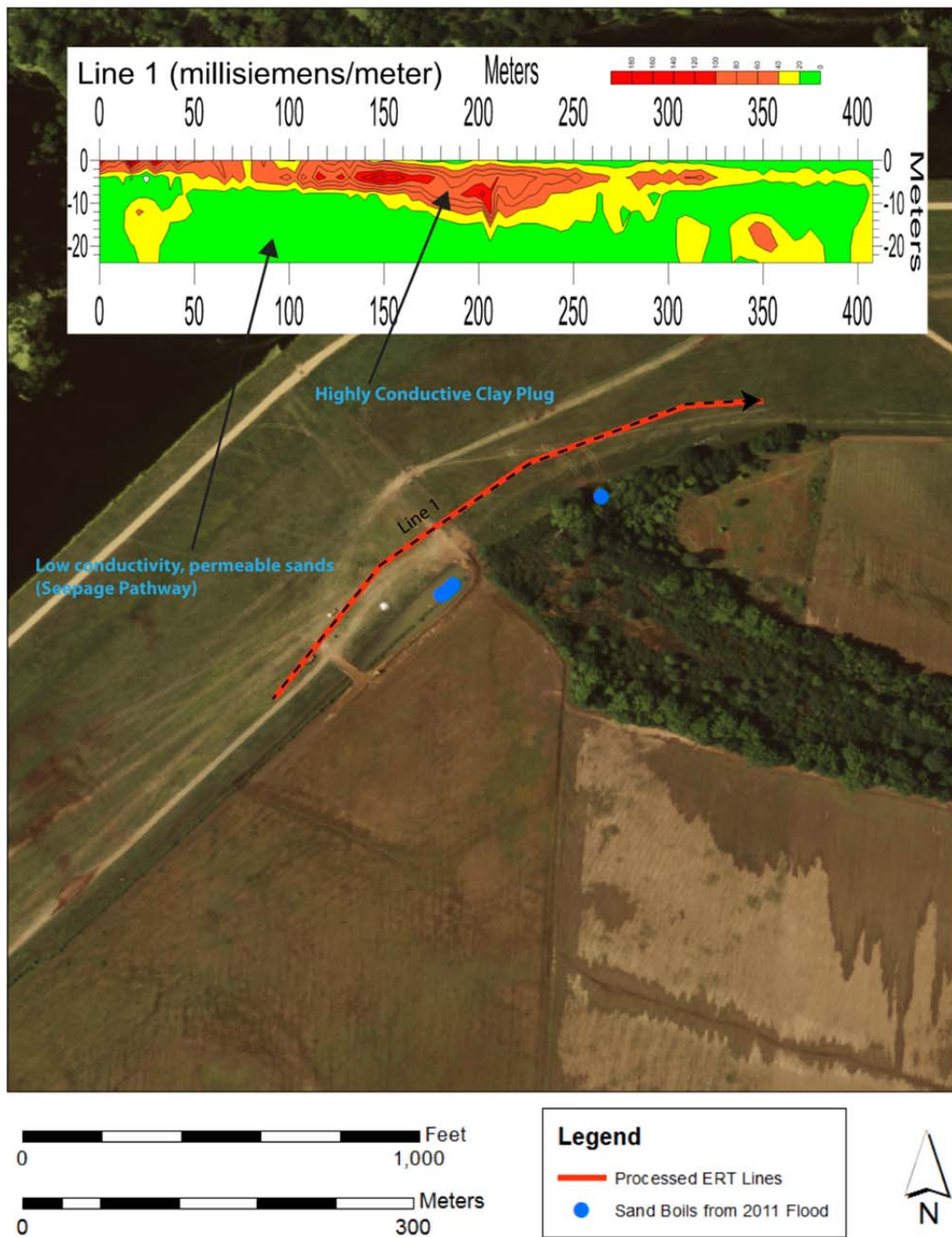


Figure 8.8 ERT line at Rena Lara. The high conductivity zone is wedge-shaped and lines up with the drainage near the levee.



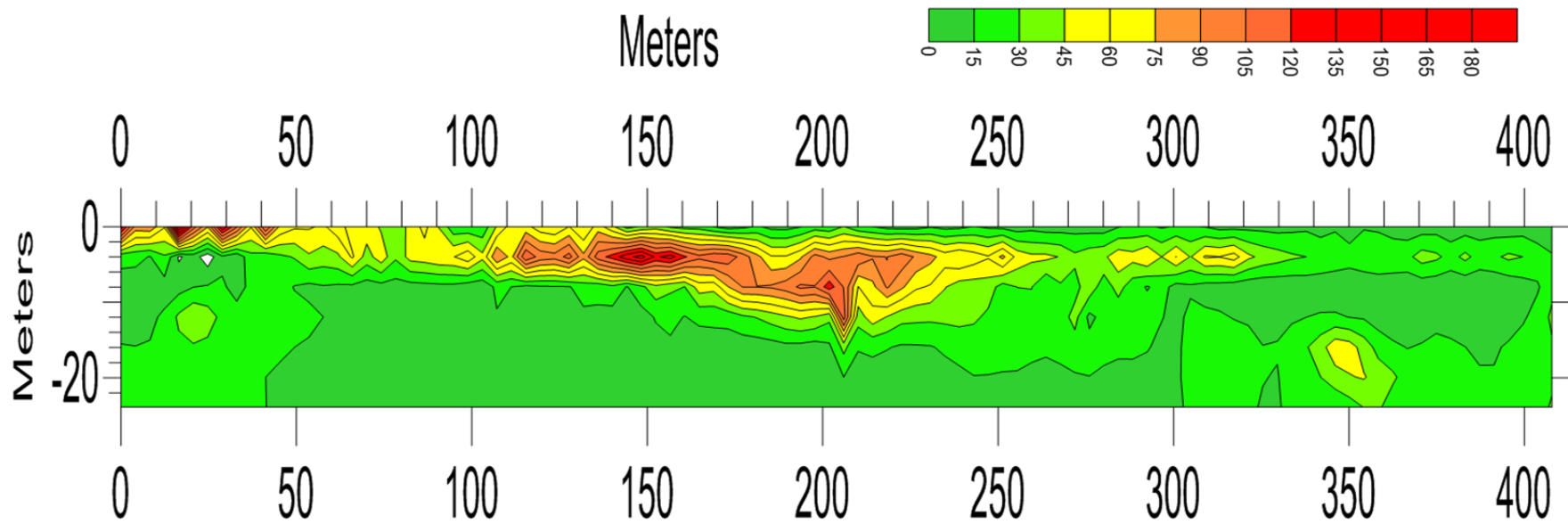


Figure 8.9 Conductivity (ms/m) section of Line 1. The results show a wedge-shaped feature of highly conductive material. This is interpreted to be a clay-filled swale.

## **CHAPTER 9**

### **Discussion of Results**

#### **9.1 Seepage Model**

In order to accurately model the seepage at each site, a general model proposed by Wilson (2003) was used as a guide. Both sites differed in subsurface geology, geomorphic features and seepage pathways, therefore, it was recognized that the occurrence of sand boils at the sites may be influenced by different factors.

##### **9.1.1 Francis Seepage Model**

At Francis, the seepage appears to be influenced by both the clay overburden landward of the levee, and a filled channel that trends beneath the levee. The occurrence of sand boils in the adjacent field were in locations where the clay overburden/top stratum was thin or not present and where the channel was running beneath the levee. It is proposed that the coarser grained sands that filled the channel are analogous to the substratum and act as a conduit for underseepage from the river-side to the land-side of the levee. This is based on the location of the sands with respect to the sand boils and seepage pathway. The water is forced through the conduit where it has a hydraulic connection to flood waters. The difference in head across the levee forces the seepage through the conduit and beneath the levee. The seepage then surfaces as

a sand boil where the overlying, impermeable overburden is thin or non-existent. This model can be seen in Figure 9.1. The model corresponds to the piping variables listed in Wilson's (2003) model (Table 9.1). The confining layer thickness (variable 2) and the horizontal permeability of the substratum (variable 5) are both believed to be the prominent factors influencing seepage at Francis.

### **9.1.2 Rena Lara Seepage Model**

Seepage at Rena Lara is influenced by a clay-filled swale extending beneath the levee. The clay within the swale has relatively low horizontal permeability, and concentrates the seepage flow towards more permeable zones on the flanks of the swale (Wilson, 2003). Groundwater forced through these zones increases the hydraulic pressures and promotes piping and sand boil formation. Wilson (2003) describes this as piping variables 9 and 10 in his model, and further notes that the orientation of the swales with the levee also influences the occurrence of sand boils (Table 9.1). An illustration of how the swales influence the seepage at Rena Lara is shown in Figure 9.2.

Although the seepage outlet at the Rena Lara site is within close proximity to the sand boils, there is not enough evidence to support a hydraulic connection between the seepage occurring beneath the levee, and that occurring from the seepage scarp. Figure 5.14 illustrates how the seepage scarp is actually occurring at an elevation above the sand boils. It is believed that the water flowing from the scarp is the result of rainwater that has penetrated the levee apron and is seeping from the toe. It is possible, however, that the scarp's formation was influenced by the degradation of the levee from piping.

From the analysis of data drawn at both Francis and Rena Lara, it was determined that two different scenarios are influencing seepage in the area. A feature common to both sites is a recent drainage channel that intersects the levee. Although the drainage features may differ in their origin and sediment composition, they both have a direct influence on seepage occurrence. These drainages may have been overlooked in similar investigations in the past, but are highlighted in this study.

## **9.1 Geophysics and Seepage Modeling**

Findings from this study demonstrated that the geology within the study varied greatly throughout each site. Although LIDAR and borehole data gave some indication of the geology at each location, further investigation was needed to determine the extent of the geologic features and how they influenced seepage behavior. Geophysics proved to be an important addition for correlating LIDAR and borehole data and supplementing these methods where data was not present.

One important example of this was the conditions at the Francis site. Borehole 7.11C (Appendix A) is located adjacent to the two sand boils that surfaced in the field adjacent to the levee. The borehole data showed that there was a 10-12 feet thick layer of clay near the surface. Based on this information alone, it would be difficult to understand how the sand boil could have surfaced through this clay zone. Line 2.2 (Figure 8.4b) of the ERT survey, however, showed that this clay zone was discontinuous, thus allowing water to surface in gaps in the clay where permeability was higher.

Geophysics at the Rena Lara site proved useful in confirming information found in the borehole and elevation data. A geologic cross section of the site showed a large clay body trending beneath the levee (Figures 5.12 and 5.13) and the LIDAR data showed a large drainage adjacent to the levee. Conducting EM and ERT data between the boreholes and the drainage helped to confirm that the surface feature was actually a swale. Geophysical results also helped delineate the size and extent of the swale and its relationship to the recent sand boils.

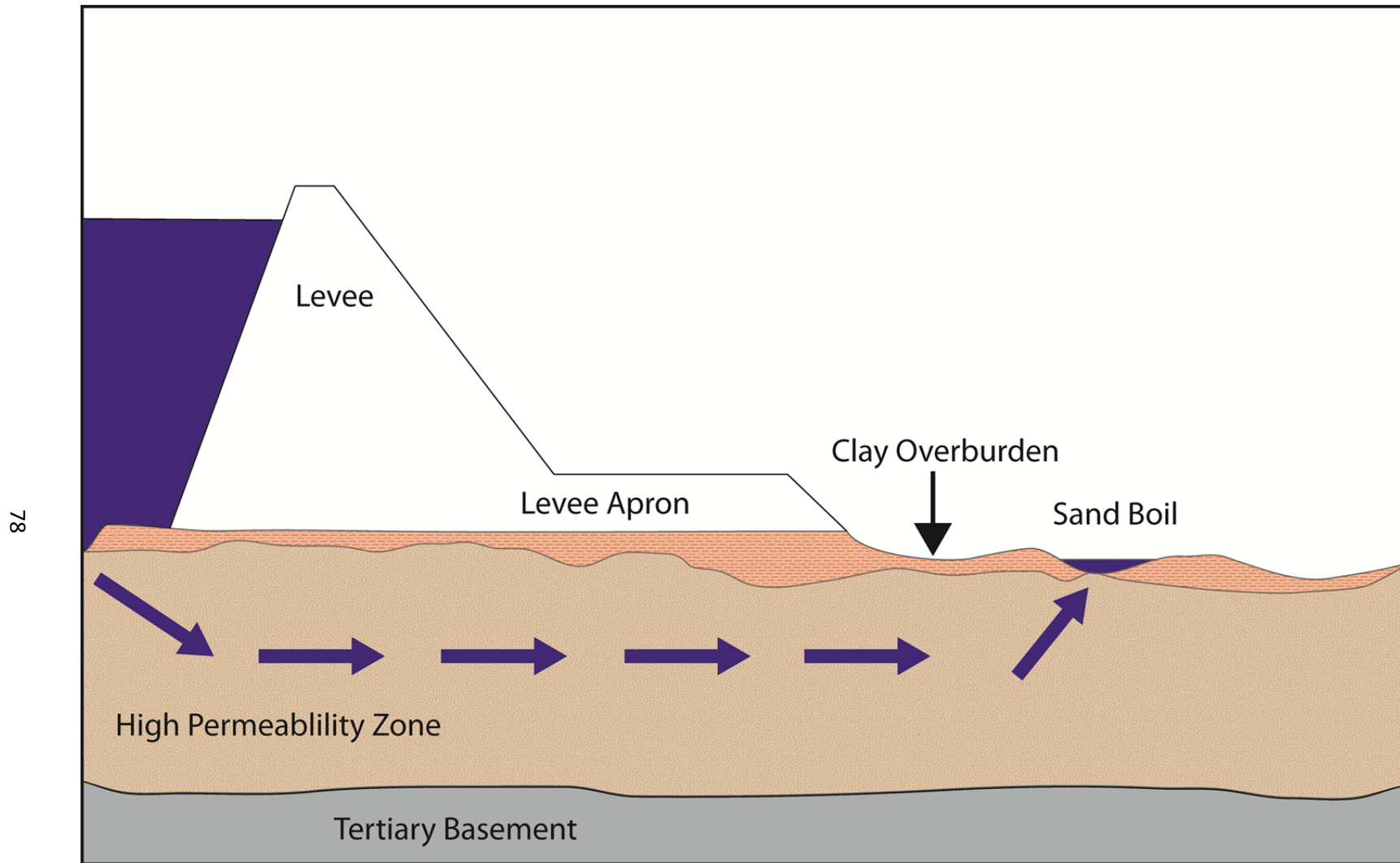


Figure 9.1 Model of seepage at Francis. The clay overburden and the high permeability zone beneath it both influence sand boil occurrence.



**Table 9.1 Piping Variables**

#	Brief Variable Description	Symbol	Noted Previous Investigators
1	Net Head on the levee (ft)	H	USACE 1956a, USACE 1956b
2	Transformed confining layer thickness (ft)	$Z_b$	Turnbull and Mansur 1959
3	Vertical permeability of riverside and landside top blanket (cm / sec <sup>2</sup> )	$k_{br}$ and $k_{bl}$	USACE 1956a, USACE 1956b
4	Effective thickness of the substratum (ft)	d	USACE 1941
5	Ratio of horizontal permeability of the substratum with vertical permeability of the top stratum	$k_h / k_v$	USACE 1956a, USACE 1956b
6	Distance from landside toe of the levee to effective seepage entry (ft)	s	USACE 1956a, USACE 1956b
7	Distance from landside toe of the levee or berm to effective seepage exit (ft)	$x_3$	USACE 1956a, USACE 1956b, USACE-STL 1976
8	Critical gradient through the top stratum landside toe of the levee	$i_c$	USACE 1941, USACE 1956a, USACE 1956b, USACE-STL 1976
9	Surface geologic deposit	based on type	Fisk 1944, USACE 1956a, USACE 1956b, Kolb 1975, Smith and Smith 1984, Saucier 1994
10	Surface geologic configuration	based on alignment with the levee	Fisk 1944, USACE 1956a, USACE 1956b, Kolb 1975, Smith and Smith 1984, Saucier 1994
11	Blocked exit	based on alignment with the levee	USACE-STL 1976

*\*Data sources given under previous investigators.*

Table 9.1 Piping variables modified from Wilson (2003). Variables 2 and 5 seem to be responsible for underseepage at Francis, while variable 9 and 10 are influencing seepage at Rena Lara.

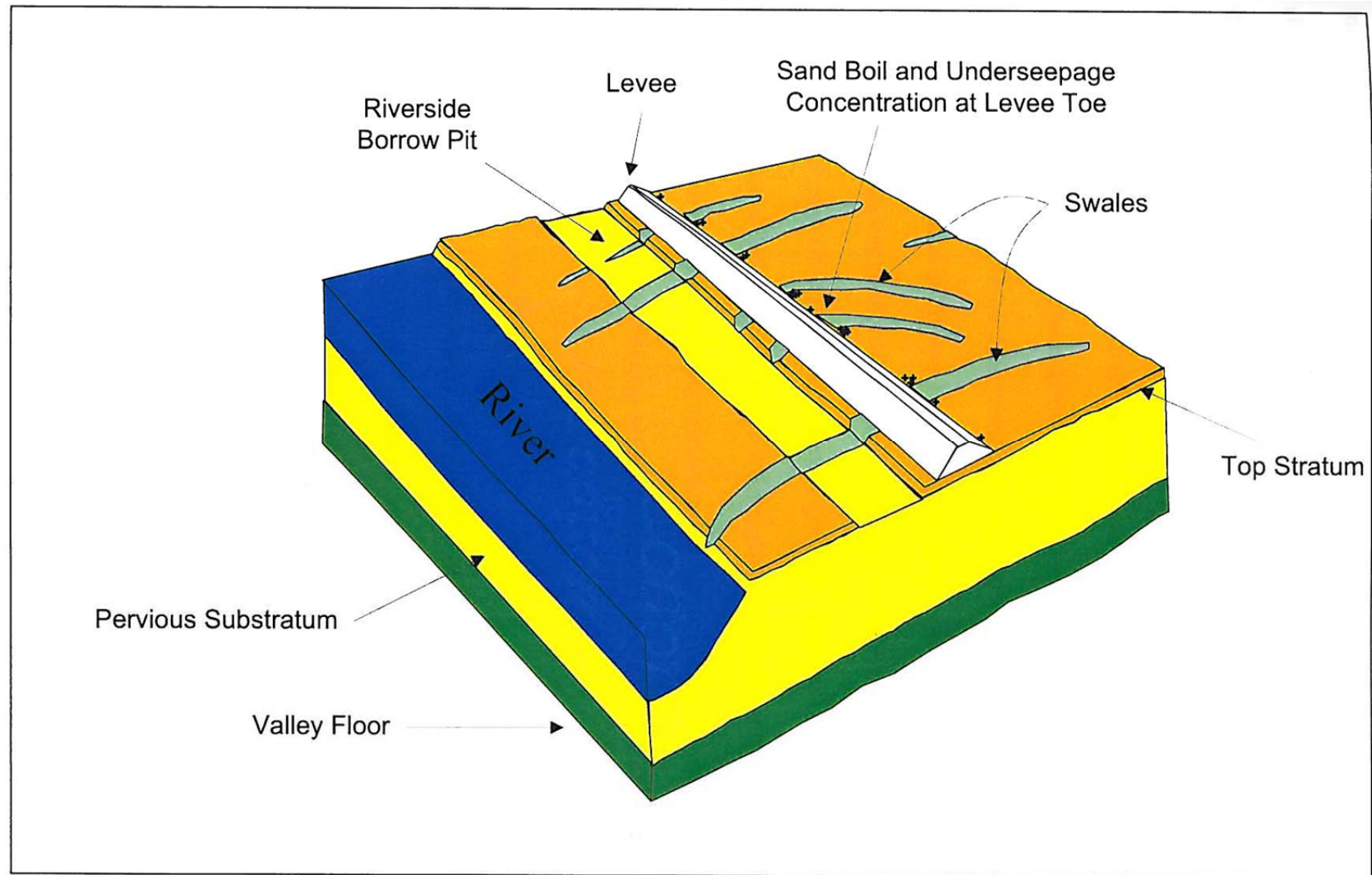


Figure 9.2 Model of seepage at Rena Lara. The clay-filled swales running beneath the levee focus seepage towards adjacent, more permeable zones. Modified from Wilson (2003).

## **CHAPTER 10**

### **Application of Results**

This study used geophysics as a means to characterize anomalies in the subsurface that may contribute to levee underseepage and piping. Results from Francis and Rena Lara demonstrate that small geomorphologic features may have an influence on seepage behavior. This information is useful in both predicting where seepage will occur during the next flood event and giving levee authorities a better understanding of the nature of the seepage as they employ mitigation measures.

The main factor in investigating seepage at Francis and Rena Lara was the correlation between local drainages and sand boil location. Sand boils occurred either within or directly adjacent to these drainages. Although each drainage has its own complexities, it is important to note how each can be easily identified using remote sensing data. Given the data, authorities may formulate a broad and general prediction model of seepage locations before a flood event.

Information on permeable and impermeable materials gathered during this study may assist in designing and placing berms and relief wells. Given that both horizontal and vertical seepage flow will not occur through the impermeable materials present, authorities may want to target more permeable zones when mitigating the seepage at both sites.

## **CHAPTER 11**

### **Recommendations for Further Work**

The geophysical data acquired during this study is verified with the geologic information used during the analysis. More geologic data and/or geophysical data, however, may be used to further understand the factors influencing underseepage and Francis and Rena Lara. The acquisition of this supplemental data is outside of the limits originally proposed by this study but may be necessary when replicating these methods at other sites.

#### **11.1 Suggestions for Supplemental Geophysical Surveys at Francis**

The focus of further geophysical analysis at Francis should be to delineate the permeable zone that runs beneath the surface drainage. This could be done with ERT or EM 34 methods. The EM34 method would require a dipole spacing of at least 20m (65 ft.) in order to measure beneath the high conductivity clay overburden. A sequence of parallel ERT lines along the drainage may also be used to trace the zone (Figure 11.1). The ERT electrode spacing should remain at one meter (3 ft.) since the zone appears to be fairly shallow. The EM and ERT methods could also be employed on the levee apron to trace the zone beneath the apron. A 20m (65ft) coil spacing and 2m (7 ft.) electrode spacing would be required to measure beneath the levee apron.

## **11.2 Suggestions for Supplemental Geophysical Work at Rena Lara**

Supplemental geophysical work at Rena Lara should be conducted on the land-side field of the levee. This would require surveying when there is less vegetation in the adjoining field. The EM 34 could be employed to determine if there is a clay overburden present at the site that is similar to Francis. This would explain the locations of the sand boils. Coil spacing should be set at 20m (65ft) and 10m (33ft) to define any possible impermeable zones. A suggested grid for supplemental EM data collection is shown in Figure 11.2.

## Proposed Lines for Supplemental ERT Surveying at Francis

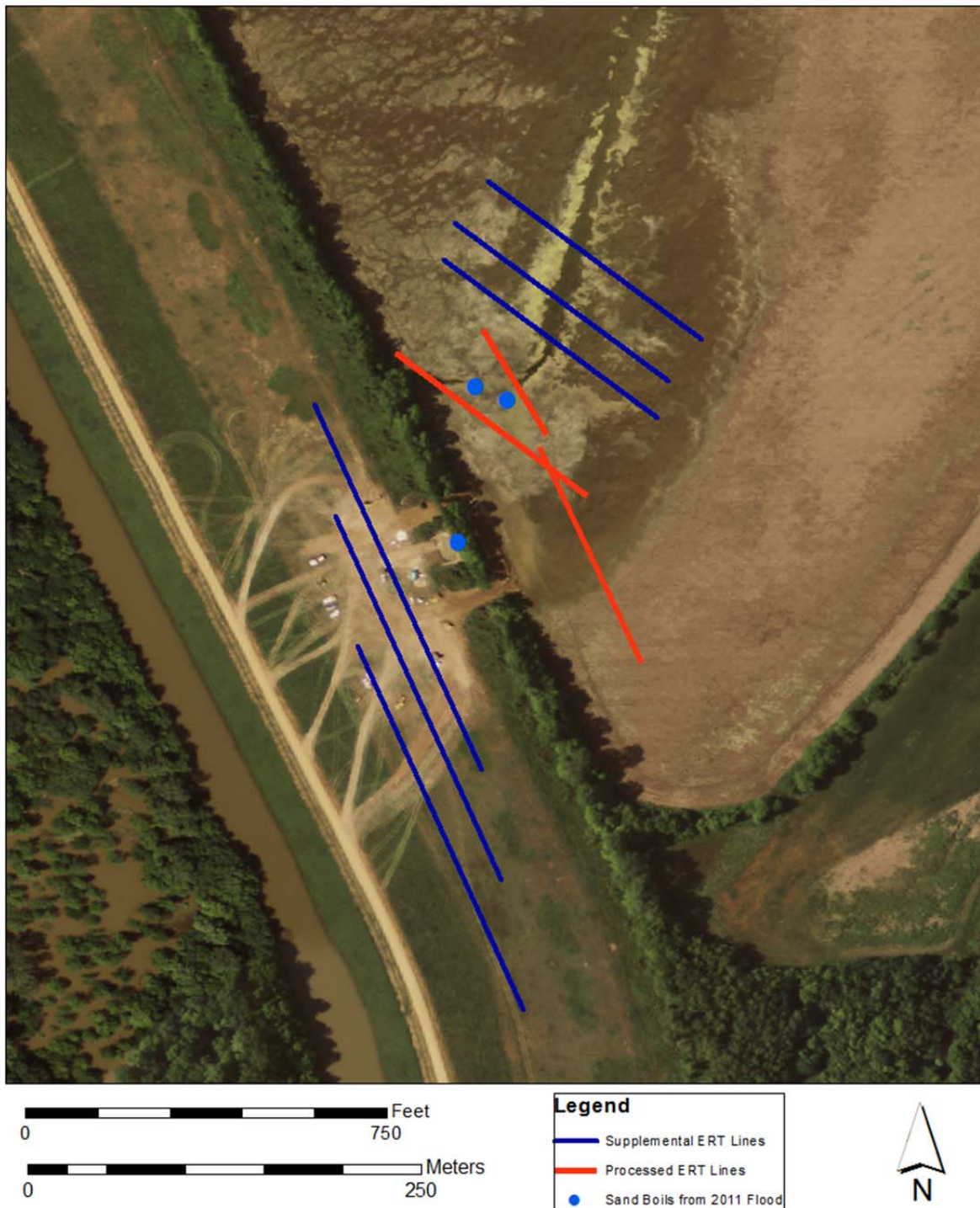


Figure 11.1 Map of suggested ERT surveys for supplemental surveying at Francis. The ERT lines should continue to cross the drainage perpendicularly in order to further identify the feature.



## Proposed Grids for Supplemental ERT Surveying at Rena Lara



Figure 11.2 Suggested grids for supplemental EM data. The layout of the grids is designed to further identify the clay-filled swale and detect a clay overburden.

## **LIST OF REFERENCES**

## LIST OF REFERENCES

- ArcGIS Resource Center, “Spline (Spatial Analysis)” ESRI, June 29, 2001, <http://help.arcgis.com/en/arcgisdesktop/10.0/help/index.html#//009z00000006q0000000.htm>, Accessed October 11, 2012.
- Aronoff, S., 2005, *Remote Sensing for GIS Managers*, Redlands, California, ESRI Press, p. 197-240.
- Chasteen, D. S., 2000, Hillhouse Mississippi Seepage Study, U.S. Army Corps of Engineers, Geotechnical Engineering Branch, Memphis, TN., 61p.
- Dunbar, J. B., Llopis, J. L., Sills, G.L., and Smith, E.W., 2007, Condition Assessment of Levees, U.S. Section of the International Boundary and Water Commission: TR-03-4, U.S. Army Corps of Engineers, Engineer Research and Development Center, Vicksburg, MS., 331p.
- Fisk, H.N., 1944, Geological Investigation of the Alluvial Valley of the Lower Mississippi River: Mississippi River Commission, Vicksburg, MS., Plate 22.
- Llopis, J.L., Smith, E.W., and North, R. E., 2007, Geophysical Surveys for Assessing Levee Foundation Conditions, Sacramento River Levees, Sacramento, CA: TR-07-21, U.S. Army Corps of Engineers, Engineer Research and Development Center, Vicksburg, MS., 57p.
- Kolb, C.R., 1975, Geologic Control of Sand Boils along Mississippi River Levees: S-75-22, U.S. Army Corps of Engineers, Waterways Experiment Station, Vicksburg, MS., 25p.
- McNeill, J.D., 1980, Electrical Conductivity of Soils and Rocks: Technical Note TN-5, Geonics Limited, 20p.
- McNeill, J.D., 1980, Electromagnetic Terrain Conductivity Measurement at Low Induction Numbers: Technical Note TN-6, Geonics Limited, 13p.
- Nimrod, P. C., and Thompson, R.M., Fall 2011, Personal Communication, Mississippi Levee Board, Greenville, MS.
- Saucier, R.T., 1994, Geology and Quaternary Geologic History of the Lower Mississippi Valley: U.S. Army Corps of Engineers, Waterways Experiment Station, Vicksburg, MS, 2 vol. 364p.

Shevnin, V., Delgado-Rodriguez O., Mousatov, A., and Ryjov, A., 2006, Estimation of Hydraulic Conductivity on Clay Content in Soil Determined from Resistivity Data, *Geofisica Internacional*, vol. 45, num. 3, p. 195-207.

Smith, R., 1997, Geotechnical Aspects of MR&T Levee Design, Construction and Maintenance, U.S. Army Corps of Engineers, Geotechnical Engineering Branch, Memphis, TN. 33p.

Sorensen, J. C., and Chowdhury, K., 2010, Levee Subsurface Investigation Using Geophysics, Geomorphology and Conventional Investigation Methods, Proceeding from the U.S. Society on Dams Conference, April 12-16, 2010, p.109-124.

Telford, W.M., Geldart, L.P., and Sheriff, R.E., 1990, *Applied Geophysics*, 2<sup>nd</sup> ed., New York, New York, Cambridge University Press, p.136-137.

Terzaghi, C., 1929, Effect of Minor Geologic Details on the safety of dams: *Geology and Engineering for Dams and Reservoirs*, Technical Publication 215, *American Institute of Mining and Metallurgical Engineers*, vol. 7, p. 31-46.

U.S. Army Corps of Engineers, 1941, Investigation of Underseepage: Lower Mississippi River Levees: TM 184-1, U.S. Army Corps of Engineers, Waterways Experiment Station, Vicksburg, MS., 25p.

U.S. Army Corps of Engineers, 1956, Investigation of Underseepage and its control. Lower Mississippi River Levees: TM 3-424, U.S. Army Corps of Engineers, Waterways Experiment Station, Vicksburg, MS, 2 vol., 421p.

U.S. Army Corps of Engineers, 1995, Design Guidance for Levee Underseepage: ETL 1110-2-569, U.S. Army Corps of Engineers, Washington, DC. 9p.

U.S. Army Corps of Engineers, 1995, Geophysical Exploration for Engineering and Environmental Investigations: EM 1110-1-1802, U.S. Army Corps of Engineers, Washington, DC. 208p.

Williams, C., 2009, Relief Wells: History of Use in Memphis District, U.S. Army Corps of Engineers, Geotechnical Engineering Branch, Memphis, TN. 32p.

Wilson, J., 2003, *Middle Mississippi River Levee Flood Performance, Assessing the Occurrence of Piping Through Empirical Modeling*, A thesis Presented for the Master of Science Degree, University of Mississippi, University, MS, 174p.

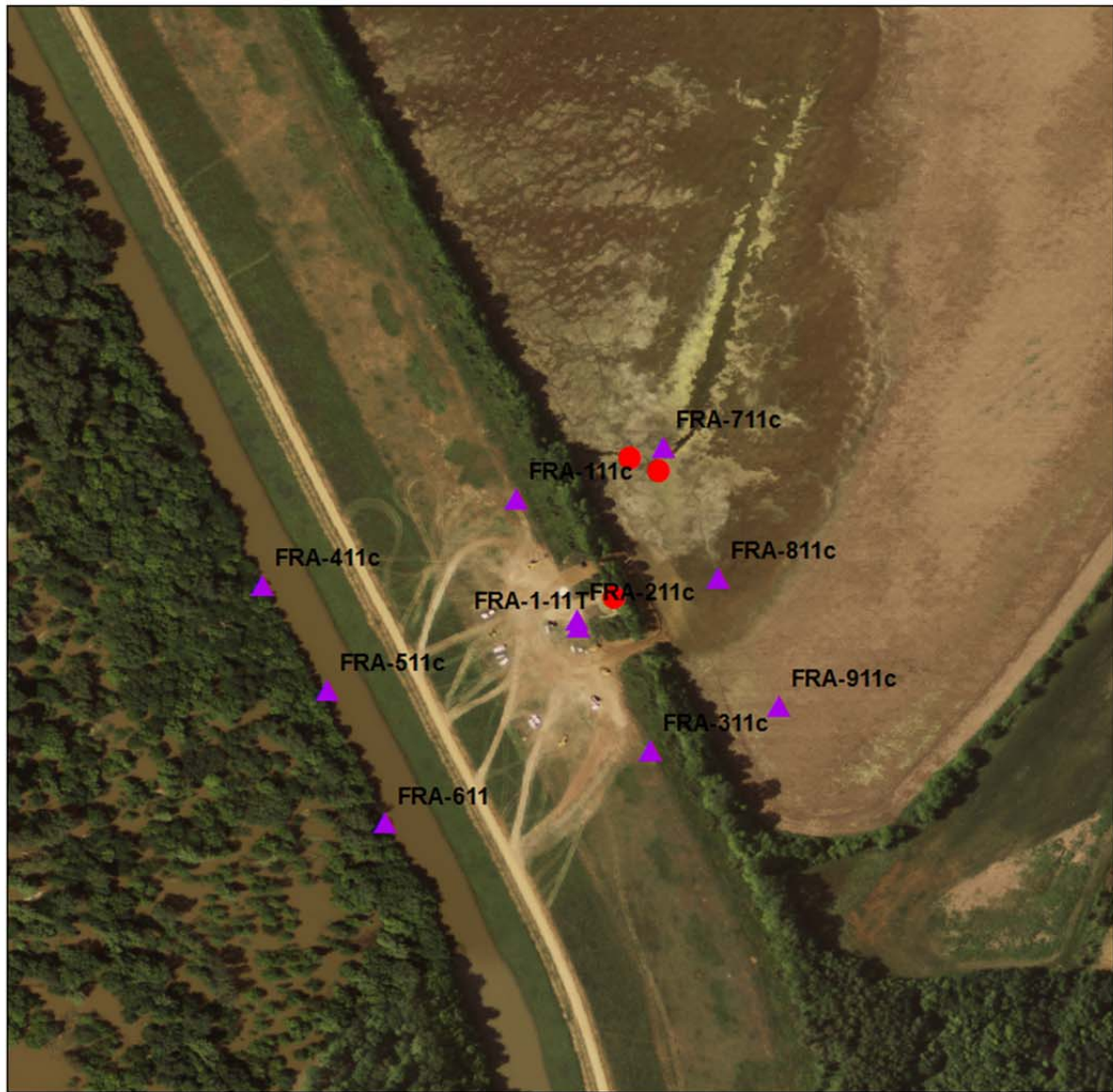
## **LIST OF APPENDICES**

## **APPENDIX A**

### **Borehole Data from Francis Site Obtained from USACE Vicksburg District**



## Francis Boreholes



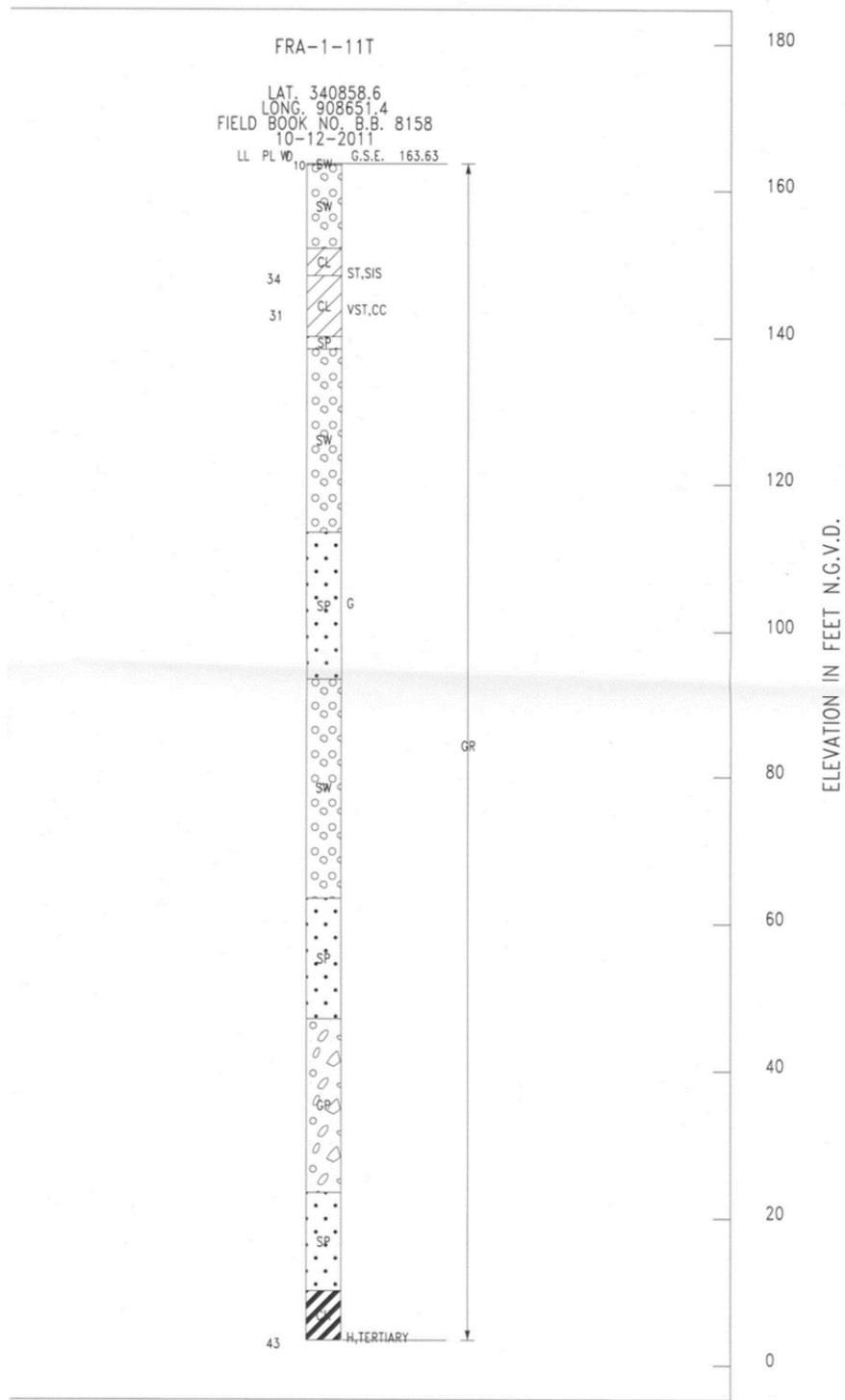
0 750 Feet

0 350 Meters

### Legend

- Sand Boils from 2011 Flood
- ▲ Francis\_Boreholes



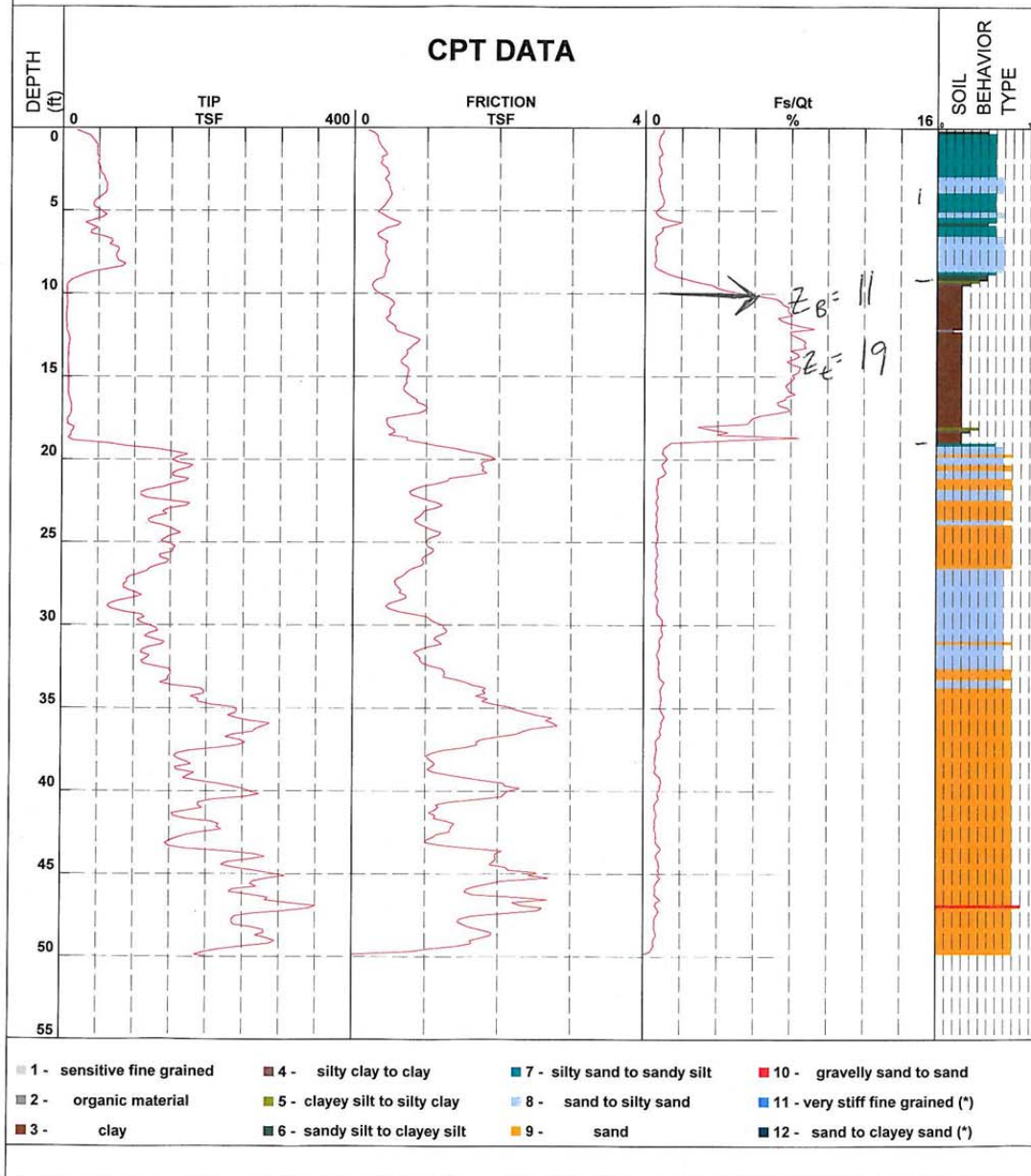




# VICKSBURG DISTRICT

FRANCIS

OPERATOR Penley CONE NUMBER DSA1050 LOCATION 34 05.197 90 51.932  
Date&Time 8/22/2011 12:48:37 PM HOLE NUMBER FRA-1.11c ELEVATION 163.77



## VICKSBURG DISTRICT

OPERATOR Penley

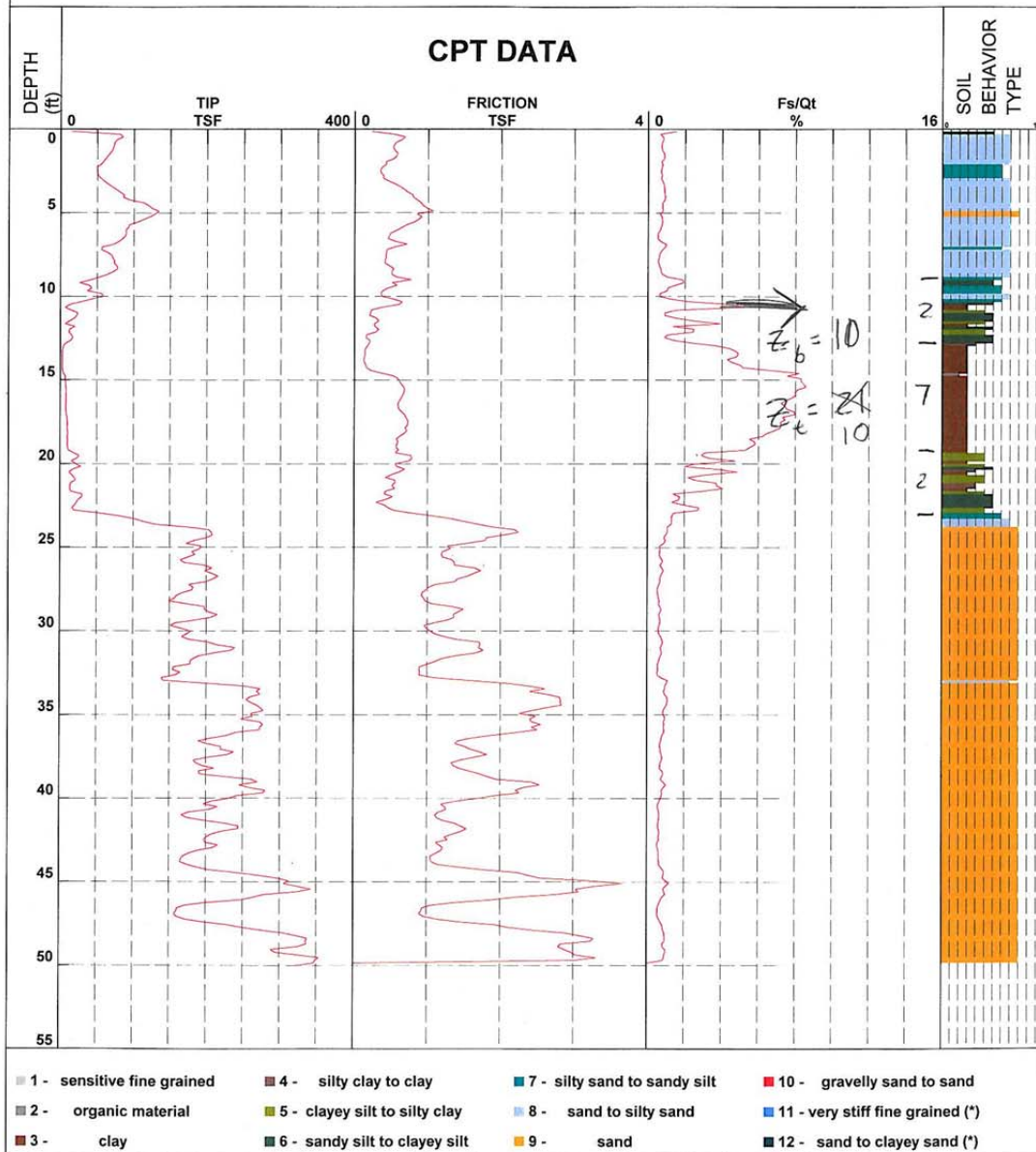
CONE NUMBER DSA1050

LOCATION 34 05.151 90 51.909

Date&Time 8/22/2011 12:04:30 PM

HOLE NUMBER FRA-2.11c

ELEVATION 163.63

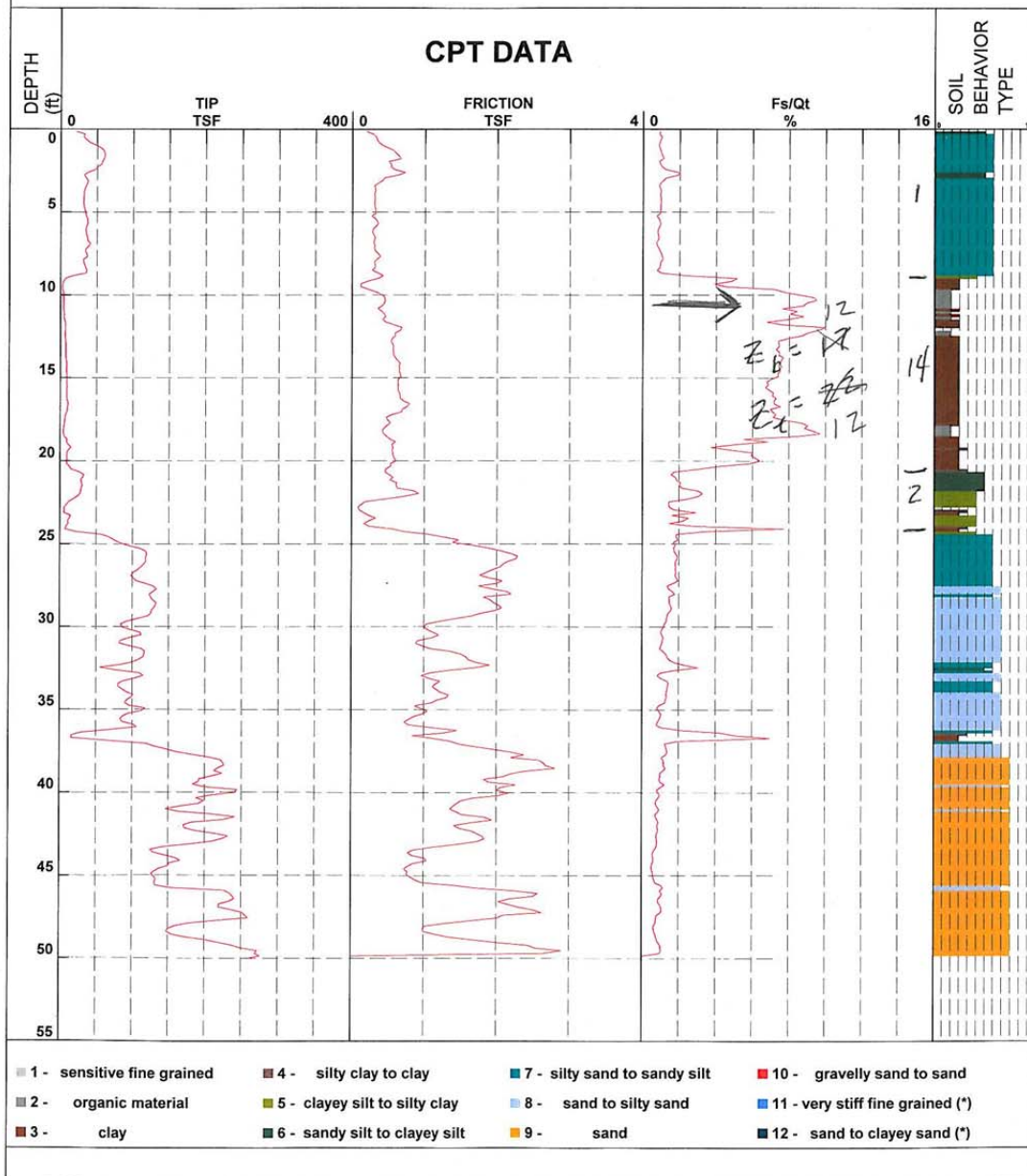






## VICKSBURG DISTRICT

OPERATOR Penley CONE NUMBER DSA1050 LOCATION 34 05.101 90 51.881  
Date&Time 8/22/2011 11:04:40 AM HOLE NUMBER FRA-3.11c ELEVATION 162.53

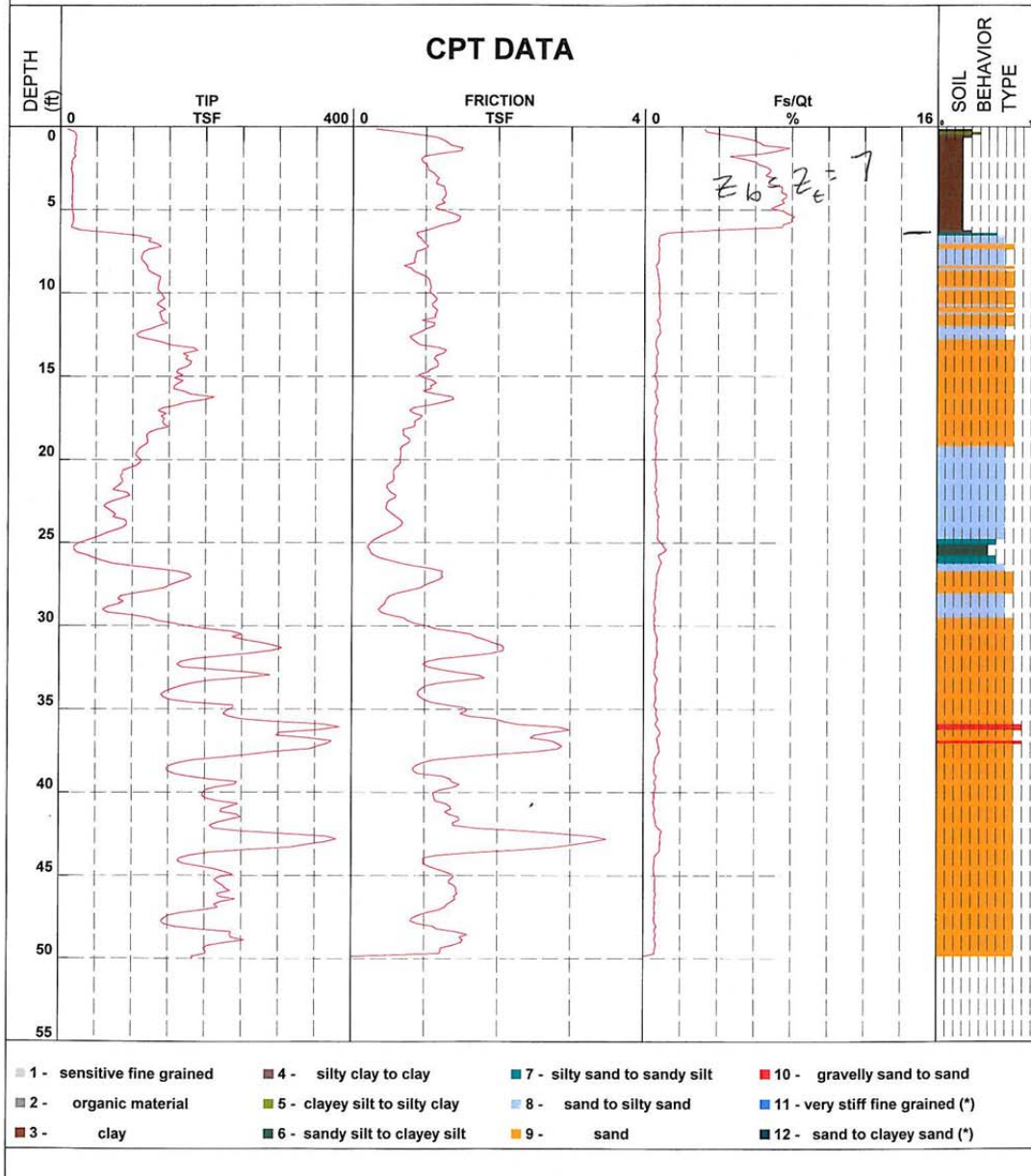




## VICKSBURG DISTRICT

OPERATOR Penley CONE NUMBER DSA1050  
Date&Time 8/22/2011 1:30:48 PM HOLE NUMBER FRA-4.11c

LOCATION 34 05.164 90 52.029  
ELEVATION 154.83







## VICKSBURG DISTRICT

OPERATOR Penley

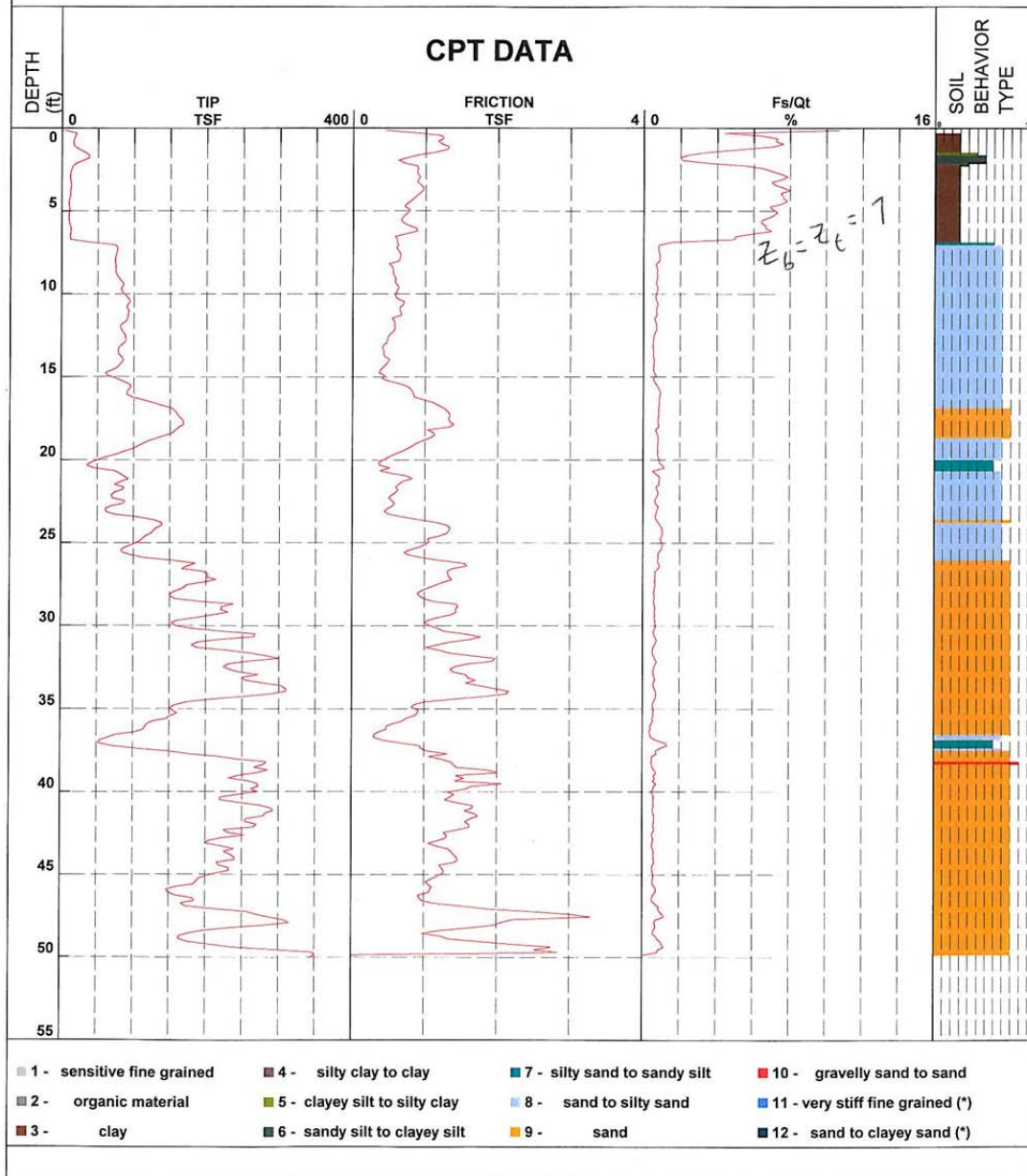
CONE NUMBER DSA1050

LOCATION 34 05.124 90 52.004

Date&Time 8/23/2011 8:12:35 AM

HOLE NUMBER FRA-5.11c

ELEVATION 154.31





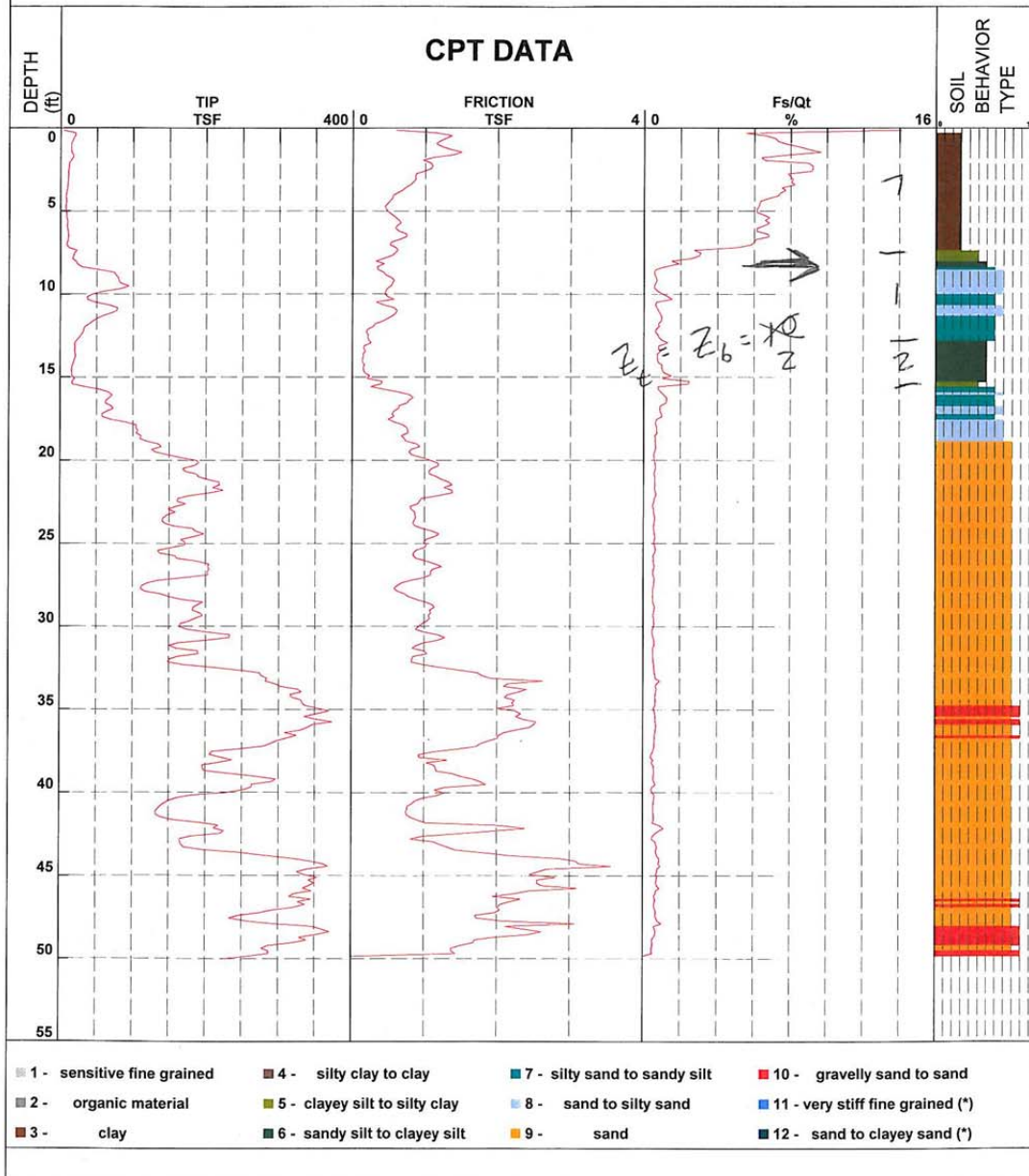
## VICKSBURG DISTRICT

OPERATOR Penley CONE NUMBER DSA1050

LOCATION 34 05.073 90 51.982

Date&Time 8/23/2011 9:05:15 AM HOLE NUMBER FRA-6.11c

ELEVATION 153.04





## VICKSBURG DISTRICT

OPERATOR Crosby

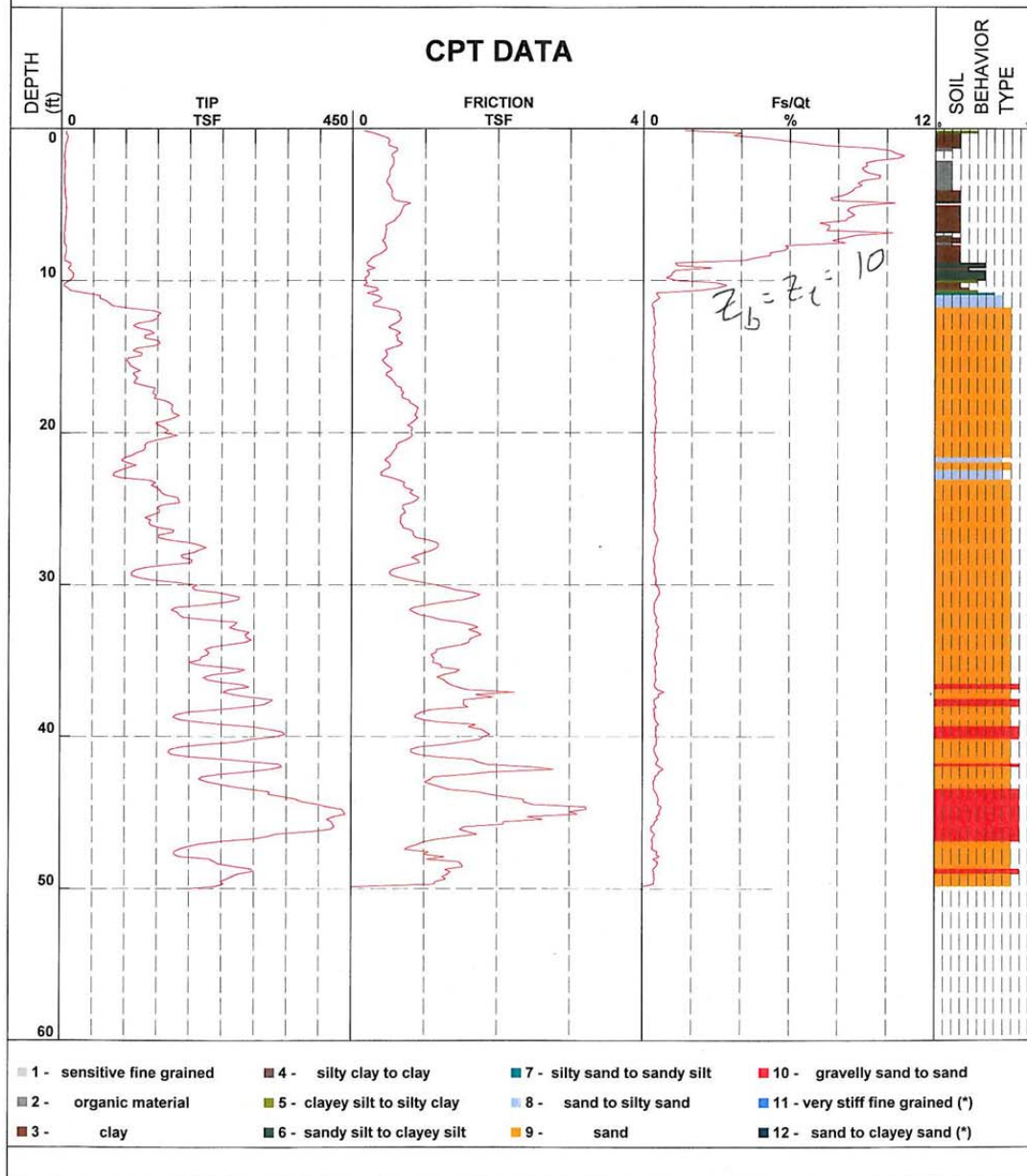
CONE NUMBER DSA1050

LOCATION 34 05.217 90 51.876

Date&Time 8/30/2011 7:40:16 AM

HOLE NUMBER FRA-7.11C

ELEVATION 150.42





## VICKSBURG DISTRICT

OPERATOR Crosby

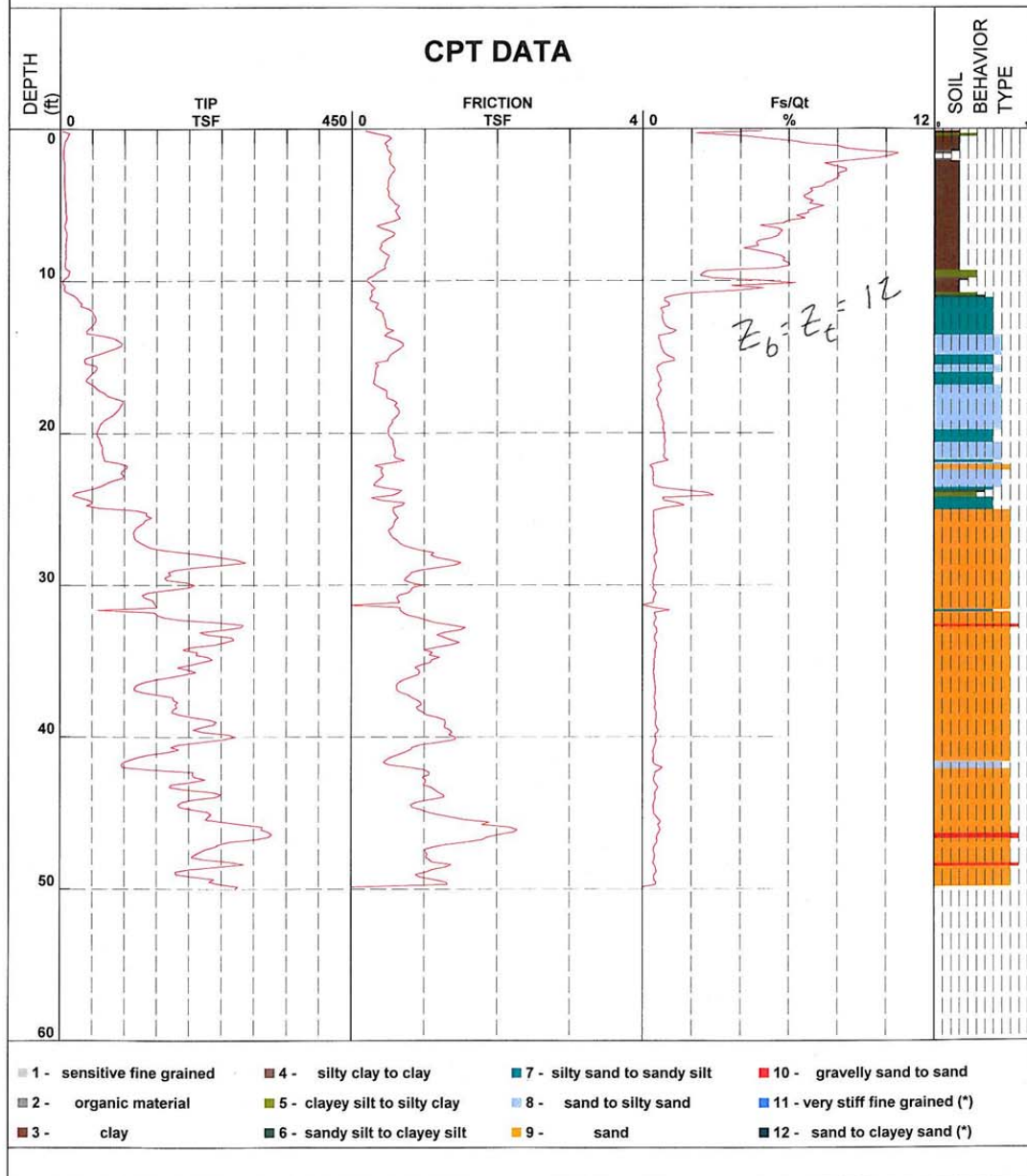
CONE NUMBER DSA1050

LOCATION 34 05.167 90 51.855

Date&Time 8/30/2011 8:18:47 AM

HOLE NUMBER FR8-7.11C

ELEVATION 151.11

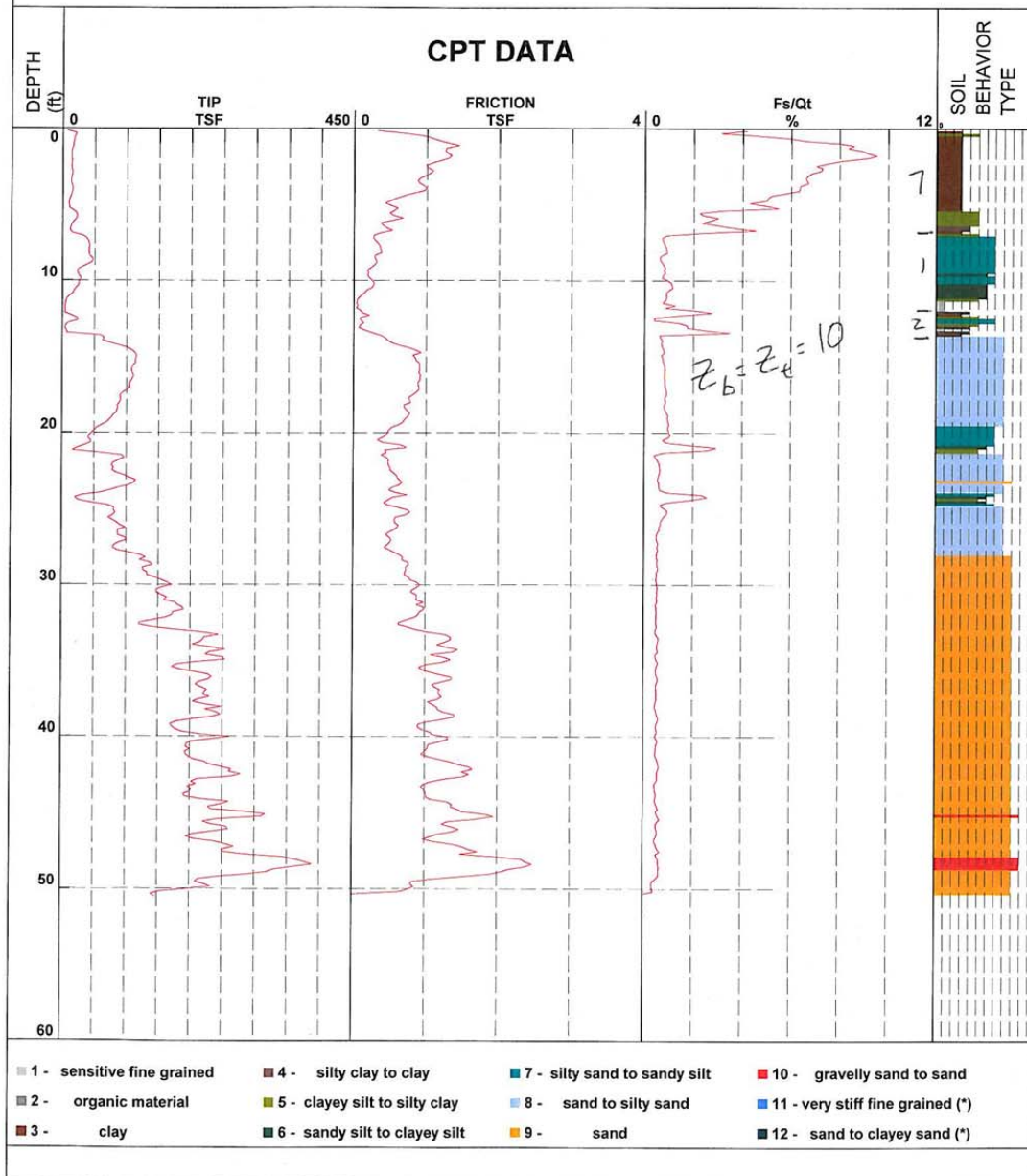






## VICKSBURG DISTRICT

OPERATOR Crosby CONE NUMBER DSA1050 LOCATION 34 05.118 90 51.832  
Date&Time 8/30/2011 9:05:35 AM HOLE NUMBER FRA-9.11C ELEVATION 151.97

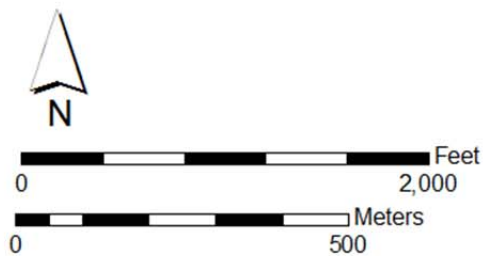


## **APPENDIX B**

### **Borehole Data from Rena Lara Site Obtained from USACE Memphis District**



## Rena Lara Boreholes



### Legend

- Seepage Point
- Sand Boils from 2011 Flood
- ▲ Rena Lara Borehole









CONDENSED SOIL DATA				WORK SHEET				SOIL LABORATORY			
Site: <u>Panda Lira Seepage Study</u>				Location: <u>160' RS. B Sta. 89/11 + 42</u>				Hole No.: <u>2-RG-83</u>			
Date of Boring: <u>12-1-83</u>		Date Received: <u>12-8-83</u>		Type of Boring: <u>Auger, S.S.</u>		Elevation of Top: <u>161.45</u>					
W = Water Content in % of Dry Weight		L.L. = Liquid Limit		P.L. = Plastic Limit		c = Cohesion in Tons/Sq. Ft.		φ = Angle of Internal Friction			
		3"		4		7d = Dry Density in Lbs./Cu. Ft.					
U. S. STANDARD SIEVE		3"		3/4"		10-		200			
COBBLES				GRAVEL				SAND		FINES	
		3"		3/4"		4.76mm		2.0mm		0.075mm	
GRAIN SIZE		3"		3/4"		4.76mm		2.0mm		0.075mm	
C.P.											
Depth Feet	Laboratory Classification	Strata Feet 0.0	W	L.L.	P.L.	φ	c	γ <sub>d</sub>	Sand	Remarks	
1 1.0-2.0	Br. <sup>fat clay</sup> <del>fine sand</del> moist: med		25							Mud - 11.5	
2 2.5-4.0	Br. <sup>fat</sup> <del>fine sand</del> clay, moist: med	CH	28	60	19					3 4 5	
3 5.0-6.5	Br. <sup>fat</sup> <del>fine sand</del> clay, moist: stiff		35	63	41					4 7 11	
4 7.5-9.0	Br. <sup>fat</sup> <del>fine sand</del> clay, moist: med	9.5	30	51	20					3 4 4	
5 10-11.5	Br. fine sand, moist.		7							2 7 7 D <sub>10</sub> = 0.16	
6 12.5-14.0	Br. fine sand, SAT	SP	7							3 5 5 D <sub>10</sub> = 0.090	
		14.5									
		17.5									

LHM Form 23A  
Rev 11 Aug 58

CONDENSED SOIL DATA WORK SHEET SOIL LABORATORY

Site: 2	1	0	0	1	Location:
---------	---	---	---	---	-----------

Kena Uva Seepage Study	
Date of Boring:	Date Completed:

DATE OF BORING.	DATE RECEIVED.	TYPE OF BORING.	ELEVATION OF TOP.	HOLE NO.:
2-1-83				0000

W = Water Content in % of Dry Weight	L.L. = Liquid Limit	$\phi$ = Angle of Internal Friction
		6-KG-83

$c$  = Cohesion in Tons/Sq. Ft.

I.L. = PLASTIC LIMIT		7d = Dry Density in Lbs./Cu. Ft.	
U. S. STANDARD SIEVE	3"	3/4"	4
			10-
			60
			100

DEPTH	COBBLES	GRAVEL	SAND	WATER
0.00				
0.25				
0.50				
0.75				
1.00				
1.25				
1.50				
1.75				
2.00				
2.25				
2.50				
2.75				
3.00				
3.25				
3.50				
3.75				
4.00				
4.25				
4.50				
4.75				
5.00				
5.25				
5.50				
5.75				
6.00				
6.25				
6.50				
6.75				
7.00				
7.25				
7.50				
7.75				
8.00				
8.25				
8.50				
8.75				
9.00				
9.25				
9.50				
9.75				
10.00				

Gravel	Fines		Medium	Fine
	Course	Fine		
	Course	Fine	Medium	Fine

GRAIN SIZE	3"	3/4"	4.76mm	2.0mm	0.42mm	0.075mm

[illegible]

30.0'

PH Form 23A  
Rev 11 Aug 58



CONDENSED SOIL DATA				WORK SHEET				SOIL LABORATORY			
Site: <u>Rena bara See page Study</u>				Location: <u>150' L.S. B sta 89/17+15</u>				Hole No.: <u>3-6G-83</u>			
Date of Boring: <u>12-5-6-83</u>		Date Received: <u>12-14-83</u>		Date Classified: <u>12-14-83</u>		Type of Boring: <u>Auger, S.S.</u>		Elevation of Top: <u>170.56</u>		Hole No.: <u>3-6G-83</u>	
W = Water Content in % of Dry Weight				L.L. = Liquid Limit				c = Cohesion in Tons/Sq. Ft.			
				P.L. = Plastic Limit				7d = Dry Density in Lbs./Cu. Ft.			
U. S. STANDARD SIEVE				3" 3/4"				10- 200			
COBBLES				GRAVEL				SAND			
				Course 3/4"				Medium 0.42mm			
GRAIN SIZE				3" 3/4"				Fine 0.074mm			
C.P.											
Depth Feet	Laboratory Classification	Strata Feet	W	L.L.	P.L.	c	7d	Sand	Remarks		
1 1.0-2.0	Br. lean clay, moist & med.	0.0	23						Med - 11.5		
2 2.5-4.0	sandy Br. lean clay, moist & med.	4.5	24	36	16			30	2 3 6		
3 5.0-6.5	lean Br. clay, moist & med.	7.5	22	39	17				5 7 8		
4 7.5-9.0	Br. fine sand, moist.								3 6 7 P.O. = 0.085		
5 10-11.5	Do	SP							3 6 7		
6 12.5-14.0	Do								9 12 11		
		14.5									
										21.6	

LIH Form 23A  
Rev 11 Aug 58



CONDENSED SOIL DATA				WORK SHEET		SOIL LABORATORY	
Site: <u>Kewa Kana Seepage Study</u>		Location:		Type of Boring: <u>By Auger, S.S.</u>		Hole No.: <u>3-6-83</u>	
Date of Boring: <u>12-5-6-83</u>		Date Received:		Elevation of Top:			
W = Water Content in % of Dry Weight		L.L. = Liquid Limit		c = Cohesion in Tons/Sq. Ft.			
P.L. = Plastic Limit		γ <sub>d</sub> = Dry Density in Lbs./Cu. Ft.					
U. S. STANDARD SIEVE <u>3"</u>		<u>3/4"</u>		<u>10-</u>		<u>200</u>	
COBBLES		GRAVEL		SAND		FINES	
Course <u>3"</u>		Course <u>3/4"</u>		Course <u>2.0mm</u>		Course <u>0.074mm</u>	
GRAIN SIZE		Fine		Medium		Fine	
		4.76mm		0.42mm		0.074mm	

Depth Feet	Laboratory Classification	Strata Feet	W	L.L.	P.L.	φ	c	γ <sub>d</sub>	Sand	Remarks
13 34-35.5	Mr. silty sand, SAT.	SM 34.0	X						66	8 10 13
14 39-40.5	Mr. fine sand, SAT.	SP 39.0	X							30 25 39 D <sub>10</sub> = 0.14
15 44-45.5	Br. & Mr. <del>fine</del> gravelly sand, SAT.	SP 44.0	X							33 30 23 D <sub>10</sub> = 0.22
16 49.5-50.0	Br. & Mr. <del>fine</del> med sand, SAT.	SP 49.5	X							12 16 14 D <sub>10</sub> = 0.26
		50.0								

JM Form 23A  
rev 11 Aug 58

50.0'

CONDENSED SOIL DATA				WORK SHEET				SOIL LABORATORY			
Site: <u>Rona Vana Seepage Study</u>				Location: <u>150' RS B Sta 89/17 +15</u>				Hole No.: <u>4-RG-83</u>			
Date of Boring: <u>1-30-83</u>		Date Received: <u>12-8-83</u>		Date Classified: <u>12-8-83</u>		Type of Boring: <u>By Auger, S.S.</u>		Elevation of Top: <u>163.28</u>		Hole No.: <u>4-RG-83</u>	
W = Water Content in % of Dry Weight				L.L. = Liquid Limit				c = Cohesion in Tons/Sq. Ft.			
P.L. = Plastic Limit				γd = Dry Density in Lbs./Cu. Ft.							
U. S. STANDARD SIEVE 3" 3/4" 4 10- 200											
COBBLES				GRAVEL				SAND			
Course 3"				Course 3/4"				Course 2.0mm			
GRAIN SIZE 3"				FINE 3/4"				FINE (Clay or Silt) 0.074mm			
C.P.											
Depth Feet	Laboratory Classification	Strata Feet	W	L.L.	P.L.	φ	c	γd	Sand	Remarks	
1 1.0-2.0	Br. & Nr. silty clay, moist & stiff	CL 2.0	22							Mud - 11.5'	
2 2.5-4.0	Br. & Nr. FAT clay, moist & stiff	CH 4.5	26	83	24					7 4 7	
3 5.0-6.5	Br. & Nr. silty clay, moist & med	CL 7.0	29	48	18					3 5 7	
4 7.5-9.0	Br. & Nr. sandy lean clay, wet & soft	CL 10.0	27	32	16				25	2 2 7	
5 10-11.5	Br. silty sand, lenses of clay, wet	SM 12.5	2							2 4 6	
6 12.5-14.0	Br. fine sand, wet	SP 17.5	2							10 14 20 γd = 0.17	

LPH Form 23A  
rev 11 Aug 58







CONDENSED SOIL DATA				WORK SHEET				SOIL LABORATORY			
Site: <u>Rona Lava Seepage Study</u>				Location: <u>150' L.S. Sta. 89/22.270</u>				Hole No.: <u>5-6G-83</u>			
Date of Boring: <u>12-6-83</u>		Date Received: <u>12-14-83</u>		Type of Boring: <u>Bx/Auger, S.S.</u>		Elevation of Top: <u>170.36</u>					
W = Water Content in % of Dry Weight				L.L. = Liquid Limit				ϕ = Angle of Internal Friction			
				P.L. = Plastic Limit				c = Cohesion in Tons/Sq. Ft.			
U. S. STANDARD SIEVE 3" 3/4"				10-200				7d = Dry Density in Lbs./Cu. Ft.			
COBBLES				GRAVEL				SAND			
Course 3"				Course 3/4"				Course 2.0mm			
GRAIN SIZE				FINE				FINE			
C.P.				0.42mm				0.074mm			
Depth Feet	Laboratory Classification	Strata Feet 0, Δ	W	L.L.	P.L.	ϕ	c	7d	Sand	Remarks	
1 1.0-2.0	Br. silty sand, moist	SM	2							Mud - 11.5	
2 2.5-4.0	Br. silty sand, moist	SM	2					79		2 7 3	
3 5.0-6.5	Br. sandy lean clay, wet & soft	CL 7.5	24	28	19			46		1 1 3	
4 7.5-9.0	Br. sandy silt, moist	ML 9.5	24					47		1 1 3	
5 10-11.5	Br. fine sand, moist	SP	2							7 5 6 0.0 = 0.14	
6 12.5-14.0	Do	15.0	2							6 13 13	
		17.5									

LHM Form 23A  
Rev 11 Aug 58

CONDENSED SOIL DATA

Site: Reva Lata Seepage Study

Date of Boring: 12-6-83

W = Water Content in % of Dry Weight

U. S. STANDARD SIEVE 3" 3/4" 4 10- 200

WORK SHEET

Location:

Date Received: 12-6-83

L.L. = Liquid Limit

P.L. = Plastic Limit

COBBLES

GRAIN SIZE 3" 3/4"

SOIL LABORATORY

Type of Boring:

Elevation of Top: 5-46-83

$\phi$  = Angle of Internal Friction

c = Cohesion in Tons/Sq. Ft.

$\gamma_d$  = Dry Density in Lbs./Cu. Ft.

SAND

COURSE

GRAVEL

FINE

FINES

(Clay or Silt)

Depth Feet	Laboratory Classification	Strata Feet	W	L.L.	P.L.	$\phi$	c	$\gamma_d$	Sand	Remarks
7 15-16.5	Br. silty sand, wet	SM 15.0	X						77	6 6 8
8 17.5-19.0	Br. fine sand, wet	SP 20.0	X							7 8 8 $D_{10} = 0.10$
9 20-21.5	Br. silty sand, wet	SM 24.0	X						69	3 4 4
10 24-25.5	Br. fine sand, SAT.	SP	X							3 7 8 $D_{10} = 0.17$
11 29-30.5	Do		X							8 10 14
12 34-35.5	Br. silty sand, SAT.	SM 37.0	X						82	9 12 14
13 39-40.5	Br. & Br. fine sand, SAT.	SP 40.5	X							10 15 24 $D_{10} = 0.17$

40.5'

LHM Form 23A  
Rev 11 Aug 58

CONDENSED SOIL DATA				WORK SHEET				SOIL LABORATORY			
Site: <u>Rena Liana Seepage Study</u>				Location: <u>145' RS</u>				Elevation of Top: <u>89/22.720</u>			
Date of Boring: <u>11-30-83</u>				Date Received: <u>12-8-83</u>				Type of Boring: <u>By Auger, S.S.</u>			
W = Water Content in % of Dry Weight				L.L. = Liquid Limit				Hole No.: <u>6-RG-83</u>			
U. S. STANDARD SIEVE 3" 3/4"				P.L. = Plastic Limit				c = Cohesion in Tons/Sq. Ft.			
COBBLES				GRAVEL				SAND			
GRAIN SIZE 3" 3/4"				Course 3/4"				Fine 0.42mm			
C.P.				2.0mm				0.074mm			
Depth Feet	Laboratory Classification	Strata Feet	W	L.L.	P.L.	c	γ <sub>d</sub>	Sand	Remarks		
1 1.0-2.0	Br. silty clay, moist & stiff	0.0	28						Mud. 11.5		
2 2.5-4.0	<del>Br. silty sand</del> silty sand	2.5	40					58	7 5 5		
3 5.0-6.5	<del>Br. silty sand</del> Br. & silty, moist	ML	18					30	4 5 5		
4 7.5-9.0	<del>Br. silty sand</del> silty sand, moist	7.5	11					53	3 7 7		
5 10.5-11.5	Br. fine sand, moist	SP	X						4 6 10 D <sub>10</sub> = 0.13		
6 12.5-14.0	Br. silty sand, moist	SM	X					76	8 7 7		
		15.0									
		17.5									

JMH Form 23A  
rev 11 Aug 58

CONDENSED SOIL DATA				WORK SHEET		SOIL LABORATORY	
Site: <u>Rena Lara Seepage Study</u>				Location:			
Date of Boring: <u>11-30-83</u>		Date Received: <u>11-30-83</u>		Type of Boring:	Elevation of Top:	Hole No.: <u>6-RG-83</u>	
W = Water Content in % of Dry Weight				L.L. = Liquid Limit	ϕ = Angle of Internal Friction		
				P.L. = Plastic Limit	c = Cohesion in Tons/Sq. Ft.		
					γd = Dry Density in Lbs./Cu. Ft.		
U. S. STANDARD SIEVE <u>3"</u>				<u>3/4"</u>	<u>10-</u>	<u>40</u>	<u>200</u>
COBBLES				GRAVEL	SAND		
				Course	Fine	Medium	Fine
GRAIN SIZE <u>3"</u>				<u>3/4"</u>	<u>2.0mm</u>	<u>0.42mm</u>	<u>0.075mm</u>
				Course	Fine	Medium	Fine
							(Clay or Silt)

Depth Feet	Laboratory Classification	Strata Feet /5,0	W	L.L.	P.L.	ϕ	c	γd	Sand	Remarks
7 15-16.5	Br. sandy silt, <del>sat</del> SAT	ML	X						41	3 2 2
8 17.5-19.0	Br. fine sand, SAT	17.5	X							7 7 7 D <sub>10</sub> = 0.18
9 20-21.5	Do	SP	X							6 10 17
10 24-25.5	Do		X							8 11 16
11 29.5-31.0	Br. silty sand, organic matter, SAT	29.0	X							6 10 11
		SM							81	
		31.0								

31.0'

## SOIL LABORATORY

12	4.70124	2.0000	0.42000	0.074000
----	---------	--------	---------	----------

Station No.	Depth Feet	Laboratory Classification	Strata Feet	W	L.L.	P.L.	φ	c	γd	Sand	Remarks
1	1.0-2.0	Br. sandy silt, moist.	0.0	16							Mud - 11.5
2	2.5-4.0	Br. <sup>fine</sup> silty clay, lenses of sand, moist & med.	2.5	32							3 6 8
3	5.0-6.5	Br. <sup>fine</sup> silty clay, moist & med.	CH	30	55	19					2 3 4
4	7.5-9.0	Br. sandy silt, wet.	7.5	20						49	2 3 4
5	10-11.5	Br. fine sand, lenses of silt, wet.	10.0	22							3 3 3 D <sub>10</sub> = 0.080
6	12.5-14.0	Br. lean clay, wet & soft.	12.5	29	30	22					2 3 5
			15.0								

16.0

CONDENSED SOIL DATA				WORK SHEET		SOIL LABORATORY	
Site: <u>Rena Lava Seepage Study</u>				Location:			
Date of Boring: <u>12-6-83</u>		Date Received: <u>7-83</u>		Type of Boring:	Elevation of Top:	Hole No.: <u>7-LG-83</u>	
W = Water Content in % of Dry Weight		L.L. = Liquid Limit		ϕ = Angle of Internal Friction			
		P.L. = Plastic Limit		c = Cohesion in Tons/Sq. Ft.			
				γ <sub>d</sub> = Dry Density in Lbs./Cu. Ft.			
U. S. STANDARD SIEVE <u>3"</u>		<u>3/4"</u>		<u>10-</u>		<u>200</u>	
COBBLES		GRAVEL		SAND		FINES	
		Course <u>3/4"</u>		Medium <u>2.0mm</u>		Fine <u>0.42mm</u>	
GRAIN SIZE <u>3"</u>		<u>3/4"</u>		<u>2.0mm</u>		<u>0.074mm</u>	

Depth Feet	Laboratory Classification	Strata Feet	W	L.L.	P.L.	ϕ	c	γ <sub>d</sub>	Sand	Remarks
7 15-16.0	<u>Br. silty SAT.</u>	<u>ML</u>	<u>X</u>						<u>27</u>	<u>2 3 7</u>
8 16-16.5	<u>Br. fine sand, moist.</u>	<u>16.0</u>	<u>X</u>							<u>2 3 7</u> <u>D<sub>10</sub> = 0.16</u>
9 17.5-19.0	<u>Br. fine sand, wet.</u>	<u>SP</u>	<u>X</u>							<u>7 12 17</u> <u>D<sub>10</sub> = 0.17</u>
10 20-21.5	<u>Do</u>		<u>X</u>							<u>8 9 10</u>
11 24-25.5	<u>Do SAT</u>		<u>X</u>							<u>6 7 11</u>
12 29-30.5	<u>Br. silty sand, SAT.</u>	<u>29.0</u>	<u>X</u>							<u>4 7 7</u>
		<u>SM</u>							<u>74</u>	<u>4 7 7</u>
		<u>39.0</u>								

LJH Form 23A  
Rev 11 Aug 58





CONDENSED SOIL DATA				WORK SHEET				SOIL LABORATORY			
Site: <u>Reva Lora Seepage Study</u>				Location: <u>145' RS</u>				Elevation of Top: <u>372 89/22 +80</u>			
Date of Boring: <u>11-29-83</u>				Date Classified: <u>12-8-83</u>				Type of Boring: <u>By Auger, SS.</u>			
W = Water Content in % of Dry Weight				L.L. = Liquid Limit				ϕ = Angle of Internal Friction			
				P.L. = Plastic Limit				c = Cohesion in Tons/Sq. Ft.			
				U. S. STANDARD SIEVE 3" 3/4" 4 10- 200				γd = Dry Density in Lbs./Cu. Ft.			
COBBLES				GRAVEL				SAND			
GRAIN SIZE 3" 3/4" 4.76mm 2.0mm 0.42mm 0.074mm				FINE (Clay or Silt)							
C.P.											
Depth Feet	Laboratory Classification	Strata Feet	W	L.L.	P.L.	ϕ	c	γd	Sand	Remarks	
1 1.0-2.0	Br. silty clay, moist & stiff	CL 2.0	24							Mud = 11.5	
2 2.5-4.0	Br. sandy silt, moist	2.0	12					45		5 5 7	
3 5.0-6.5	Br. sandy silt, wet	ML	12					49		3 3 4	
4 7.5-9.0	Do	10.0	16							2 4 5	
5 10-11.5	Br. fine sand, wet.	SP	X							3 5 10 D <sub>10</sub> = 0.20	
6 12.5-14.0	Br. fine sand, wet.	15.6	X							13 12 10 D <sub>10</sub> = 0.16	
17.5											

LJH Form 23A  
Rev 11 Aug 58

CONDENSED SOIL DATA				WORK SHEET		SOIL LABORATORY			
Site: <u>Realt's Seepage Study</u>		Location:		Type of Boring:		Elevation of Top:		Hole No.:	
Date of Boring:		Date Received:		Date Classified:		Date of Test:		Date of Report:	
W = Water Content in % of Dry Weight		L.L. = Liquid Limit		P.L. = Plastic Limit		U. S. STANDARD SIEVE		FINES	
3"		3/4"		4		10-		200	
COBBLES		GRAVEL		SAND		FINE		FINES	
3"		3/4"		4.76mm		2.0mm		0.075mm	
GRAIN SIZE		Course		Fine		Medium		Clay or Silt	
3"		3/4"		4.76mm		2.0mm		0.075mm	

Depth Feet	Laboratory Classification	Strata Feet	W	L.L.	P.L.	$\phi$	c	$\gamma_d$	Sand	Remarks
15-16.5	<u>Silty sand</u>	SM	X						62	7 7 6
17.5-19.0	<u>Fine sand</u>	SP	X						90	10 12 10
20-21.5	<u>Silty sand</u>	SM	X						71	4 5 6
24-25.5	<u>Do</u>	SP	X							5 7 11
29-30.5	<u>Dr. fine sand SAT.</u>	SP	X							14 18 24 D <sub>10</sub> = 0.10
34-35.5	<u>Do</u>	SP	X							25 35 35
38.5-40.0	<u>Do</u>	SP	X							14 20 25

40.0'

U.S. Form 23A  
Rev 11 Aug 58

CONDENSED SOIL DATA				WORK SHEET				SOIL LABORATORY			
Site: <u>Rena Lara Seepage Study</u>				Location: <u>150' L.S. Sta. 89/33+00</u>							
Date of Boring: <u>12-7-83</u>		Date Received: <u>12-14-83</u>		Type of Boring: <u>By Auger, S.S.</u>		Elevation of Top: <u>120.24</u>		Hole No.: <u>9-46-83</u>			
W = Water Content in % of Dry Weight				L.L. = Liquid Limit				c = Cohesion in Tons/Sq. Ft.			
				P.L. = Plastic Limit				γ <sub>d</sub> = Dry Density in Lbs./Cu. Ft.			
U. S. STANDARD SIEVE 3" 3/4" 4 10- 200											
COBBLES				GRAVEL				SAND			
Course 3"				Course 3/4"				Course 2.0mm			
GRAIN SIZE 3"				FINE 3/4"				FINE (Clay or Silt) 0.074mm			
C.P.											
Depth Feet	Laboratory Classification	Strata Feet	W	L.L.	P.L.	φ	c	γ <sub>d</sub>	Sand	Remarks	
1 1.0-2.0	Br lean clay, moist & med.	CL 0.0	25							Mad - 11.5 12-7-83	
2 2.5-4.0	Br silty clay, wet & soft.	CL 2.0	30	43	17					γ <sub>d</sub> 12.8 12-7-83	
3 5.0-6.5	Br <del>stiff</del> clay, moist & med.	CL 5.0	27	51	18					1 3 4	
4 7.5-9.0	Br fat clay, moist & med.	CH	40	70	22					1 2 3	
5 10-11.5	Do		36							1 2 3	
6 12.5-14.0	Do		37							1 3 4	
28.0											

LHM Form 23A  
Rev 11 Aug 58

CONDENSED SOIL DATA				WORK SHEET		SOIL LABORATORY	
Site: <u>Rena Vana Seepage Study</u>				Location:		Hole No.: <u>9-66-83</u>	
Date of Boring: <u>12-7-83</u>		Date Received: <u>12-7-83</u>		Type of Boring:	Elevation of Top:		
W = Water Content in % of Dry Weight		L.L. = Liquid Limit		ϕ = Angle of Internal Friction			
		P.L. = Plastic Limit		c = Cohesion in Tons/Sq. Ft.			
U. S. STANDARD SIEVE <u>3"</u>		<u>3/4"</u>		γ <sub>d</sub> = Dry Density in Lbs./Cu. Ft.			
COBBLES		GRAVEL		SAND		FINES	
GRAIN SIZE <u>3"</u>		Course <u>3/4"</u>		Medium <u>2.0mm</u>		Fine <u>0.42mm</u>	
						(Clay or Silt) <u>0.074mm</u>	

Depth Feet	Laboratory Classification	Strata Feet S, D	W	L.L.	P.L.	ϕ	c	γ <sub>d</sub>	Sand	Remarks
7 15-16.5	Mr. FATCLAY, lenses of silt, moist & stiff.		28							5 4 9
8 17.5-19.0	Do		29							3 6 6
9 20-21.5	Mr. FATCLAY, organic, wet & soft.		57	95	29					1 3 3
10 24-25.5	Mr. FATCLAY, wet & soft.		50	84	25					3 5 4
11 29-30.5	Mr. sandy silt, lenses of clay, wet.	29.0	32							1 2 3
12 34-35.5	Mr. sandy silt, wet.	31.0	30						76	6 8 8
		SM								
		44.0								

LIH Form 23A  
Rev 11 Aug 58

CONDENSED SOIL DATA WORK SHEET SOIL LABORATORY

Site:	Location:
1	0
2	1
3	2
4	3
5	4
6	5
7	6
8	7
9	8
10	9
11	10
12	11
13	12
14	13
15	14
16	15
17	16
18	17
19	18
20	19
21	20
22	21
23	22
24	23
25	24
26	25
27	26
28	27
29	28
30	29
31	30
32	31
33	32
34	33
35	34
36	35
37	36
38	37
39	38
40	39
41	40
42	41
43	42
44	43
45	44
46	45
47	46
48	47
49	48
50	49
51	50
52	51
53	52
54	53
55	54
56	55
57	56
58	57
59	58
60	59
61	60
62	61
63	62
64	63
65	64
66	65
67	66
68	67
69	68
70	69
71	70
72	71
73	72
74	73
75	74
76	75
77	76
78	77
79	78
80	79
81	80
82	81
83	82
84	83
85	84
86	85
87	86
88	87
89	88
90	89
91	90
92	91
93	92
94	93
95	94
96	95
97	96
98	97
99	98
100	99

Date of Boring:	Date Received:	Date Classified:	Type of Boring:	Elevation of Top:	Hoile No.:
Aug 28 1908	Sept 1 1908	Sept 1 1908			

2-7-83	Date received.	Date Classified:	Type of Boring:	Elevation of Top:	Hole No.:
					9-10-17

W = Water Content in % of Dry Weight	L.L. = Liquid Limit	$\phi$ = Angle of Internal Friction
--------------------------------------	---------------------	-------------------------------------

$c$  = Cohesion in Tons/Sq. Ft.

U. S. STANDARD SIEVE	I. I. I. - PASCAL LIMIT	W = DRY DENSITY IN LBS./CU. FT.
3"	3/4"	40
	10-	200

DEPTH	COBBLES	GRAVEL	SAND	OTHER
0				
1				
2				
3				
4				
5				
6				
7				
8				
9				
10				
11				
12				
13				
14				
15				
16				
17				
18				
19				
20				
21				
22				
23				
24				
25				
26				
27				
28				
29				
30				
31				
32				
33				
34				
35				
36				
37				
38				
39				
40				
41				
42				
43				
44				
45				
46				
47				
48				
49				
50				
51				
52				
53				
54				
55				
56				
57				
58				
59				
60				
61				
62				
63				
64				
65				
66				
67				
68				
69				
70				
71				
72				
73				
74				
75				
76				
77				
78				
79				
80				
81				
82				
83				
84				
85				
86				
87				
88				
89				
90				
91				
92				
93				
94				
95				
96				
97				
98				
99				
100				

	FINE	COURSE	MEDIUM	FINE
(Clay or Silt)				

GRAIN SIZE	3"	3/4"	4.76mm	2.0mm	0.42mm	0.074mm

Station	Depth Feet	Laboratory Classification	Strata Feet	W	L.L.	P.L.	Ø	c	γ <sub>d</sub>	Sand	Remarks
13	39-40.5	Med. <del>sandy</del> silty sand, SAT.	31.0	X							3 5 12
14	44-45.5	Br. fine sand, SAT.	44.0	X							10 25 28 10 = 0.25
15	49-50.5	Do	SP	X							13 22 32
16	53-55.0	med to fine Br. & Gr. <del>fine</del> sand, SAT.	52.0	X							8 10 30 0.0 = 0.25
			SP								
			55.0								

FD-302 (Rev. 11 Aug 58)



CONDENSED SOIL DATA WORK SHEET SOIL LABORATORY

Site: <u>Renakara Seepage Study</u>		Location: <u>145<sup>th</sup> RS. &amp; Sta. 89/33+00</u>	
Date of Boring: <u>11-29-83</u>	Date Received: <u>12-8-83</u>	Type of Boring: <u>Br/Auger, S.S.</u>	Elevation of Top: <u>160.68</u>
W = Water Content in % of Dry Weight		L.L. = Liquid Limit	Hole No.: <u>10-RG-83</u>
P.L. = Plastic Limit		$\theta$ = Angle of Internal Friction	
4		c = Cohesion in Tons/Sq. Ft.	
10-		$\gamma_d$ = Dry Density in Lbs./Cu. Ft.	
200			
U. S. STANDARD SIEVE 3"		3/4"	
COBBLES	Course	GRAVEL	Course
	3/4"	3/4"	3/4"
GRAIN SIZE	3"	4.75mm	2.0mm
c p		0.075mm	
		FINE (Clay or Silt)	

Station No.	Depth Feet	Laboratory Classification	Strata Feet	W	L.L.	P.L.	Ø	c	Yd	Sand	Remarks
1	1.0-2.0	Br. silty clay, moist & med.	0.0	25							Mud - 14.0
2	2.5-4.0	Br. & Nr. <sup>fat</sup> <del>stiff</del> clay, moist & stiff	2.0	28	6.5	2.0					3 8 10
3	5.0-6.5	Do		32							3 5 7
4	7.5-9.0	Br. & Nr. FAT clay, moist & med.	CH	40	10.1	2.3					3 7 5
5	10-11.5	Br. & Nr. FAT clay, lenses of silt, moist & med.		34							3 7 5
6	12.5-14.0	Br. & Nr. FAT clay, moist & stiff	15.0	31	7.8	2.2					4 7 5

CONDENSED SOIL DATA				WORK SHEET				SOIL LABORATORY			
Site: <u>Reva Lara Seepage Study</u>		Location:		Type of Boring:		Elevation of Top:		Hole No.:			
Date of Boring: <u>11-29-83</u>		Date Received:		L.L. = Liquid Limit		P.L. = Plastic Limit		Angle of Internal Friction			
W = Water Content in % of Dry Weight		3"		3/4"		4"		10-200			
U. S. STANDARD SIEVE		3"		3/4"		4"		40			
COBBLES		GRAVEL		SAND		FINE		FINES			
GRAIN SIZE		3"		3/4"		4"		40			
3"		3/4"		4"		40		0.075mm			
3"		3/4"		4"		40		0.075mm			
Depth Feet	Laboratory Classification	Strata Feet / 5.0	W	L.L.	P.L.	$\phi$	c	$\gamma_d$	Sand	Remarks	
7 15-16.5	Br. silty clay, wet & soft	CL	39	47	19					0 1 2	
8 17.5-19.0	Do	20.0	42							0 1 1	
9 20-21.5	Br. sandy silt, lenses of clay, wet	24.5	37							2 3 4	
10 24-25.5	Br. fine sand, SAT.		X							0 10 12 D <sub>10</sub> = 0.075	
11 29-30.5	Br. & M. fine sand, SAT.	SD	X							9 5 8 D <sub>10</sub> = 0.20	
12 33.5-35.0	Do	35.0	X							5 6 8	
		35.0'									

LHM Form 23A  
Rev 11 Aug 58

## SOIL LABORATORY

Site: <u>Pen a Larz Seepage Study</u>	Location: <u>150' L.S. B Sta</u>	<u>89/38 toe</u>	
Date of Boring: <u>12-7, 8-83</u>	Date Classified: <u>12-14-83</u>	Type of Boring: <u>Bx Auger, S.S.</u>	Elevation of Top: <u>170.42</u>
W = Water Content in % of Dry Weight		L.L. = Liquid Limit	θ = Angle of Internal Friction
U. S. STANDARD SIEVE 3"		P.L. = Plastic Limit	c = Cohesion in Tons/Sq. Ft.
3/10"			γ <sub>d</sub> = Dry Density in Lbs./Cu. Ft.
			<u>11-65-83</u>

GRAIN SIZE	GRAVEL		SAND			FINES (Clay or Silt)
	Course	Fine	Course	Medium	Fine	
3"	3/4"		4.76mm	2.0mm	0.42mm	0.074mm

Depth Feet	Laboratory Classification	Strata Feet	W	L.L.	P.L.	Ø	c	γ <sub>d</sub>	Sand	Remarks
1 1.0-2.0	Br. sandy lean clay, moist & med.	0.0	26							Med - 11.5
2 2.5-4.0	Br. sandy lean clay, moist & med.	CL	24	36	15				35	2 3 4
3 5.0-6.5	Br. & Mc. fat clay, moist & stiff	5.0	30	84	23					3 4 6
4 7.5-9.0	Do	SH	33							3 3 4
5 10-11.5	Do		29							3 3 6
6 12.5-14.0	Do	15.0	35							3 6 7

JPM Form 23A  
 Rev 11 Aug 58

CONDENSED SOIL DATA				WORK SHEET				SOIL LABORATORY			
Site: <u>Renata Geopage Study</u>				Location:							
Date of Boring: <u>11-66-83</u>		Date Received: <u>11-66-83</u>		Type of Boring: <u>3</u>		Elevation of Top: <u>11-66-83</u>		Hole No.: <u>11-66-83</u>			
W = Water Content in % of Dry Weight				L.L. = Liquid Limit				ϕ = Angle of Internal Friction			
				P.L. = Plastic Limit				c = Cohesion in Tons/Sq. Ft.			
								γd = Dry Density in Lbs./Cu. Ft.			
U. S. STANDARD SIEVE <u>3"</u>				<u>3/4"</u>				<u>10-</u>			
COBBLES				GRAVEL				SAND			
				Course <u>3/4"</u>				Medium <u>2.0mm</u>			
GRAIN SIZE <u>3"</u>				Fine <u>4.76mm</u>				Fine <u>0.42mm</u>			
								FINES (Clay or Silt) <u>0.074mm</u>			

Depth Feet	Laboratory Classification	Strata Feet	W	L.L.	P.L.	ϕ	c	γd	Sand	Remarks
7 15-16.5	Br. fine sand, lenses of clay	SP 15.0	X							11 14 16
8 17.5-19.0	Br. silty sand, wet	SM 17.0	23						54	6 7 9
9 20-21.5	Br. sandy silt, SAT.	ML 24.0	X						43	3 4 9
10 22-25.5	Br. fine sand, SAT.		X							13 22 27 0.10 = 0.16
11 29-34.5	Do	SP	X							11 13 11
12 34-35.5	Do		X							9 12 16
13 38.5-40.0	Do	40.0	X							22 29 43
										40.0'

JM Form 23A  
rev 11 Aug 58

CONDENSED SOIL DATA				WORK SHEET				SOIL LABORATORY			
Site: <u>Rona Liza Seepage Study</u>				Location: <u>145' R5 B Ste 89/ 38 +10</u>				Hole No.: <u>12-RG-83</u>			
Date of Boring: <u>11-28-83</u>				Date Received: <u>12-8-83</u>				Type of Boring: <u>By Auger, S.S.</u>			
W = Water Content in % of Dry Weight				L.L. = Liquid Limit				c = Cohesion in Tons/Sq. Ft.			
U. S. STANDARD SIEVE 3" 3/4"				P.L. = Plastic Limit				γd = Dry Density in Lbs./Cu. Ft.			
COBBLES				GRAVEL				SAND			
GRAIN SIZE 3" 3/4"				Course 3/4"				Fine 0.42mm			
GR. 0.075mm				2.0mm				0.075mm			
Depth Feet	Laboratory Classification	Strata Feet 0.0	W	L.L.	P.L.	φ	c	γd	Sand	Remarks	
1 1.0-2.0	Br. silty clay, moist, med	CL	23							med - 11.5	
2 2.5-4.0	Br. silty clay, moist, stiff	CH	29	20	19					5 10 14	
3 5.0-6.5	Br. silty sand, moist	SL	1						87	7 10 12	
4 7.5-9.0	Br. fine sand, wet	SP	1							4 10 11 γd = 0.26	
5 10-11.5	Do	SP	1							3 7 10	
6 12.5-14.0	Do		1							4 14 20	
19.0											

MS Form 23A  
rev 11 Aug 58

## CONDENSED SOIL DATA

4.0000

[illegible]

0.51



## SOIL LABORATORY

[illegible]

Sample No.	Depth Feet	Laboratory Classification	Strata Feet	W	L.L.	P.L.	φ	c	γ <sub>d</sub>	Sand	Remarks
1	1.0-2.0	Br. fine sand, lenses of clay, moist.	SP 0.0	2							Mud - 11.5
2	2.5-4.0	Br. & Gr. silty clay, lenses of sand, moist & med.	CL 5.0	27							1 2 3
3	5.0-6.5	Br. & Gr. fat clay, moist & stiff.	CH	31	23	21					3 6 7
4	7.5-9.0	Br. & Gr. fat clay, moist & med.	9.5	36	26	23					1 3 5
5	10-11.5	Br. & Gr. silty clay, moist & med.	CL 12.5	29	44	18					2 5 5
6	12.5-14.0	Br. fine sand, wet.	SP	2							6 11 18 D <sub>10</sub> = 0.12

LDH Form 23A  
Rev 11 Aug 58

---

SOIL LABORATORY

Site: <i>Rena Para Seepage Study</i>		Location:	
Date of Boring: <i>12-8-83</i>	Date Received:	Type of Boring:	Elevation of Top:
W = Water Content in % of Dry Weight		Hole No.: <i>13-LG-83</i>	
L.L. = Liquid Limit			

W = Water Content in % of Dry Weight	L.L. = Liquid Limit	$\phi$ = Angle of Internal Friction	13-L.G-83
	P.L. = Plastic Limit	c = Cohesion in Tons/Sq. Ft.	
U. S. STANDARD SIEVE 30		$\gamma_d$ = Dry Density in Lbs./Cu. Ft.	
			3/4"

U. S. STANDARD SIEVE	P.L. = Plastic Limit	$\gamma_d$ = Dry Density in Lbs./Cu. Ft.
3"	4	10-
3/4"	4	40
		200

COBBLES	GRAVEL		SAND			FINES (Clay or Silt)
	Course	Fine	Course	Medium	Fine	
GRAIN SIZE	3"	3/4"	4.76mm	2.0mm	0.42mm	0.075mm

Depth Feet	Laboratory Classification	Strata Feet Z.S.	W	L.L.	P.L.	Ø	c	γ <sub>d</sub>	Sand	Remarks
7 15-16.5	Br. fine sand, wet		X							10 16 22
8 17.5-19.0	Do		X							7 13 19
9 20-21.5	Do		X							7 13 19
10 24-25.5	Br. fine sand, SAT.	29.0	X							5 8 12 P <sub>20</sub> = 0.12
11 29-30.5	Br. silty sand, SAT.	SM	X						66	4 5 6
12 34-35.5	Br. fine sand, SAT.	34.0	X							7 7 8 P <sub>20</sub> = 0.16

A6.0



CONDENSED SOIL DATA				WORK SHEET				SOIL LABORATORY			
Site: <u>Rena Lana Seepage Study</u>				Location: <u>132.85 S. Sta. 89/43 +27</u>				Hole No.: <u>14-RG-83</u>			
Date of Boring: <u>11-29-83</u>		Date Received: <u>12-8-83</u>		Type of Boring: <u>Bx/Auger, S.S.</u>		Elevation of Top: <u>162.41</u>					
W = Water Content in % of Dry Weight				L.L. = Liquid Limit				c = Cohesion in Tons/Sq. Ft.			
				P.L. = Plastic Limit				γd = Dry Density in Lbs./Cu. Ft.			
U. S. STANDARD SIEVE 3" 3/4"				GRAVEL				SAND			
COBBLES				Course 3/4"				Course 10-200			
GRAIN SIZE 3" 3/4"				Fine				FINE (Clay or Silt)			
C.P.				4.76mm				0.42mm 0.075mm			
Depth Feet	Laboratory Classification	Strata Feet G.O.	W	L.L.	P.L.	φ	c	γd	Sand	Remarks	
1 1.0-2.0	Br. clay, moist & med.	CL	27							Mud - 11.5	
2 2.5-4.0	Br. <sup>lean</sup> clay, moist & med.	5.0	26	39	16					3 4 5	
3 5.0-6.5	Br. fine sand, moist.		X							4 8 13 D <sub>0</sub> = 0.15	
4 7.5-9.0	D <sub>0</sub>	SP	X							6 15 25	
5 10-11.5	D <sub>0</sub>		X							4 6 10	
6 12.5-14.0	D <sub>0</sub>		X							8 10 15	
7 15-16.5	Br. fine sand, wet.	16.5	X							6 8 10 D <sub>0</sub> = 0.15	
		16.5'									

LM Form 23A  
Rev 11 Aug 58

CONDENSED SOIL DATA				WORK SHEET				SOIL LABORATORY			
Site: <u>REVA LAB Seepage Study</u>				Location: <u>150' x 50' Sta 90/2+50</u>				Hole No.: <u>15-LG-83</u>			
Date of Boring: <u>12-12-83</u>		Date Received: <u>Box Aug 28 '83</u>		Type of Boring: <u>Box Auger</u>		Elevation of Top: <u>170.32</u>		Type of Boring: <u>Box Auger</u>		Elevation of Top: <u>170.32</u>	
W = Water Content in % of Dry Weight				L.L. = Liquid Limit				c = Cohesion in Tons/Sq. Ft.			
U. S. STANDARD SIEVE 3" 3/4" 4 10- 200				P.L. = Plastic Limit				γd = Dry Density in Lbs./Cu. Ft.			
COBBLES				GRAVEL				SAND			
GRAIN SIZE 3" 3/4" 4.76mm 2.0mm 0.42mm 0.075mm				FINE				FINE			
C.P.				C.P.				C.P.			
Depth Feet	Laboratory Classification	Strata Feet	W	L.L.	P.L.	φ	c	γd	Sand	Remarks	
1 1.0-2.0	Br. silty sand, wet.	0.0	2							Mud @ 11.5	
2 2.5-4.0	Br. sandy silt, lenses of clay, moist	SM 2.5	17							4-4-4	
3 5.0-6.5	Br. & Br. silty clay, lenses of sand, moist & med	ML 5.0	30							4-8-10	
4 7.5-9.0	Do	CL 10.0	25							2-3-5	
5 10.0-11.5	Br. & Br. FAT clay, moist & stiff	CH 12.5	28							3-6-8	
6 12.5-14.0	Br. silty sand, wet.	SM 15.0	2						85	5-8-10	
40.0											

LM Form 23A  
Rev 11 Aug 58





## CONDENSED SOIL DATA

Site: <u>Reva Liza Seepage Study</u>		Location: <u>140' RS 0 57m 90/2 +65'</u>	
Date of Boring: <u>11-28-83</u>	Date Received: <u>12-8-83</u>	Type of Boring: <u>BS/Auger, S.S.</u>	Elevation of Top: <u>161.74</u>
W = Water Content in % of Dry Weight		L.L. = Liquid Limit	Hole No.: <u>16-RG-83</u>
		P.L. = Plastic Limit	$\theta$ = Angle of Internal Friction
U. S. STANDARD SIEVE <u>3"</u>		<u>4</u>	<u>7d = Cohesion in Tons/Sq. Ft.</u>
		<u>3/4"</u>	<u>7d = Dry Density in Lbs./Cu. Ft.</u>
COBBLES		GRAVEL	<u>40</u>
	Course	Course	<u>200</u>
	Fine	SAND	
		Medium	
GRAIN SIZE <u>3"</u>	<u>4.76mm</u>	Fine	
	<u>3/4"</u>	<u>2.0mm</u>	(Clay or Silt)
C.P.		<u>0.42mm</u>	<u>0.074mm</u>

Station	Depth Feet	Laboratory Classification	Strata Feet O, O	W	L.L.	P.L.	$\phi$	c	$\gamma_d$	Sand	Remarks
1	1.0-2.0	Br. silty clay, moist & med.	CL 2.5	28							Mud - 11.5
2	2.5-3.5	Br. silty sand, moist.	SM 3.5	2						86	4 5 5
3	3.5-4.0	Br. & Br. lean clay, wet & soft.	CL 5.0	26							
4	5.0-6.5	lenses of sand. Br. fine sand, wet.		2							4 8 10 D <sub>10</sub> = 0.090
5	7.5-9.0		SP	2							8 15 21
6	10-11.5			2							5 10 12

LLM Form 23A  
Rev 11 Aug 58



## VITA

Thomas Chapman Brackett “Chap” was born in Savannah, Georgia on June 29, 1987. Upon graduating from Benedictine Military School in 2006, he enrolled in the University of Mississippi’s Geological Engineering program. During his junior year of undergrad, Chap was hired by the Mississippi Mineral Resources Institute as a student research assistant. He graduated in the Fall of 2010 with a Bachelor’s of Science degree in Geological Engineering.

Due in part to the encouragement of Dr. Greg Easson and other MMRI staff, Chap continued his studies at the University. In the Spring of 2011 chap enrolled in the School of Engineering’s graduate program, working towards a Master’s of Science in Engineering with emphasis in Geological Engineering. During his graduate career, Chap maintained his job with MMRI where he participated in the project *Characteristics of the Flood Hazard in the Delta Region of Mississippi*. He was also awarded the Robert Woolsey Award in the Fall of 2011. Upon graduation, Chap moved to Houston, Texas where he currently is employed by Maverick Exploration Company.